USGS
science for a changing world

In cooperation with the Texas Department of Transportation

Depth-Duration Frequency of Precipitation for Texas

Water-Resources Investigations Report 98–4044

U.S. Department of the Interior
U.S. Geological Survey

Depth-Duration Frequency of Precipitation for Texas

By William H. Asquith

U.S. GEOLOGICAL SURVEY
Water-Resources Investigations Report 98–4044

In cooperation with the Texas Department of Transportation

Austin, Texas
1998

U.S. DEPARTMENT OF THE INTERIOR

Bruce Babbitt, Secretary

U.S. GEOLOGICAL SURVEY

Thomas J. Casadevall, Acting Director

Second printing

For additional information write to

District Chief
U.S. Geological Survey
8011 Cameron Rd.
Austin, TX 78754–3898

Copies of this report can be purchased from
U.S. Geological Survey
Branch of Information Services
Box 25286
Denver, CO 80225–0286

CONTENTS

PLATE

(Plate is in pocket)

FIGURES

TABLES

Depth-Duration Frequency of Precipitation for Texas

By William H. Asquith

Abstract

The U.S. Geological Survey, in cooperation with the Texas Department of Transportation, conducted a study of the depth-duration frequency of precipitation for Texas. Depth-duration frequency is an estimate of the depth of precipitation for a specified duration and frequency or recurrence interval. For this report, precipitation durations of 15, 30, and 60 minutes; 1, 2, 3, 6, 12, and 24 hours; and 1, 2, 3, 5, and 7 days were investigated. The recurrence intervals for the frequencies range from 2 to 500 years.

The time series of precipitation annual maxima for 173 fifteen-minute, 274 hourly, and 865 daily National Weather Service precipitation stations with at least 10 years of record in Texas provide the basis of depth-duration frequency for each identified duration. In total, about 3,030; 10,160; and 38,120 cumulative years of record are available for the 15-minute, hourly, and daily stations, respectively.

L-moment statistics of the precipitation annual maxima were calculated for each duration and for each station using unbiased L-moment estimators. The statistics calculated were the mean, L-scale, L-coefficient of variation, L-skew, and L-kurtosis. The mean for each station and duration was corrected for the bias associated with fixed-interval recording of precipitation. The generalized logistic distribution was determined, using L-moment ratio diagrams, as an appropriate probability distribution for modeling the frequency of annual maxima for durations of 15 minutes to 24 hours; whereas, the generalized extreme-value distribution was determined as appropriate for durations of 1 to 7 days.

The location, scale, and shape parameters of the distributions for each duration and each station were calculated from the L-moments. These parameters were contoured using spatial interpolation, based on the geostatistical method of kriging, to produce 37 maps that depict the spatial variation and magnitude of each parameter. Contour maps of the shape parameter for the generalized extreme-value distribution for durations of 1 to 7 days are not presented; the root mean square errors of preliminary maps for 1- to 7-day shape parameters were not appreciably smaller than the statewide standard deviation. Therefore, a single statewide mean shape parameter was used for 1- to 7-day durations. The depth-duration frequency for any location in Texas can be estimated using the contour maps and the equation of the corresponding distribution.

INTRODUCTION

Precipitation depths for various durations and frequencies, referred to as depth-duration frequency (DDF) in this report, have many uses. A common use of DDF is for the design of structures that control and route localized runoff—such as parking lots, storm drains, and culverts. Another use of DDF is to drive river-flow models that incorporate precipitation characteristics. Accurate DDF estimates are important for cost-effective structural designs at stream crossings and for developing reliable flood prediction models. In 1996, the U.S. Geological Survey (USGS), in cooperation with the Texas Department of Transportation, began a 3-year study of precipitation characteristics for Texas. The major objectives of the study are (1) to define the DDF of precipitation for Texas, (2) to determine appropriate areal-reduction factors for the 1-day design storm for Texas, and (3) to investigate the extreme precipitation potential for Texas.

Purpose and Scope

The purpose of this report is to present procedures to determine DDF of precipitation for any location in Texas. This report updates previous DDF studies for Texas. For this report, precipitation durations of 15, 30, and 60 minutes; 1, 2, 3, 6, 12, and 24 hours; and 1,

2, 3, 5, and 7 days were investigated. The frequencies (expressed as recurrence intervals) range from 2 to 500 years. Selection of a bound on recurrence interval is difficult. In general, as recurrence interval increases, the accuracy of DDF estimate decreases. An upper recurrence interval of 500 years is considered reasonable since most hydraulic design criteria for engineered structures and controls incorporating DDF require recurrence intervals equal to or less than 500 years. The reciprocal of a recurrence interval is an exceedance probability. For example, a 100-year precipitation has an annual exceedance probability of 0.01, which by definition means that there is a 1-percent chance in each and every given year that this precipitation will be equaled or exceeded.

Accurate DDF analysis using data from any one station is difficult because the data for one station represent a poor spatial and (or) temporal sampling of precipitation. For example, storms occur over areas that might or might not contain a station; and generally, only short record is available at a single station. Additionally, the distribution of precipitation associated with any one station tends to be highly nonuniform. More accurate DDF estimates can be developed by "pooling" or "regionalizing" data from many nearby stations (see Stedinger and others, 1993, p. 18.33). The regionalization procedures used are explained in the "Regionalization of Precipitation Annual Maxima" section of this report. The procedures were developed using a data base of precipitation annual maxima for 173 (15-minute), 274 (hourly), and 865 (daily) National Weather Service (NWS) stations, each with at least 10 years of record in Texas. In total, about 3,030 cumulative years of record is available for the 15-minute stations, 10,160 years for the hourly stations, and 38,120 years for the daily stations.

Previous Studies

DDF information for the area of the United States east of the Rocky Mountains, including Texas, is available from two principal sources. The first source, commonly known as TP–40 (Hershfield, 1962), presents DDF for durations of 30 minutes to 24 hours and recurrence intervals of 2 to 100 years. The work of Hershfield was extended by Frederick and others (1977) and commonly is known as HYDRO–35. The HYDRO–35 study presents DDF for durations of 5 to 60 minutes and recurrence intervals of 2 to 100 years.

In recent years, other investigations of precipitation frequency have been conducted. Schaefer (1990) and Parrett (1997) presented precipitation frequency investigations based on the generalized extreme-value (GEV) distribution for Washington State and Montana, respectively. Also, the GEV distribution was selected by Huff and Angel (1992) to model the frequency of annual precipitation maxima for durations of 5 minutes to 10 days for the midwestern United States (Illinois, Indiana, Iowa, Kentucky, Michigan, Minnesota, Missouri, Ohio, and Wisconsin). For the western United States (Arizona, Nevada, New Mexico, Utah, and parts of California, Colorado, Idaho, Oregon, Texas, and Wyoming), the generalized Pareto distribution was selected to model the frequency of annual precipitation maxima for durations of 1 hour to 7 days (L.T. Julian, National Weather Service, written commun., 1997). The NWS study covers only a small part of the Texas Panhandle and the northern one-half of the Trans-Pecos region of West Texas. Wilks and Cember (1993) selected the Beta-P distribution to model the frequency of annual precipitation maxima for durations of 1 to 10 days for northeastern United States and southeastern Canada. Other studies of precipitation frequency, which are at or near completion, are for Canada (Younes Alila, University of British Columbia, Vancouver, Canada, written commun., 1998), for southern British Columbia (M.G. Schaefer, MGS Consultants, Lacey, Wash., written commun., 1998), and for Oklahoma (R.L. Tortorelli, U.S. Geological Survey, written commun., 1998).

Climate of Texas

The climate of Texas varies considerably across the State, and the climate for any given location in Texas is highly variable and nonuniform. This variability and nonuniformity is due in part to the influences of four principal types of air masses that periodically move through the State (Bomar, 1995). Two of these air masses generally are characterized as warm and moist. The "continental tropical" originates in the Pacific Ocean and moves into Texas from the west; and the "maritime tropical" originates in the Gulf of Mexico, southeast of Texas. The "maritime polar" and "continental polar," or Arctic, arrive from the northwest and north, respectively, and generally are characterized as cold and dry. Additionally, tropical cyclones, which also contribute to the climatic variability and nonuniformity, occasionally affect Texas during the summer and early fall. These cyclones have produced many daily

rainfall totals in excess of 20 inches (in.) for many locations in the State.

A comprehensive discussion of the climate and weather phenomenon in Texas is found in recent works by Bomar (1995) and by the Office of the State Climatologist (1987). A report by Carr (1967) also presents a discussion of the State's climate, and a discussion of climate change and related topics for Texas is presented by Norwine and others (1995).

The climatic characteristics of Texas magnify the two extremes of the hydrologic spectrum—floods and droughts. Destructive flooding, caused by excessive precipitation, occurs somewhere in the State nearly every year. Conversely, short- and long-term droughts also occur throughout the State. At least one drought has occurred in some part of Texas in the majority of decades of the 20th century (Bomar, 1995; Jones, 1991).

Many near-world-record precipitation events have occurred in Texas (World Meteorological Organization, 1986). For example, a total of 38.2 in. of rain fell in 24 hours during September 9–10, 1921, near Thrall [about 30 miles (mi) northeast of Austin]; a storm on May 31, 1935, near D'Hanis (about 40 mi west of San Antonio) produced 22 in. of rain in 2 hours 45 minutes; and about 10 in. of rain fell in 1 hour at New Braunfels (about 20 mi north of San Antonio) on May 11, 1972. These and other greatest precipitation depths in Texas are compared to the greatest worldwide precipitation depths (represented by an equation) in figure 1.

The number in parenthesis shown in figure 1 is the ratio of selected greatest-observed precipitation depths in Texas to the corresponding 100-year depth (derived from this report) for that locality. The greatest depths generally are documented at sites without systematic precipitation-recording stations. The maximum statewide 100-year depths shown in figure 1 were derived from this report.

In general, the maximum depths shown in figure 1 are larger than the maximum depths measured at precipitation stations. This observation is significant because it indicates that the potential exists for very large depths to be measured at precipitation stations in the future. Also, even with about 3,030; 10,160; and 38,120 cumulative years of data for the 15-minute, hourly, and daily stations, respectively, some of the largest depths have gone unrecorded by systematic data-collection activities because of limited spatial and (or) temporal sampling. A trend is indicated for maximum depths in Texas to approach world maximum depths as duration decreases. This trend could be caused by a physical upper limit (meteorologically affected) of precipitation potential for short durations or, possibly reflect the scantiness of short-duration data on a worldwide basis. Additionally, the large ratios of maximum-known to 100-year depths indicate that the potential exists for precipitation depths greatly in excess of those that can be reliably[1] estimated from available data. These depths have estimated recurrence intervals considerably greater than 1,000 years.

For purposes of investigation and scrutiny of the data, a regional division of the State is considered necessary. The regions used in this report represent those developed and used by the NWS (Bomar, 1995; Carr, 1967). However, for this study the southeastern boundary of the Edwards Plateau region was positioned one county farther southeast to incorporate Bexar, Comal, Hays, and Travis Counties. This alternative positioning is considered necessary because large storms in these counties are similar to those in adjacent counties to the northwest (Slade, 1986). Additionally, the Lower Valley (Rio Grande) region was combined with the South Texas region because of the lack of substantial precipitation data in the Lower Valley region due to its small geographic area. The climatic regions of Texas used in this study are shown in figure 2, with the Lower Valley also identified.

Data Base of Precipitation Annual Maxima

Data Sources

Information concerning precipitation data for 15-minute, hourly, and daily NWS stations is available through the National Climatic Data Center in Asheville, N.C. (Internet address <http://www.ncdc.noaa.gov/ncdc.html>). The precipitation annual maxima for the selected durations for the NWS stations were compiled

[1]"Reliability" in this context means that minor changes in (1) spatial and (or) temporal sampling of precipitation annual maxima, (2) distribution choice for modeling the frequency of annual maxima, or (3) method of sample summarization—that is, distribution parameter estimation—can lead to large differences in estimates for very large recurrence intervals. For example, the relative percent differences between 100-, 1,000-, and 10,000-year estimates from the generalized logistic and extreme-value distributions (fitted to a data set characteristic of annual maxima in Texas) are 5.5, 20, and 40 percent, respectively. The relative percent differences increase dramatically for large recurrence intervals although the generalized logistic and extreme-value distributions are closely related.

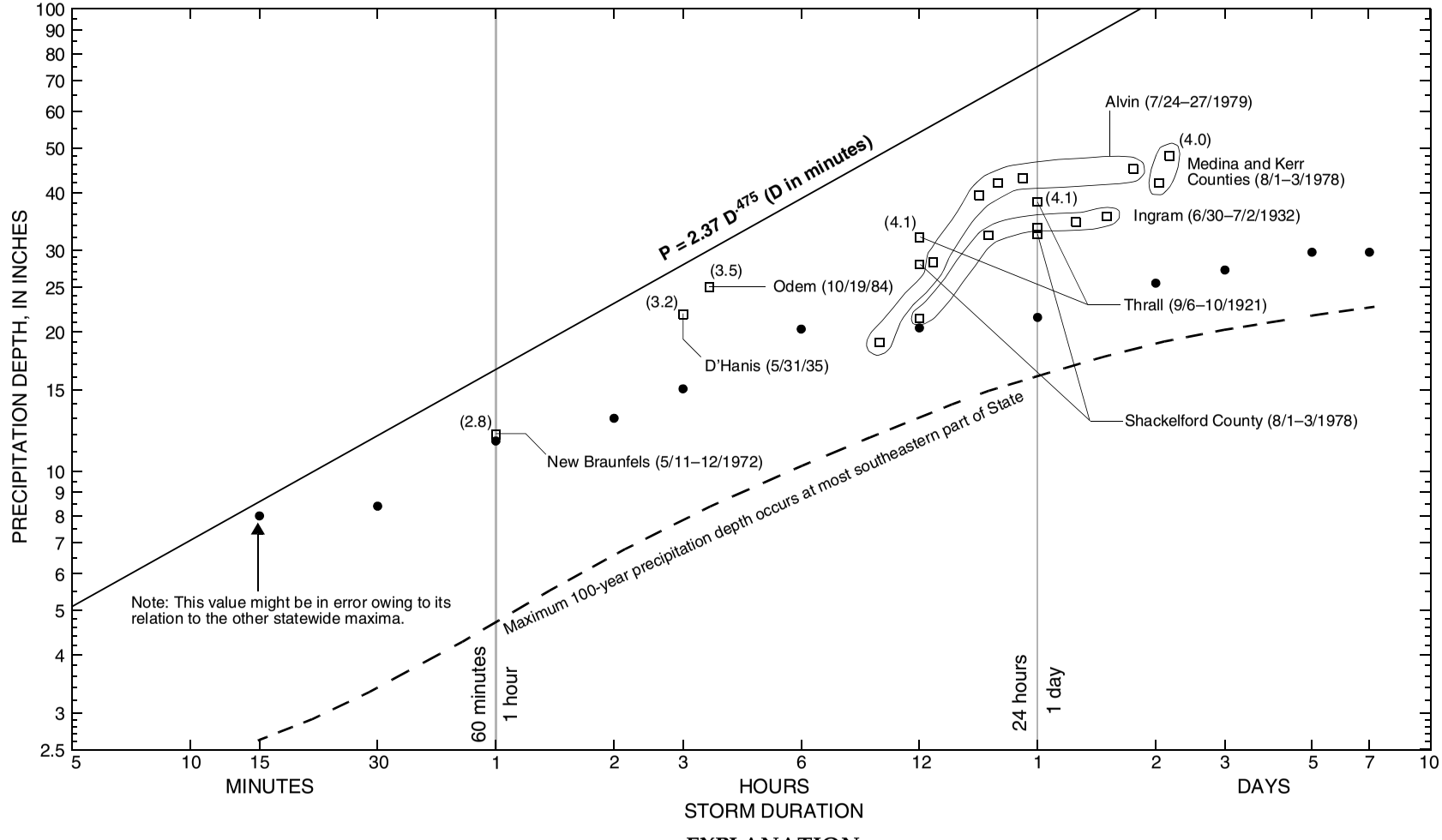

EXPLANATION

World maximum depth-duration relation (World Meteorological Organization, 1986)—Equation computes envelope curve

Maximum statewide 100-year precipitation depth—derived from depth-duration frequency analysis in report

Statewide maximum at recording precipitation stations for corresponding duration—derived from Texas precipitation data base

(2.8) **Selected greatest precipitation depths in Texas (John Patton, National Weather Service, written commun., 1996)**—Number in parenthesis is ratio of depth to 100-year depth for corresponding locality derived from depth-duration frequency analysis, figures 10–46

Figure 1. Relation between precipitation depth and storm duration for world record, Texas record, and Texas data-base maxima.

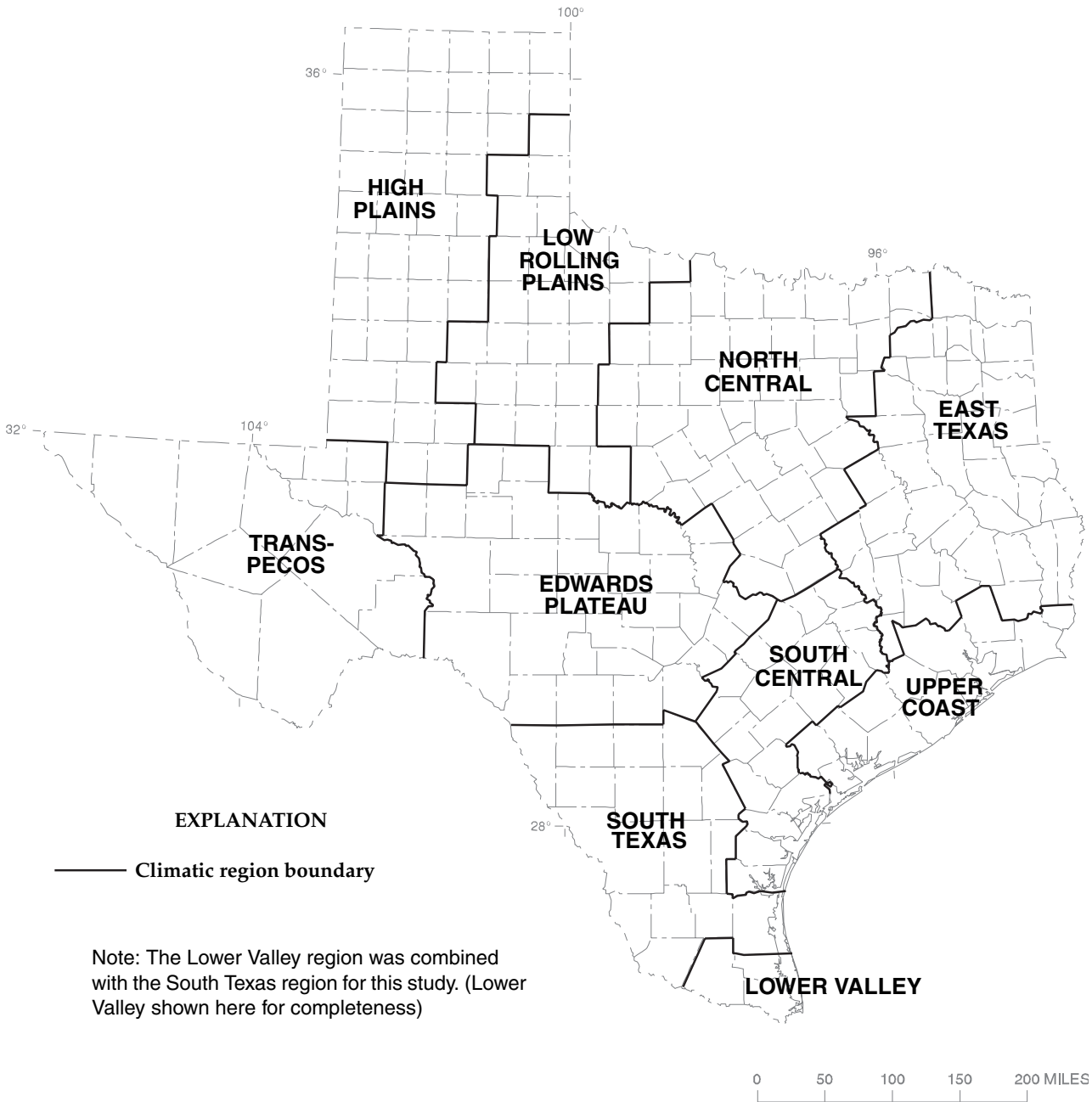

Figure 2. Modified National Weather Service climatic regions of Texas (modified from Carr, 1967).

by Hydrosphere Data Products, Inc. (1996). The 15-minute data generally are available for 1972–94. Hourly precipitation data generally are available for 1948–94. Daily precipitation data are available for about 1910–94. Additionally, the precipitation record was extended for nine hourly stations from data provided by the NWS (John Vogel, written commun., 1996).

The 15-, 30- and 60-minute annual maxima were compiled from the 15-minute data. The 1-, 2-, 3-, 6-, 12-, and 24-hour annual maxima were compiled from the hourly data; likewise, the 1-, 2-, 3-, 5-, and 7-day annual maxima were compiled from the daily data. To clarify potentially confusing terminology in this report, the term "60-minute" duration is associated with the aggregation of four consecutive 15-minute data values as opposed to the 1-hour data from a single value. Similarly, the term "24-hour" duration is associated with the aggregation of 24 consecutive 1-hour data values as

opposed to the 1-day data from a single value. For some years, the influence of missing record or deleted record caused inconsistencies in the availability of depths for all the durations. In these instances, the missing or deleted year was removed from the data base. Removal of some years did not greatly reduce the available precipitation data for Texas.

Only those stations that have at least 10 years of data were selected for inclusion in this study. The author believes that a minimum of 10 years of data for stations in Texas is needed before the data become representative of the true precipitation characteristics. A basis for the 10-year minimum record length is that droughts or periods of abundant rainfall in Texas seldom last more than 4 to 5 years. Therefore, using data with at least 10 years of record is an attempt to insure that the collected data are not unduly biased by the cyclical nature of the climate.

The 15-minute, hourly, and daily NWS stations used for this study are listed in the Appendices. The locations of the 15-minute, hourly, and daily stations are shown on plate 1.

Each of the three types of precipitation stations generally are uniformly distributed around the State; however, of the three, the daily precipitation stations have the densest network. The areal densities in stations per 1,000 square miles (mi^2) for each of the station types are 0.646, 1.02, and 3.23 for the 15-minute, hourly, and daily stations, respectively. The distribution of record length for each region and station type are shown in figure 3. The figure indicates that the record length is reasonably well distributed among the regions for each of the station types. However, there are clear differences in the record availability between the station types. In general, the daily stations have the longest records of the three station types; whereas, the 15-minute stations have the shortest records.

To illustrate the inherent variability of a series of 1-day precipitation annual maxima, graphs are shown for each climatic region using data from a long-term station (figs. 4–6). Similar variability is indicated by graphs of the 15-minute and hourly stations (not included in this report). Additionally, figures 4–6 show the median and mean beginning and ending years of daily precipitation stations for each climatic region.

Occasionally an existing station is relocated to a nearby site, and new stations might be established near an existing station. If the distance between two or more stations is small, then their records were assumed equivalent and combined into one longer record. Geographic proximity (about 3 mi north to south or 2 mi east to west) is the basis for combining the records of a few stations. For this study, (1) the records of 8 fifteen-minute stations were combined into 4 records; (2) the records of 30 hourly stations were combined into 15 records; and (3) the records of 47 daily stations were combined into 23 records. The combined records are not separately identified; however, they can be determined from the station names in the Appendices.

Correction of Precipitation Annual Maxima for Fixed-Interval Recording

The ratios of 60-minute to 1-hour maxima and 24-hour to 1-day maxima were analyzed. Both the 1-hour and 1-day maxima generally are less than the 60-minute and 24-hour maxima, respectively, because the 1-hour and 1-day maxima are collected on a fixed-interval basis (beginning to end of each hour or midnight to midnight); whereas, the 60-minute and 24-hour maxima are determined with four consecutive or "moving" 15-minute windows or 24 consecutive 1-hour windows, respectively. In total, 170 stations have concurrent 15-minute (therefore 60-minute) and hourly maxima, which comprise about 2,900 values; and 144 stations have concurrent hourly (therefore 24-hour) and daily maxima, which comprise about 4,800 values. A 60-minute to 1-hour weighted-mean ratio of 1.13 [weighted standard deviation (SD) = 0.054] and a 24-hour to 1-day weighted-mean ratio of 1.13 (weighted SD = 0.082) were determined for the entire State. The weighting is based on record length for each station. The spatial distribution of the two mean ratios was investigated. The mean ratios show no apparent spatial dependence.

Weiss (1964) considered the ratio of true to fixed-interval maxima on the basis of probability theory and determined a theoretical "correction" factor of 1.143 for the true 60-minute to hourly maxima and for the true 24-hour to daily maxima. Miller and others (1973) used an empirically derived factor of 1.13. Both factors are either reasonably close to or match those determined for this report. On a conceptual basis, both empirical factors from this report would be expected to be slightly less than the theoretical factor because both the 60-minute and 24-hour maxima were developed from finite samples (15-minute or 1-hour intervals) and therefore are biased slightly downward themselves.

However, it is possible that Weiss's corrections are too large, given that 1.13 has been determined by

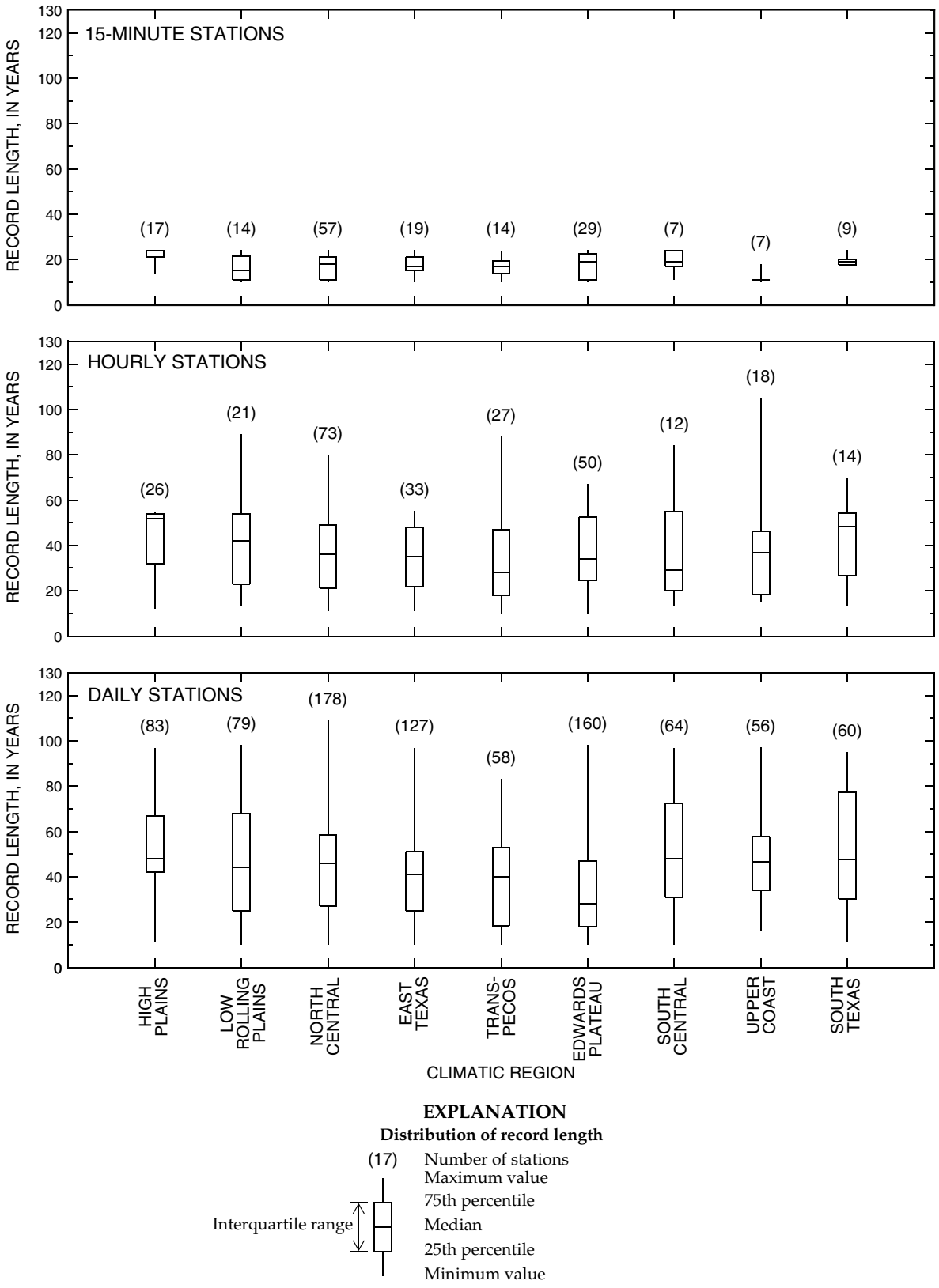

Figure 3. Record-length distribution for 15-minute, hourly, and daily precipitation stations in climatic regions of Texas.

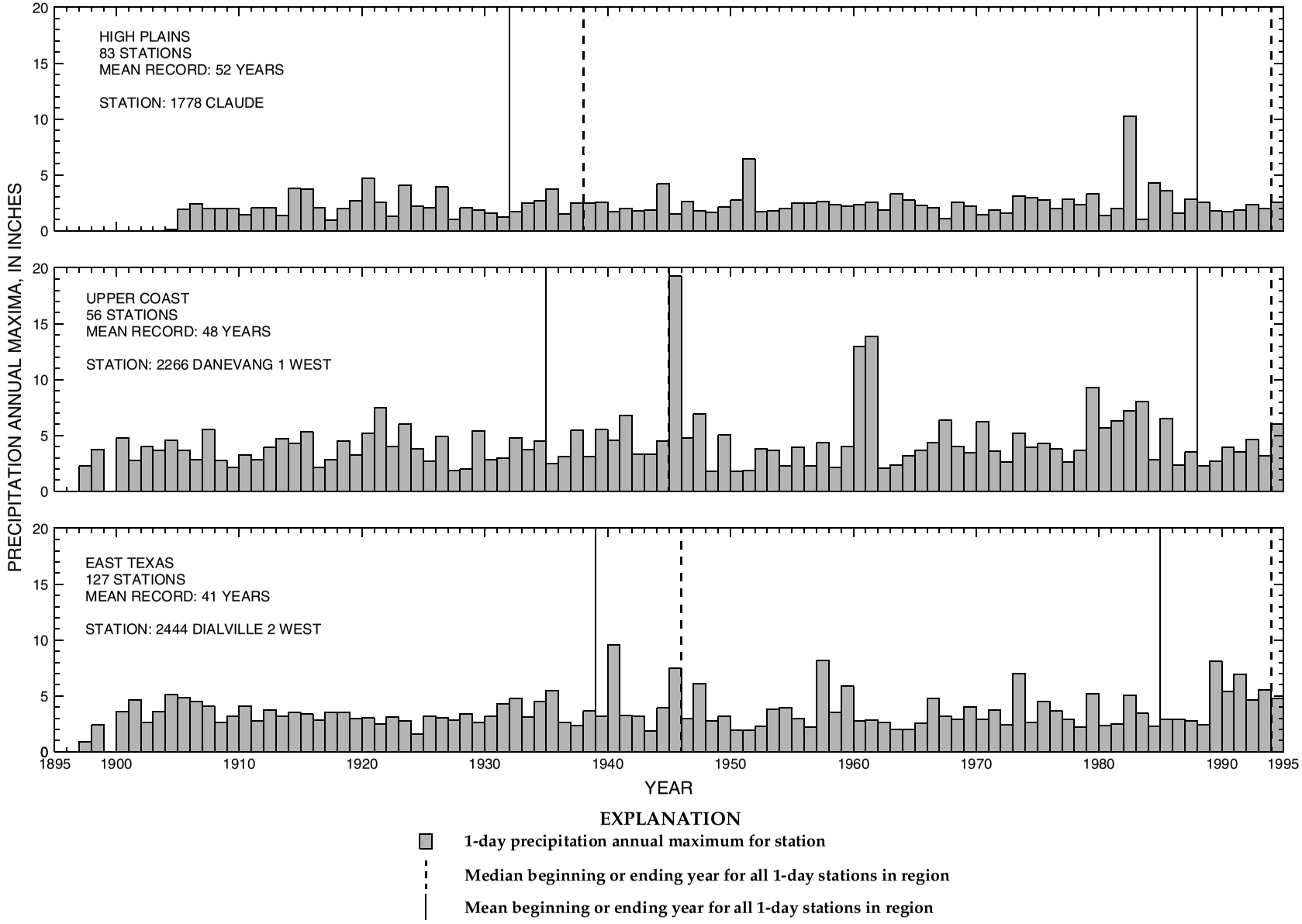

Figure 4. Time series of 1-day precipitation annual maxima for long-term stations (1778, 2266, and 2444) and distribution of available record in corresponding climatic regions of Texas.

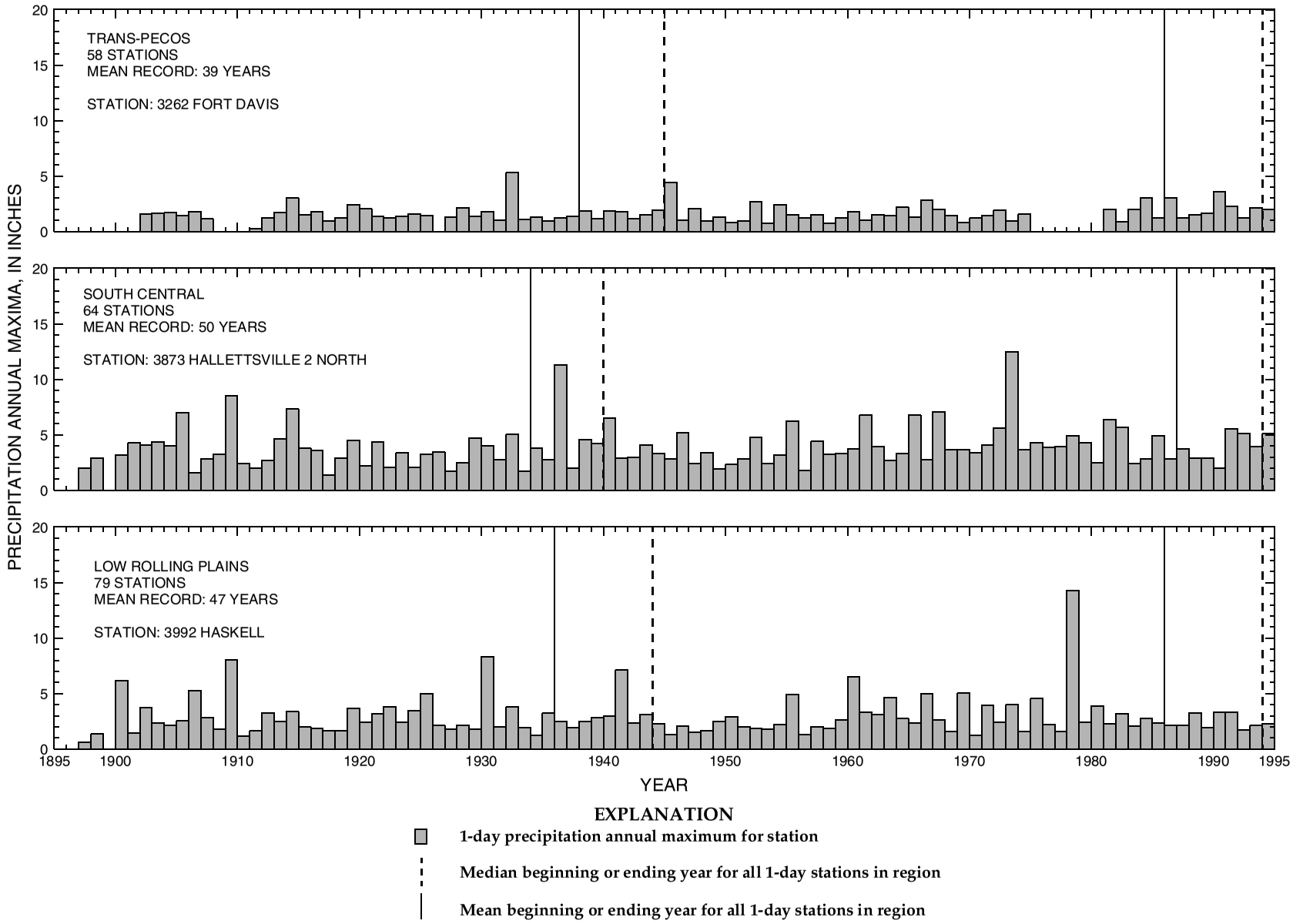

Figure 5. Time series of 1-day precipitation annual maxima for long-term stations (3262, 3873, and 3992) and distribution of available record in corresponding climatic regions of Texas.

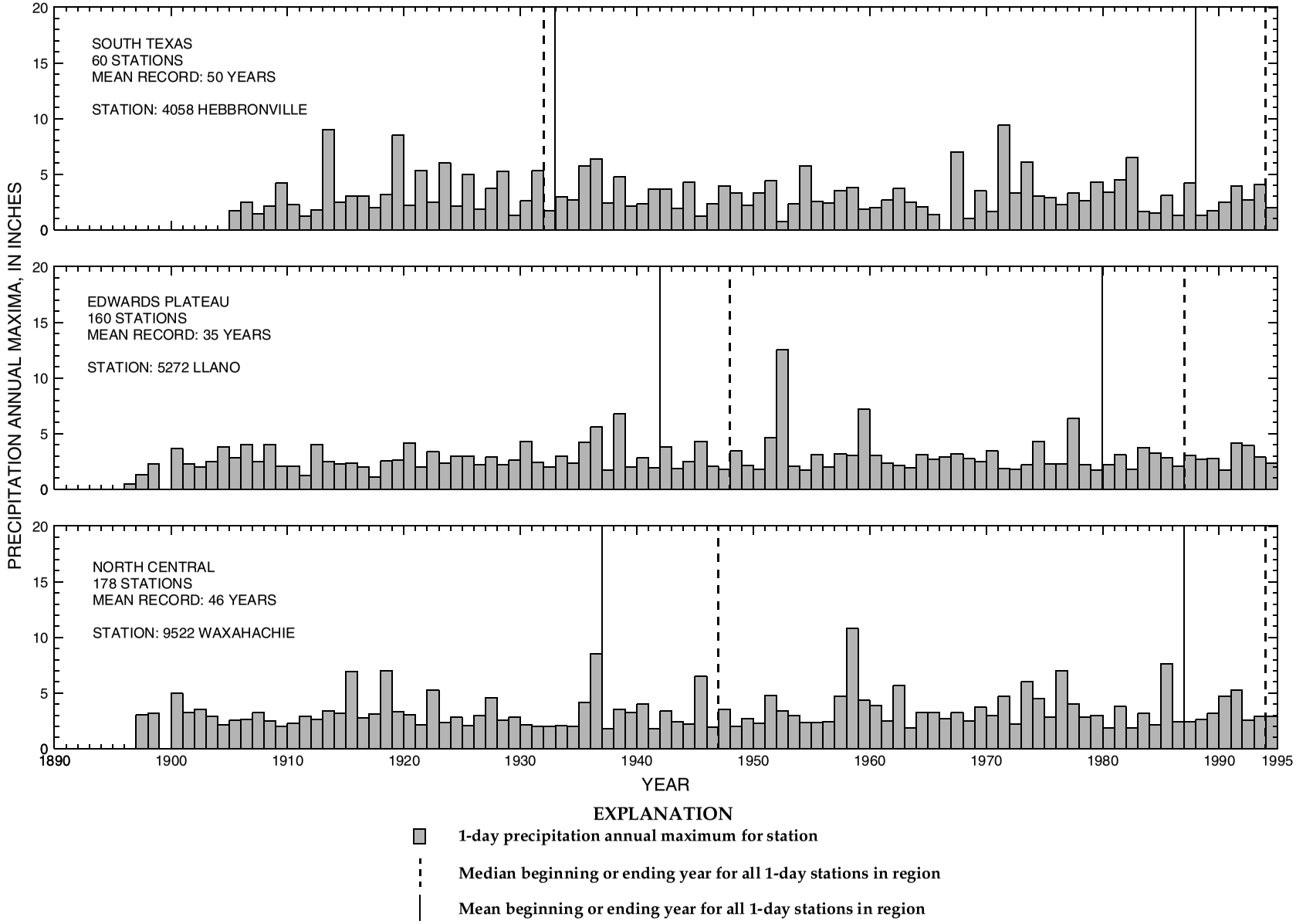

Figure 6. Time series of 1-day precipitation annual maxima for long-term stations (4058, 5272, and 9522) and distribution of available record in corresponding climatic regions of Texas.

Table 1. Correction factors for mean annual maxima of precipitation

[Note: Correction factors (Weiss, 1964) are from the equation {n/n – 0.125}, where n is the number of subintervals for a given duration; min, minutes; n/a, empirical correction factor not determined for this report; hr, hours]

Duration (variable)	Corresponding fixed intervals or time steps	No. subintervals	Weiss correction factor[1] (dimensionless)	Empirical correction factors for Texas (dimensionless)
15 min	15 min	1	1.143	n/a
30 min	do.	2	1.067	n/a
60 min	do.	4	1.032	n/a
1 hr	1 hr	1	1.143	1.13
2 hr	do.	2	1.067	n/a
3 hr	do.	3	1.044	n/a
6 hr	do.	6	1.022	n/a
12 hr	do.	12	1.011	n/a
24 hr	do.	24	1.005	n/a
1 day	1 day	1	1.143	1.13
2 days	do.	2	1.067	n/a
3 days	do.	3	1.044	n/a
5 days	do.	5	1.026	n/a
7 days	do.	7	1.018	n/a

[1] Weiss, 1964.

others, and 1.13 was determined for this report. This difference (between 1.143 and 1.13) might be due to Weiss's assumption that the probability of a storm event occurring is equal throughout any time interval and the assumption that the distribution of precipitation during the time interval is uniform. In reality, in the Panhandle and West Texas, large storms occur more frequently during the late afternoon and early evening; while in Central Texas, large storms frequently occur at night. Disregarding Weiss's assumptions could produce slightly smaller correction factors. However, the percent change of 1.143 to 1.13 is only about –1.1 percent. The theoretical correction factors developed by Weiss were used for this study because of (1) the small difference between Weiss's 1.143 and Miller's empirical 1.13 and (2) the fact that corrections were needed for the 15-, 30-, and 60-minute durations and for durations greater than 1 hour or 1 day. The correction factors are applicable only on the mean annual maxima for a given duration and are not actually applied to the individual data points (Weiss, 1964, p. 79). The theoretical correction factors from Weiss (1964), pertinent to this study, are listed in table 1. Schaefer (1990, p. 127) concludes that correction factors such as Weiss's or Miller's affect only the location (mean) and scale (SD) measures of a given data set and do not affect higher measures of the data such as shape (skew). The adjustment to the scale measure of the annual maxima is discussed later in the "Spatial Averaging of L-coefficient of Variation and L-skew and Estimation of L-scale" section.

Acknowledgments

The author expresses his gratitude to Sue Giller and Ben Hardison of Hydrosphere Data Products, Inc., for their compilation (on diskette) of precipitation annual maxima for the identified durations and to John Vogel of the NWS for providing some noncomputer-stored hourly data. Furthermore, the author expresses his gratitude to the thorough and timely review of early drafts by Mel Schaefer of MSG Consultants, and Charles Parrett and Robert Tortorelli of the USGS.

REGIONALIZATION OF PRECIPITATION ANNUAL MAXIMA

The concept of "regionalization" in the context of a precipitation frequency analysis is the process by which the precipitation characteristics surrounding a particular station are combined or "pooled together" to develop more accurate statistical summaries of precipitation characteristics than can be derived from a single station. Additionally, once regionalization is completed, precipitation frequency can be estimated for locations other than precipitation stations.

The underlying assumption of the regionalization approach adopted for Texas is that the parameters of the distribution selected to model the frequency of annual maxima can be expressed as either spatially continuous variables or as single statewide means. A parameter is considered expressible by contours on a map (instead of a single statewide mean) provided that the root mean square error (RMSE) associated with the mapped contours of a parameter is appreciably smaller than the statewide SD of the parameter. If the percent decrease from the statewide SD to the RMSE is not at least 15 percent, then a contour map is considered no better than a single statewide mean. A tenet of the underlying assumption is that a single distribution is appropriate for modeling the frequency of annual maxima for a given duration.

The five primary elements of the regionalization approach of precipitation annual maxima for this report are (1) to compute the L-moment statistics for each station and determine an appropriate distribution for modeling the frequency of annual maxima; (2) to improve the estimation of the L-coefficient of variation and L-skew by spatial averaging; (3) to estimate a corrected L-scale from the product of the corrected mean depth and the spatially averaged L-coefficient of variation; (4) to transform the L-moment statistics to the parameters of the distribution; and (5) to contour the parameters using "spatial interpolation" based on the geostatistical method of kriging to produce maps that depict the magnitude and spatial variation of the parameters. The precipitation depth (X) for a specified nonexceedance probability (F) and duration (d) for any location in Texas is determined by obtaining the distribution parameters from the contour maps and computing the quantiles, $X_d(F)$, from the equation defining the distribution.

L-moments

This section presents a brief introduction to the theory of L-moments and the technique for selecting an appropriate probability distribution. Comprehensive discussion pertinent to L-moments, their historical development, and distribution selection can be found in Hosking (1986, 1990), Hosking and Wallis (1993, 1997), and Vogel and Fennessey (1993).

Consider a random variable X (precipitation depth in this report) with a cumulative probability distribution function F (nonexceedance probability). The quantities

$$M_{ijk} = E[X^i F^j (1-F)^k] = \int_0^1 X^i F^j (1-F)^k dF, \quad (1)$$

where E = the expectation operator, are known as probability-weighted moments (PWM) as defined by Greenwood and others (1979). By letting $M_{ijk} = M_{1r0}$, the PWM for moment r can be expressed as

$$\beta_r = E[XF^r]. \quad (2)$$

An unbiased sample estimate of β_r (PWM) for any distribution is computed from the following (Landwehr and others, 1979):

$$b_r = \frac{1}{n} \sum_{j=1}^{n-r} \left[\frac{\binom{n-j}{r}}{\binom{n-1}{r}} \right] x_j, \quad (3)$$

where

b_r = unbiased sample estimate of β_r for moment number $r = 0, 1, 2, \ldots$ and

$x_{(j)}$ = ordered values of X where $x_{(1)}$ is the largest observation and $x_{(n)}$ is the smallest.

In a sense, the PWM are somewhat analogous to the more widely known product moments (mean, SD, coefficient of variation, skew, kurtosis). For example, b_0 is equal to the mean; however, interpretation of the higher-order PWM is difficult. To facilitate PWM interpretation, Hosking (1986, 1990) developed L-moments as specific linear combinations of the PWM. Unbiased L-moment sample estimates are obtained by substituting the sample estimates of β_r into the following equation:

$$\lambda_{r+1} = \sum_{k=0}^{r} \beta_k (-1)^{r-k} \binom{r}{k} \binom{r+k}{k}. \quad (4)$$

The L-moments can be formulated into values that are exactly analogous, though not equal, to the product moments (Hosking, 1990). The mean, scale, coefficient of variation, skewness, and kurtosis of a distribution estimated using equation 4 are expressed by the following L-moments (λ_r) and L-moment (τ_r) ratios:

$$\lambda_1 \equiv \text{mean, and } \lambda'_1 \equiv 1.022(\lambda_1) \text{ corrected mean (Weiss, 1964);} \quad (5)$$

$$\lambda_2 \equiv \text{L-scale;} \quad (6)$$

$$\tau_2 = \frac{\lambda_2}{\lambda_1} \equiv \text{L-coefficient of variation (L–CV);} \quad (7)$$

$$\tau_3 = \frac{\lambda_3}{\lambda_2} \equiv \text{L-skew; and} \quad (8)$$

$$\tau_4 = \frac{\lambda_4}{\lambda_2} \equiv \text{L-kurtosis.} \quad (9)$$

For this report, the L-moments and the L-moment ratios were calculated for each duration and for each station using unbiased estimators. The use of the unbiased estimators for L-moment computation decreases the chance of selecting an inappropriate distribution to fit to a given data set (Hosking and Wallis, 1995, p. 2,024).

L-moment ratio diagrams allow simple comparisons between the sample estimates of τ_3 and τ_4 and their theoretical counterparts from selected distributions. Discussion of L-moment ratio diagrams is available in the previously identified sources at the beginning of this section and others in the "Selected References." Vogel and Fennessey (1993) demonstrated the significant differences between product-moment ratio diagrams (skew and kurtosis) and L-moment ratio diagrams; furthermore, they concluded that L-moment ratio diagrams always should be preferred over product-moment ratio diagrams for distribution selection.

The relation between values of τ_3 and τ_4 and weighted-mean values of τ_3 and τ_4 for the State to the theoretical τ_3 and τ_4 relations (Hosking, 1991b) from the generalized extreme value (GEV), generalized logistic (GLO), and log-normal distributions are shown in figure 7. The gray points represent the τ_3 and τ_4 for each station. The scatter around the cluster of regional (weighted) means and around the single statewide (weighted) mean, in general, represents sampling variability—that is, stations with long record are more likely to have τ_3 and τ_4 that plot closer to the cluster of regional means and to the single statewide mean. The generalized Pareto and Pearson Type III distributions (Hosking, 1990; Stedinger and others, 1993) were evaluated, and the τ_3 and τ_4 relation from the data was found to be clearly different from the generalized Pareto and Pearson Type III distributions. Therefore, the generalized Pareto and Pearson Type III distributions are not shown in figure 7. Figure 7 indicates that the data for the corresponding weighted mean of τ_3 and τ_4 generally plot between the GLO and GEV distributions. The figure further indicates that the data for 15-minute duration and the corresponding weighted values of τ_3 and τ_4 cluster around the GLO distribution; and the data for the 7-day duration and the corresponding weighted values cluster around the GEV distribution. Additionally, there exists a steady trend away from the GLO to the GEV distribution as duration increases, as shown by the movement of the weighted-mean statewide data point as duration increases. This trend is supported in similar L-moment ratio diagrams (not reported here) for the durations not shown in figure 7. The log-normal distribution can be dismissed on the basis of its general relation to the data points.

From the L-moment ratio diagrams, the author concludes that the distribution shifts from GLO like to GEV like between the 12-hour and 1-day duration. Although a change from the GLO to GEV distribution is observed between the 12-hour and 1-day duration, determination of an exact duration for which the change occurs is difficult. Therefore, the GLO distribution was selected for durations up to and including 24 hours, and the GEV distribution was selected for durations of 1 day or more.

Goodness-of-fit measures (Z-statistics) of the GLO and GEV distributions were computed for each duration following the methods of Hosking and Wallis (1993) by considering the entire State as a single region (see weighted statewide mean in fig. 7). The Z-statistics of the GLO and GEV distributions of each duration are listed in table 2. The Z-statistics of the GLO distribution are less than those of the GEV distribution for 15 minutes to 24 hours, whereas the Z-statistics of the GEV distribution are smaller than those of the GLO distribution for 1 to 7 days.

The goodness-of-fit measure can be interpreted in two ways. The first interpretation (Hosking and Wallis, 1993) is that a distribution is considered appropriate if the absolute value of the Z-statistic is less

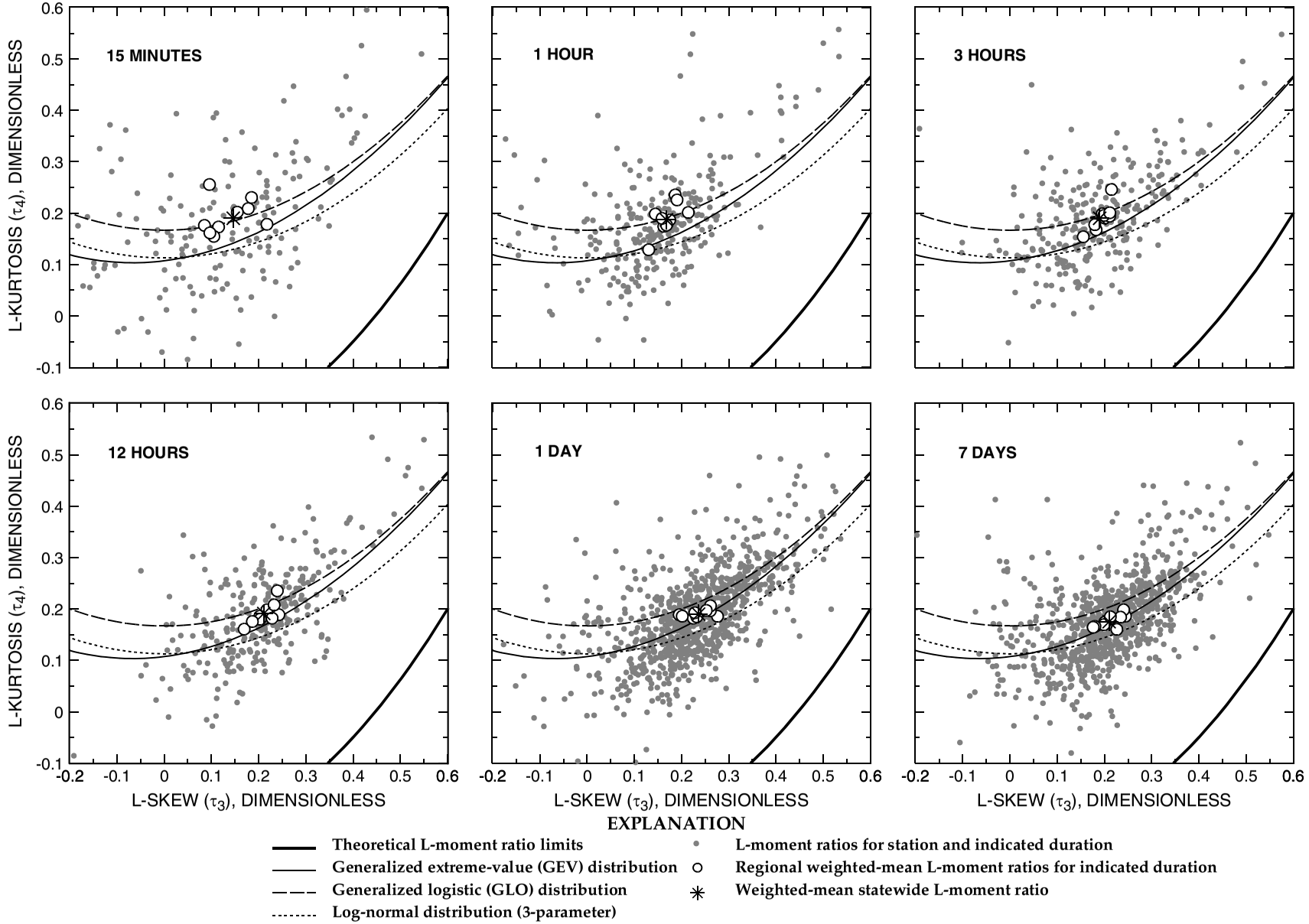

Figure 7. L-moment ratio diagrams for selected precipitation durations in Texas.

Table 2. Summary of goodness-of-fit and heterogeneity measures for Texas

[GLO, generalized logistic distribution; GEV, generalized extreme-value distribution; min, minutes; hr, hours]

Duration (variable)	Data-base source	No. of stations	Goodness-of-fit measure (Z-statistic[1])		Heterogeneity measure (H-statistic[1])
			GLO	GEV	
15 min	15-minute stations	173	–2.0	–7.1	4.4
30 min	do.	do.	2.1	–3.8	4.8
60 min	do.	do.	2.0	–3.4	2.3
1 hr	Hourly stations	274	–.17	–9.1	12
2 hr	do.	do.	.83	–7.8	9.4
3 hr	do.	do.	.35	–7.8	8.3
6 hr	do.	do.	.62	–6.9	6.5
12 hr	do.	do.	1.5	–6.0	5.4
24 hr	do.	do.	2.2	–5.2	4.5
1 day	Daily stations	865	7.6	–6.0	9.7
2 days	do.	do.	7.3	–6.6	12
3 days	do.	do.	8.3	–6.0	13
5 days	do.	do.	8.8	–6.1	14
7 days	do.	do.	11	–4.8	16

[1] Hosking and Wallis, 1993.

than about 1.64; this interpretation has validity only if the region containing the data is "homogeneous" (see Hosking and Wallis, 1993, 1997). Homogeneous is interpreted to mean that, except for a location-specific scaling factor, (1) the form of the distribution for the homogeneous region is known, and (2) the distribution is exactly defined (defined by specification of its parameters). The heterogeneity measures (H-statistic) for the entire State were computed for each duration following the methods of Hosking and Wallis (1993). The H-statistics (table 2) are larger than 2.0, which Hosking and Wallis (1993, p. 275) conclude is indicative of a heterogeneous region; thus, strict interpretation of the goodness-of-fit measure is questionable. The second interpretation of the goodness-of-fit is that the form of the distribution with the smallest Z-statistic is considered appropriate, but the distribution parameters might require additional specification. Applying the second interpretation to the Z-statistics (table 2), the GLO distribution is judged appropriate for annual maxima for durations of 15 minutes to 24 hours; whereas the GEV distribution is judged appropriate for annual maxima for durations of 1 to 7 days. Various geographic regions much smaller in areal extent than Texas were delineated, and the goodness-of-fit and heterogeneity measures were computed. Frequently, regions with areal extents less than about 10 percent of the total area of Texas show (1) H-statistics close to 1.0 (thus, near homogeneous), (2) absolute values of Z-statistics of the GLO distribution less than about 1.64 for the 15-minute to 24-hour durations, and (3) absolute values of Z-statistics of the GEV distribution less than about 1.64 for the 1- to 7-day durations.

The previous studies, TP–40 (Hershfield, 1962) and HYDRO–35 (Frederick and others, 1977), each used the two-parameter Gumbel distribution, which is a special case of the GEV distribution, where τ_3 and τ_4 are equal to 0.1699 and 0.1504, respectively (Stedinger and others, 1993, p. 18.9). Either the GLO or GEV distribution fits the data better than the Gumbel distribution because the Gumbel distribution, which plots as a single point in figure 7 (but is not shown for clarity), is

not as close to the data as the GLO or the GEV distributions. The two-parameter Gumbel distribution is not as "flexible" for fitting to data having different τ_3.

The investigation of precipitation frequency in Washington (Schaefer, 1990) determined that the GEV distribution was appropriate for durations of 2, 6, and 24 hours, although subsequent investigation by Schaefer (1993) determined that the four-parameter Kappa distribution (Hosking, 1994) was a better choice[2]. The investigations of precipitation frequency by Huff and Angel (1992) and Parrett (1997) determined that the GEV distribution was appropriate for durations of 1 or more days for the midwestern United States and Montana, respectively.

Generalized Logistic and Generalized Extreme-Value Distributions

The GLO distribution (Hosking, 1990) was selected as appropriate for the entire State and for durations of 15 minutes to 24 hours. Computation of the precipitation depth for a given frequency, $X_d(F)$, from the GLO distribution is as follows:

$$X_d(F) = \xi + \frac{\alpha}{\kappa}\left\{1 - \left[\frac{(1-F)}{F}\right]^{\kappa}\right\}, \qquad (10)$$

where

ξ, α, and κ = location, scale, and shape parameters, respectively, of the GLO distribution, and

F = annual nonexceedance probability, 1 – exceedance probability, or $[1 - (1/T)]$ where T is recurrence interval.

Alternatively, if a storm depth for a given duration is known, the storm's point nonexceedance probability can be estimated by the following inversion of equation 10:

$$F = \frac{1}{1 + \left\{1 - \frac{\kappa}{\alpha}[X_d(F) - \xi]\right\}^{1/\kappa}}. \qquad (11)$$

Equations for estimating the parameters of the GLO distribution are in Hosking (1990). The parameters of the GLO distribution are estimated from L-moments by the following:

$$\kappa = -\tau_3; \qquad (12)$$

$$\alpha = \frac{\lambda_2}{\Gamma(1+\kappa)\Gamma(1-\kappa)}, \qquad (13)$$

where

$\Gamma(-)$ = the gamma function;

$$\xi = \lambda_1 + \frac{(\lambda_2 - \alpha)}{\kappa}. \qquad (14)$$

The ξ parameter of the GLO distribution describes the location of the distribution and is interpreted as the median depth, or alternatively, as the 2-year depth for a given duration. The scale and shape of the distribution are described by α and κ, respectively. Both ξ and α have units of inches, and κ is dimensionless.

The GEV distribution (Stedinger and others, 1993, p. 18.16–19) was selected as appropriate for the entire State for 1-day and greater durations. Computation of $X_d(F)$ from the GEV distribution is as follows:

$$X_d(F) = \xi + \frac{\alpha}{\kappa}\{1 - [-ln(F)]^{\kappa}\}, \qquad (15)$$

where

ξ, α, and κ = location, scale, and shape parameters, respectively, of the GEV distribution; and

$ln\,(F)$ = natural logarithm of annual nonexceedance probability.

Alternatively, if a storm depth for a given duration is known, the storm's "point" annual nonexceedance probability can be estimated by the following inversion of equation 15:

$$F = e^{-\left\{1 - \frac{\kappa}{\alpha}[X_d(F) - \xi]\right\}^{1/\kappa}}. \qquad (16)$$

[2] The four-parameter Kappa distribution is a more flexible distribution than the three-parameter distributions. On an L-moment ratio diagram, the Kappa distribution plots as an area, not a line, and therefore can take on τ_3 and τ_4 values between the theoretical GLO and GEV distribution lines (Hosking, 1994). The four-parameter Kappa distribution was considered briefly for this report; however, it was not chosen because (1) its use requires the specification of another parameter and (2) the differences between these three distributions (GLO, GEV, and Kappa) are mitigated by the upper recurrence interval bound of 500 years.

Equations for estimating the parameters of the GEV distribution are presented in Hosking (1990). The parameters of the GEV distribution are estimated from L-moments by the following:

$$Z = \frac{2}{(3+\tau_3)} - \frac{ln(2)}{ln(3)}, \quad (17)$$

$$\kappa \approx 7.8590Z + 2.9554Z^2, \quad (18)$$

$$\alpha = \frac{\lambda_2 \kappa}{(1-2^{-\kappa})\Gamma(1+\kappa)}, \quad (19)$$

$$\xi = \lambda_1 + \frac{\alpha}{\kappa}\{\Gamma(1+\kappa) - 1\}. \quad (20)$$

The GEV distribution parameters (ξ, α, and κ) are somewhat analogous to their counterparts in the GLO distribution. However, ξ in the GEV distribution is not interpreted as the median depth because of the different formulation of the GEV distribution from the GLO distribution. Both ξ and α have units of inches, and κ is dimensionless.

Spatial Averaging of L-coefficient of Variation and L-skew and Estimation of L-scale

The values for τ_2 and τ_3 were spatially averaged in an effort to (1) reduce the random component in their values and (2) improve the accuracy of their estimates. Also, averaging τ_2 and τ_3 has the desirable effect of reducing the influence of any one station on the eventual contouring of the ξ, α, and κ parameters. Efficient investigation of "discordant" data (see Hosking and Wallis, 1993, p. 272–273) within the entire data base was not feasible because of the large number of stations and durations—in total, some 261,000 individual data values. The first L-moment, the mean, was not spatially averaged because (1) the mean depths exhibit very strong spatial dependence and (2) the estimates of the mean depth of each station are the most accurate of the λ_2, τ_2, and τ_3 statistics.

A formal justification and development of the spatial-averaging method involves the following relation:

$$\Phi^S{}_i(x,y) = \Phi^T{}_i(x,y) + \Phi^N{}_i(r), \quad (21)$$

where

$\Phi^S{}_i(x,y)$ = the value of τ_2 or τ_3 for station i at location (x,y);

$\Phi^T{}_i(x,y)$ = the "true" but always unknown value of τ_2 or τ_3 for station i; and

$\Phi^N{}_i(r)$ = the unknown random component of τ_2 or τ_3, which is a function of record length (r) at the station (with a model-error component included).

In equation 21, $\Phi^T{}_i(x,y)$ is a constant for the location (x,y), whereas both $\Phi^S{}_i(x,y)$ and $\Phi^N{}_i(r)$ are random variables. The references to spatial location and record length in equation 21 are dropped without a loss of generality, and $\Phi^T{}_i$ is computed as:

$$\Phi^T{}_i = \Phi^S{}_i - \Phi^N{}_i. \quad (22)$$

Continuing, assume that $\Phi^T{}_i$ is fixed within the area defined by n neighboring stations (call this the neighborhood or "mini" region). Specifically, the station of interest is $i = 1$, the first nearest station is $i = 2$, the farthest station is $i = n$; thus, the neighborhood contains n stations:

$$\Phi^T{}_1 = \Phi^T{}_2 = \Phi^T{}_3 = \Phi^T{}_4 = \Phi^T{}_n. \quad (23)$$

When $\Phi^T{}_i$ is assumed fixed, $\Phi^T{}_i$ becomes spatially constant on small geographic scales. On large geographic scales, this assumption is not true; however, if the neighborhood is small, then the gradient of $\Phi^T{}_i$ is close to zero, and $\Phi^T{}_i$ can be considered constant. Reformulating equation 22 for a neighborhood of five stations ($n = 5$) yields

$$5\Phi^T = \sum_{i=1}^{5} (\Phi^S{}_i - \Phi^N{}_i). \quad (24)$$

Next, expand the terms in the summation in equation 24:

$$\Phi^T = \frac{1}{5}\sum_{i=1}^{5} \Phi^S{}_i - \frac{1}{5}\sum_{i=1}^{5} \Phi^N{}_i. \quad (25)$$

If the expected value of Φ^N is zero, then the expected value of Φ^T becomes the mean of $\Phi^S{}_i$. However, consider that the random components are time biased; that is, as record length (r) gets large, $\Phi^N{}_i$ must get small because $\Phi^S{}_i$ must approach $\Phi^T{}_i$. Therefore, it is practical to incorporate record length as a weighting factor on $\Phi^S{}_i$:

$$\Phi^T = \frac{\sum_{i=1}^{n} r_i \Phi^S_i}{\sum_{i=1}^{n} r_i}. \quad (26)$$

The choice of the weights in equation 26 is somewhat arbitrary. Other weights could have been chosen, such as those based upon separation distance from station $i = 1$ to station $i = n$ or those based on cross correlations in the data.

Equation 26 represents the spatial averaging method used on τ_2 and τ_3 where n represents the number of nearest (neighborhood) stations to average together. Equation 26 is equivalent to the regional moment estimation equation frequently seen in "index-flood" regional analyses (for example, Hosking and Wallis, 1993, p. 271, eq. 2). Because equation 26 is applied to each duration and each station in the data base, the approach here can be considered a "moving index-flood." The spatially averaged τ_2 and τ_3 are represented by the following:

$$\tau'_2 = \text{spatially averaged L–CV, and} \quad (27)$$

$$\tau'_3 = \text{spatially averaged L-skew.} \quad (28)$$

If $n = 1$ in equation 26, then no averaging takes place and τ'_2 and τ'_3 are equal to the values for each station; likewise, if n equals the total number of stations ($n = 173$, 274, or 865), the computed values are weighted statewide means. The assumption that Φ^T_i is constant weakens as n gets larger. To determine an appropriate value for n, various values of n were tried, and the effects of different n values were evaluated on the basis of changes in the geographic distribution of τ_2 and τ_3 and the overall reduction in statewide variance for τ_2 and τ_3. A value of $n = 5$, which corresponds to a "mini" region containing five stations being generated for each station, was selected as appropriate. Values of n much greater than about 8 had the effect of severely reducing the variance of τ_2 and τ_3 across the State and obscuring local variations.

The effects of spatial averaging on the statewide distributions of τ_2 and τ_3 are shown in figures 8 and 9. The spatial averaging of τ_2 and τ_3 results in an appreciable reduction in the interquartile range (IQR); and the deviations of values outside the IQR are largely reduced. The median values remain nearly the same after averaging, suggesting that the values for τ_2 and τ_3 have not been unduly biased.

The bottom graph of figure 8 illustrates the effects of the spatial averaging on τ_2. The median of τ'_2 increases steadily as the duration increases from 15 minutes to about 24 hours. (The 15- and 30-minute medians are about equal.) The median of τ'_2 takes a downward step from 24 hours to 1 day, after which the median of τ'_2 is nearly constant. The origin of this step trend is unknown. The IQR and the deviations of values outside the IQR are greatly reduced. Also, after spatial averaging (bottom graph), the deviation of values greater than the IQR is similar to the deviation of values less than the IQR, suggesting that a more normal-like distribution of τ_2 has been generated.

Analogous to figure 8, the effects of the spatial averaging on the statewide distribution of τ_3 are shown in figure 9. The top graph of figure 9 illustrates that the median of τ_3 increases with increasing duration from the 30-minute to 1-day duration and then levels off somewhat (or possibly declines). The top graph also illustrates that the IQR is larger for the 15- to 60-minute durations and nearly constant for all other durations. This pattern might be partially due to the shorter record length (thus more sampling variance) of the 15-minute stations (fig. 3). Unlike the deviations of values of τ_2 greater than and less than the IQR (top graph of fig. 8), the deviations of values of τ_3 greater than and less than the IQR (top graph of fig. 9) are relatively similar for all durations.

The bottom graph of figure 9 illustrates the effects of spatial averaging on τ_3. The median of τ_3 still increases with increasing duration from the 30-minute to 1-day duration and then levels off somewhat. The 15-minute median τ_3 in both graphs is larger than the 30-minute median (whose origin is unknown). The IQR and the deviations of values outside the IQR are greatly reduced.

The author believes that a more accurate estimate of L-scale (λ_2) can be determined because more accurate values of L–CV (τ'_2) are available from the spatial averaging and because the mean (λ_1) has been corrected for fixed-time-interval bias (λ'_1). Recalling that τ_2 is the ratio between L-scale and the mean (eq. 7), it follows that a more accurate estimate of L-scale than λ_2 can be derived from

$$\lambda'_2 = \lambda'_1(\tau'_2). \quad (29)$$

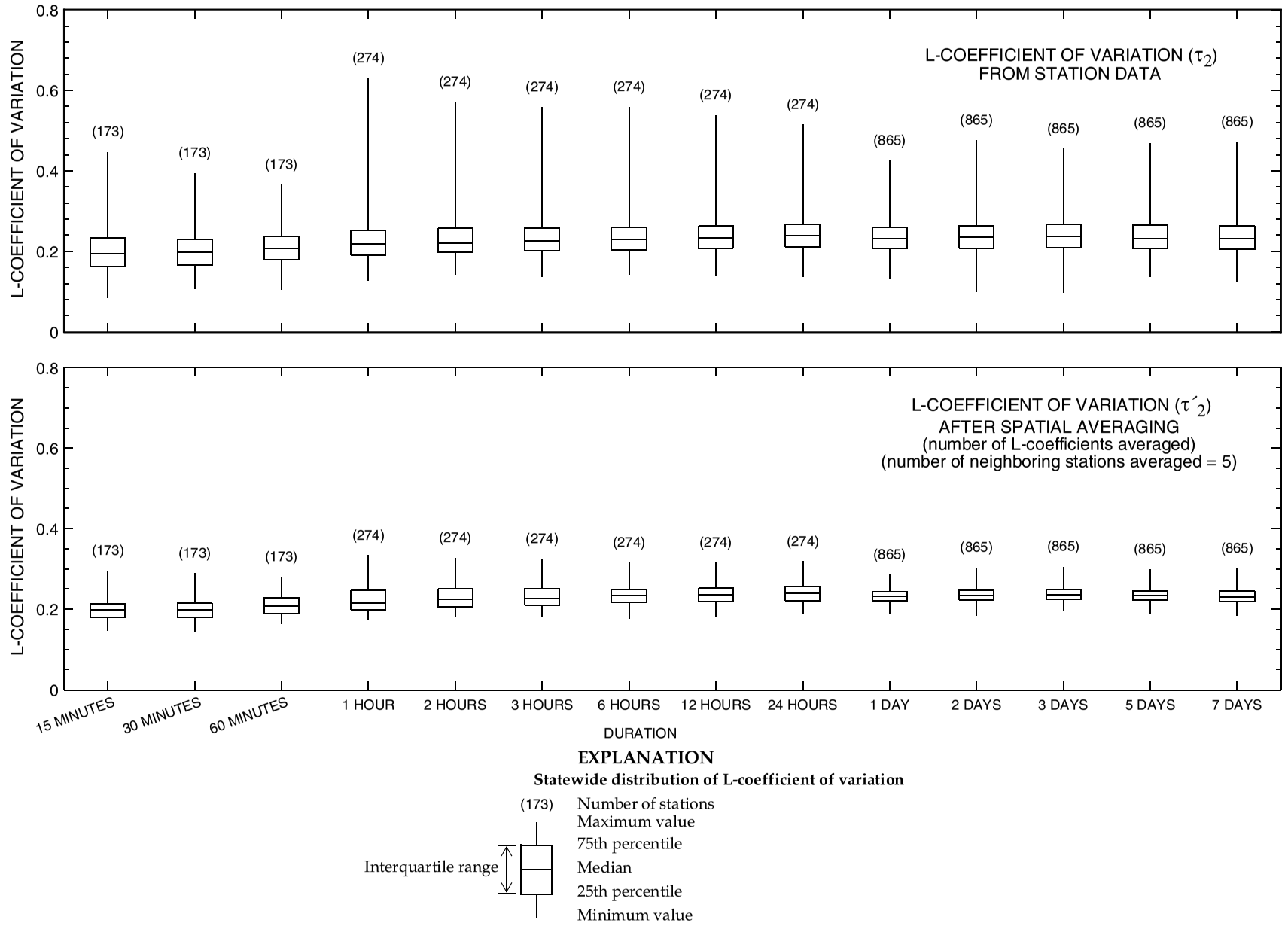

Figure 8. Effects of spatial averaging on the statewide distribution of L-coefficient of variation for each precipitation duration.

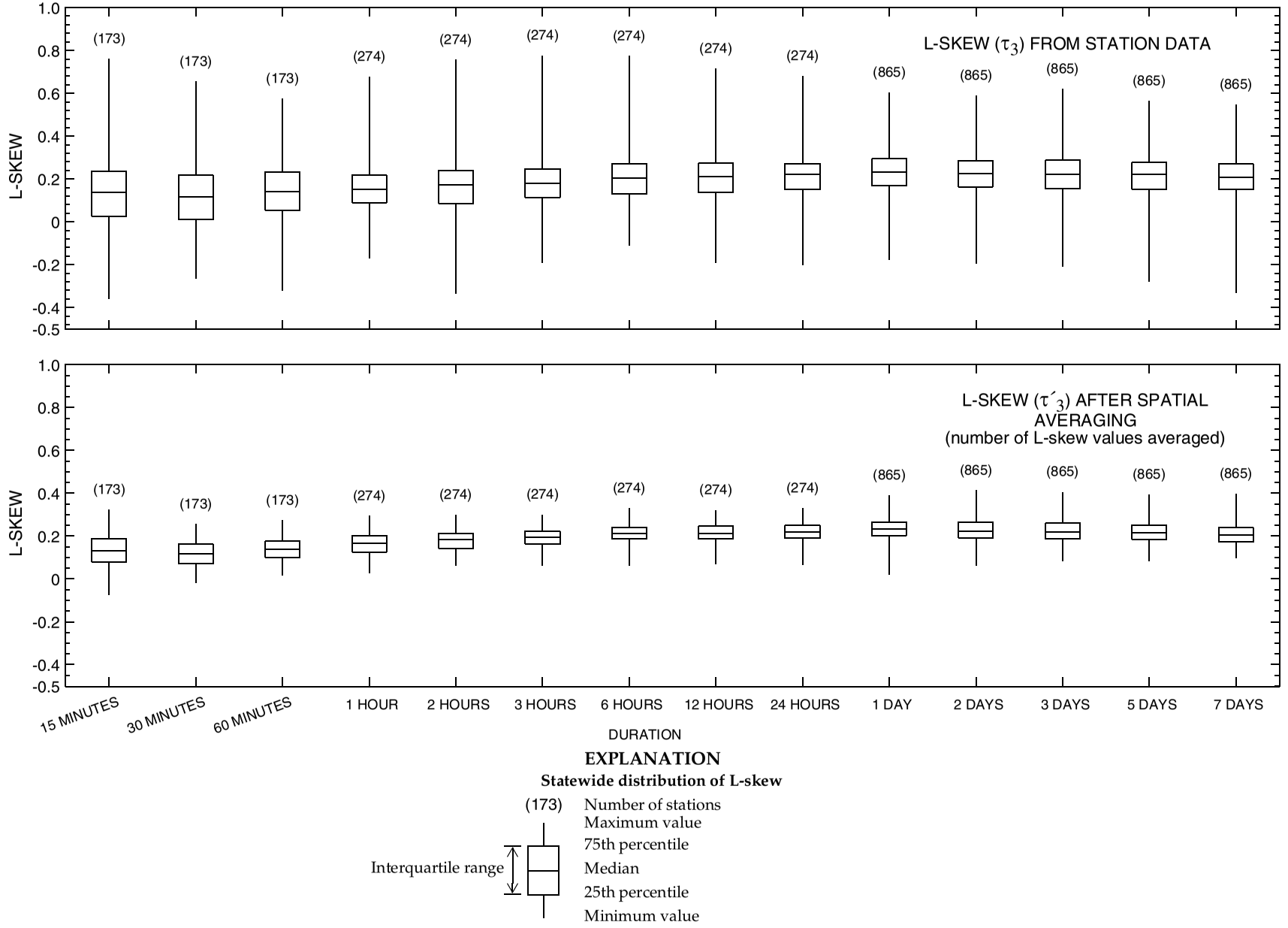

Figure 9. Effects of spatial averaging on the statewide distribution of L-skew for each precipitation duration.

Contouring Distribution Parameters

The values for λ'_1, λ'_2, and τ'_3 were transformed into the ξ, α, and κ parameters (see eqs. 12–14 and 17–20) of either the GLO distribution (15-minute to 24-hour duration) or the GEV distribution (1- to 7-day duration). The resulting parameters then were contoured using interpolation based on the geostatistical method of kriging to produce 37 maps representing the spatial magnitude and variation of the parameters.

A complete discussion of the kriging method is beyond the scope of this report. Standard geostatistical terminology is used in this section. A thorough discussion of the kriging method is available in Carr (1995), Davis (1986), and Deutsch and Journel (1992).

A linear form of the theoretical semivariogram was chosen to model the semivariance of each parameter for all durations. A variety of search radii, sample sizes, and grid densities were investigated for generation of the contour maps. A maximum search radius of about 185 mi and a grid spacing of about 3 mi were used. This grid spacing translates to approximately 67,000 grid cells for the State. A sample size of 10 stations was used for the 15-minute and hourly data (15-minute to 24-hour duration), and a sample size of 20 stations was used for the daily data. The larger sample size for the daily data is justifiable because the density of the daily stations (3.23 per 1,000 mi^2) is much greater than that of either the 15-minute or hourly stations (0.646 or 1.02 stations per 1,000 mi^2).

DEPTH-DURATION FREQUENCY OF PRECIPITATION FOR TEXAS

The DDF for any location in Texas can be estimated from the maps (figs. 10–46 at end of report) and from procedures discussed in this section. Contour maps depicting the location (ξ) parameters for durations of 15 minutes to 7 days are shown in figures 10–23. Contour maps depicting the scale (α) parameters for durations of 15 minutes to 7 days are shown in figures 24–37. Contour maps depicting the shape (κ) parameters for durations of 15 minutes to 24 hours are shown in figures 38–46. The figures have been checked for internal consistency; for example, ξ parameters of one duration are less than ξ parameters of a larger duration for a given location in Texas.

Analysis of the error associated with each of the maps was done. The error associated with a station is defined as

$$\in(p)_i = \Phi^S(p)_i - \Phi^C(p)_i, \qquad (30)$$

where

$\in(p)_i$ = error associated with parameter p (ξ, α, or κ) at station i;

$\Phi^S(p)_i$ = value of the parameter for the station (control point); and

$\Phi^C(p)_i$ = value of the parameter for the station from the contours.

The error thus defined is only indicative of the true error because each station was used in the development of the contour maps. An independent means to measure error is not available.

The results of the map error analysis are listed in table 3. The table lists the mean across the State for each parameter and its SD. Also listed are the mean contour error, mean absolute contour error, RMSE, and percent change from SD to RMSE for each parameter. Each of these statistics is a weighted value, which means that record length of each station was considered in the computation.

The mean contour error is the mean difference between values of the control points and values from the map; mean contour errors near zero are desirable. This error reflects potential bias in the map. Additionally, the RMSE was calculated by the following:

$$RMSE = \sqrt{\frac{\sum_{i=1}^{n} r_i[\in(p)_i]^2}{\sum_{i=1}^{n} r_i}}, \qquad (31)$$

where

r_i = record length associated with station i; and

$\in(p)_i$ = error associated with parameter p (ξ, α, or κ) at station i.

RMSE is analogous to the SD, and therefore the RMSE is comparable to the SD of the control points. The percent change from SD to RMSE, 100*[(RMSE – SD) / SD], is considered indicative of the improvement in parameter estimation by using the map contours rather than simply using the corresponding statewide mean. Percent changes from SD to RMSE for all parameters and durations, except for 1- to 7-day κ, are all greater than 15 percent. Thus, the author believes the use of the contour maps results in more accurate estimates of the parameters than by simply using a statewide mean. The statewide means in table 3 are used for

Table 3. Summary statistics of distribution-parameter maps for each precipitation duration in Texas

[Note: Contour error is defined as parameter value for control point minus value from contour map. SD, standard deviation; RMSE, root mean square error; min, minutes; hr, hours; --, maps for κ not presented because SD to RMSE percent change is less than 15 percent]

Duration	Control points (stations)			Contours			SD to RMSE percent change
	Statewide mean of control points	SD of statewide mean	Ratio of SD to mean	Mean contour error	Mean absolute contour error	RMSE of contour map	
Location parameter (ξ), in inches							
15 min	0.896	0.178	0.199	–0.00312	0.0755	0.127	–28.7
30 min	1.24	.206	.166	–.00730	.0897	.119	–42.2
60 min	1.58	.275	.174	.00289	.117	.154	–43.9
1 hr	1.52	.317	.209	–.0171	.102	.150	–52.5
2 hr	1.87	.422	.226	–.0229	.121	.181	–57.2
3 hr	2.03	.474	.233	–.00819	.137	.196	–58.5
6 hr	2.33	.563	.242	–.0156	.152	.219	–62.2
12 hr	2.66	.667	.258	–.0294	.163	.240	–64.0
24 hr	3.00	.783	.261	–.0270	.184	.270	–65.6
1 day	2.84	.673	.237	–.00536	.158	.223	–66.8
2 days	3.22	.776	.241	–.0293	.172	.242	–68.8
3 days	3.43	.839	.245	–.0438	.193	.267	–68.2
5 days	3.77	.922	.245	–.0134	.204	.283	–69.3
7 days	4.08	1.00	.245	–.0135	.216	.305	–69.6
Scale parameter (α), in inches							
15 min	.179	.0357	.199	–.00400	.0193	.0276	–22.5
30 min	.247	.0387	.141	–.000862	.0227	.0288	–25.6
60 min	.331	.0499	.151	.00199	.0300	.0392	–21.4
1 hr	.338	.0518	.153	.000967	.0281	.0393	–24.1
2 hr	.426	.0751	.176	.000453	.0343	.0466	–38.0
3 hr	.469	.0928	.198	–.00105	.0377	.0506	–45.5
6 hr	.547	.118	.216	–.000018	.0457	.0617	–47.9
12 hr	.624	.147	.236	–.00183	.0511	.0700	–52.4
24 hr	.713	.178	.250	–.00844	.0604	.0794	–55.4
1 day	1.08	.258	.234	–.00429	.0949	.121	–53.2
2 days	1.25	.317	.254	.00108	.111	.145	–54.4
3 days	1.36	.334	.246	–.00239	.122	.157	–52.9
5 days	1.49	.374	.251	–.00721	.130	.168	–55.1
7 days	1.61	.397	.247	–.00958	.143	.185	–53.4
Shape parameter (κ), dimensionless							
15 min	–.132	.0782	.592	.0104	.0426	.0612	–21.7
30 min	–.119	.0602	.506	.00307	.0342	.0438	–27.2
60 min	–.142	.0551	.388	–.00694	.0311	.0410	–25.7
1 hr	–.165	.0540	.327	–.000655	.0327	.0423	–21.7
2 hr	–.180	.0503	.279	–.00359	.0313	.0400	–20.5
3 hr	–.190	.0508	.267	–.00543	.0326	.0390	–23.2
6 hr	–.209	.0538	.257	.000309	.0284	.0362	–32.7
12 hr	–.213	.0502	.236	.00330	.0274	.0346	–31.1
24 hr	–.219	.0463	.211	.000238	.0261	.00331	–28.4
1 day	–.0954	.0765	.802	--	--	--	--
2 days	–.0867	.0825	.952	--	--	--	--
3 days	–.0862	.0818	.949	--	--	--	--
5 days	–.0750	.0769	1.03	--	--	--	--
7 days	–.0615	.0755	1.23	--	--	--	--

the 1- to 7-day κ. The shape (κ) parameter of the GEV distribution for durations of 1 to 7 days was not contoured because an appreciable amount of the variability could not be explained by preliminary contours—RMSEs of preliminary contour maps for 1- to 7-day shape parameters were not appreciably smaller than statewide SDs.

General observations about the ξ parameters are:

1. The ξ parameter has a systematic upward trend with increasing duration from 15 minutes to 24 hours and from 1 to 7 days. The upward trend is less pronounced in West Texas where long-duration (multiple-day) storms are not as frequent as in southeast Texas where considerably longer duration rainfall occurs. The contour lines generally exhibit a north-to-south azimuth except in Central Texas and near the coast where the general direction parallels the coast. A rapid upward trend in ξ appears to exist where the southern coast (north to south) turns northeast ("coastal bend"). This trend might be due to a change in moisture flux across the coast—in general the moisture flux along the Texas coast trends to the northwest.

2. A clear tendency for the ξ to trend upward at a reduced rate exists northwest to southeast "down" the Colorado River valley; whereas the area immediately south of the Colorado River (southeast Edwards Plateau region) shows a "mounding" of ξ (fig. 23, for example). This mounding could be attributed to an orographic influence of the Balcones escarpment where it parallels the southeastern and southern boundary of the Edwards Plateau region.

3. Furthermore, ξ shows mounding in the area of the Guadalupe, Davis, and Chisos Mountains. This mounding is particularly pronounced for the 1- to 7-day durations due to the greater number of control points (fig. 23, for example). The cause of this mounding in the mountains is certainly due to orographic influences of these mountain ranges.

4. Finally, the southernmost part of the State within the delta of the Rio Grande shows larger values of ξ than those in the area immediately to the north for durations of 30 minutes to 3 days (figs. 11–21).

The α parameters, in general, exhibit trends similar to those of the ξ parameters. The similarity of trends is not surprising because of the relation between λ'_1 and λ'_2 (eq. 29). However, less spatial detail or localized variations are seen in the contour lines of α. The α parameter for the 1- to 7-day durations appears to mound near the southeastern edge of the Edward Plateau region, which corresponds very closely to the location of the Balcones escarpment (fig. 34, for example).

Of the three parameters, physical interpretation of κ is the most difficult. As listed in table 3 and shown on the 15-minute to 24-hour κ maps, the magnitude of κ generally increases with duration, up to about the 24-hour duration, and then begins decreasing with increasing duration. (κ is calculated differently for 24 hours and less (eq. 12) than for 1 day and more (eqs. 17–18).) This upward and then downward trend with increasing duration is due to τ'_3 (bottom graph, fig. 9) increasing up to about the 1-day duration and then decreasing as duration increases beyond 1 day.

Examples of Depth-Duration Frequency Computation

Two examples of DDF computations illustrate the use of the maps. Suppose estimates of the 100-year, 6-hour depth and the 100-year, 2-day depth are needed for Amarillo, Tex. The ξ, α, and κ parameters for the 6-hour duration are estimated from figures 16, 30, and 44. The ξ and α parameters for the 2-day duration are estimated from figures 20 and 34; whereas, the κ parameter is estimated from table 3. The ξ, α, and κ estimates for the 6-hour duration are 1.68 in., 0.42 in., and –0.20, respectively. The values of ξ, α, and κ for the 2-day duration are 2.37 in., 0.925 in., and –0.0867, respectively.

For the 6-hour duration, the GLO distribution is used. The 100-year nonexceedance probability (F) is equal to 0.99. From equation 10,

$$X_{6\,\mathrm{hour}}(0.99) = 1.68 + \frac{0.42}{-0.20}\left\{1 - \left[\frac{(1-0.99)}{0.99}\right]^{-0.20}\right\} = 4.84 \text{ in.}$$

Likewise, the 25-year, 6-hour precipitation depth (F = 0.96) is 3.55 in., and the 500-year depth (F = 0.998) is 6.86 in. Often a depth duration is converted to a precipitation intensity, which is measured in inches per hour (in/hr). The 100-year, 6-hour precipitation intensity for Amarillo therefore is 0.81 in/hr (4.84 in/6 hr).

For the 2-day duration, the GEV distribution is used. The nonexceedance probability (F) is equal to 0.99. From equation 15,

$$X_{2\,\mathrm{day}}(0.99) = 2.37 + \frac{0.925}{-0.0867}$$

$$\{1 - [-ln(0.99)]^{-0.0867}\} = 7.60 \text{ in.}$$

When the depth is estimated as previously discussed, potential errors exist that might positively or negatively bias the value of $X_d(F)$. One potential error is the author's interpretation associated with the kriging procedure near "outliers," near areas with sparse data, or near the boundaries of the State. Another possible error is the interpolation error associated with obtaining the parameters from the contour maps—interpolated parameters for the same location could be slightly different. Interpolation in the far western part of the State, where several mountain ranges exist, is subject to greater error than elsewhere in the State because there are fewer control points, and the effects of rapid changes in altitude (orographic influence on precipitation characteristics) might not be reflected in the contour maps.

Examples illustrating the sensitivity of map interpolation—measured by percent change—of the GLO and GEV distributions from the above examples ($F = 0.99$) to the values of the three parameters are as follows:

For the GLO distribution, a 10-percent increase in ξ (1.85), in α (0.462), in κ (–0.22) yields a depth of 5.52 in., which is a 14-percent change; and a 10-percent decrease in ξ (1.51), in α (0.378), in κ (–0.18) yields a depth of 4.21 in., which is a negative 13-percent change. For the GEV distribution, a 10-percent increase in ξ (2.61), in α (1.02), in κ (–0.0954) yields a depth of 8.50 in., which is a 12-percent change; and a 10-percent decrease in ξ (2.13), in α (0.833), in κ (–0.0780) yields a depth of 6.74 in., which is a negative 11-percent change. Other examples of parameter sensitivity could be obtained.

The potential error of a DDF for a particular locality depends on the potential error in estimating the three parameters, on the magnitude of recurrence interval, and on the actual geographic site of the locality (for example, in the Chisos Mountains). However, for much of the State, a 10-percent difference in a parameter value obtained from the maps represents a very large geographic distance; thus, the examples of parameter sensitivity are considered extreme.

Precipitation Intensity-Duration Frequency Curve

To moderate the potential errors in calculating the DDF for a given location, the author suggests that a log-log graph showing the relation between precipitation intensity (in inches per hour) and duration be generated, and a "best-fit" line hand plotted on the graph. The best-fit line or "precipitation intensity-duration frequency" (IDF) curve represents the final precipitation depth for the selected location. A reason to use a log-log intensity-duration graph, in addition to the linearizing effect, is that the percent differences in the intensities between durations become independent of the magnitude of the intensity. A representative IDF curve for El Paso is shown in figure 47 (at end of report). In addition to showing the precipitation intensity for each duration for El Paso, the figure shows the precipitation intensity duration for selected localities in Texas. The relatively smooth transition of the IDF curve from short to long durations, in which nearly independent data sources are used, is notable and encouraging. In other words, the parameter maps produce consistent precipitation depths.

A potential error involves large potential discrepancies between the two estimates at the 1-hour (60-minute and 1-hour estimates) and 1-day (24-hour and 1-day estimates) durations. These discrepancies might occur because of the differences in mean record length between the 15-minute stations and the hourly stations and between the hourly and the daily stations (fig. 3); the longer-duration data are more accurate, in general, than the shorter-duration data. Additionally, the distribution and density of the control points (stations) vary between the 15-minute and hourly stations and between the hourly and daily stations, resulting in potential errors associated with the contouring. Finally, at the 1-day duration, there is a change from the GLO to the GEV distribution, which can contribute to discrepancies between the 24-hour and the 1-day estimates. Because both estimates at the 1-hour or 1-day duration are considered valid, the generation of an IDF curve as shown in figure 47 helps resolve discrepancies.

A final potential problem in calculating DDF for a given location is that the DDF for one duration might be greater than the DDF for a greater duration. This problem could be attributed to the potential errors

previously identified. The generation of an IDF curve for each location resolves this problem as well.

Comparison to Previous Studies

Exact comparisons to previous studies [TP–40 (Hershfield, 1962) and HYDRO–35 (Frederick and others, 1977)] are not easy to document within the context of this report. However, a comparison between the depths for the 6-hour 100-year storm from TP–40 and the depths calculated using parameters obtained from the appropriate contour maps (figs. 16, 30, and 44) is shown in figure 48 (at end of report). The depths in figure 48 were not adjusted using a "best fit" IDF curve as previously described. According to the figure, the depths calculated using the methods in this report are similar (generally ±0.5 in.) to those in TP–40 except in the coastal and south-central Texas areas. The contours of the depths using the methods in this report show greater spatial detail than the depths available from TP–40. Along the coast, the depths from this report are about 15 percent greater than the depths from TP–40. In the south-central part of the State (especially near the Balcones escarpment), the depths from this report are about 40 percent greater than the depths from TP–40. The differences in south-central Texas are not surprising given the occurrence of large storms in this part of the State (Slade, 1986).

The IDF curve for Amarillo and Orange, Tex., derived from the methods of this report and the curves generated from TP–40 and HYDRO–35 are compared in figure 49 (at end of report). The similarity in shape of the curves from this report to the curves from the previous studies is notable. However, the precipitation-intensity values for Amarillo from this report are about 16 percent larger than those from the previous studies for durations less than or equal to about 3 hours; and the precipitation-intensity values for Orange from this report are about 10 percent larger than those from TP–40 for durations greater than or equal to about 3 hours.

Many other comparisons of IDF or DDF estimates from this report were made with estimates from the previous studies (not reported here); results similar to those shown in figures 48 and 49 were observed. IDF or DDF estimates or curves derived from this report are considered more accurate than estimates from previous studies because of (1) the greater number of stations and longer periods of record available for this study, (2) the use of more powerful statistics (L-moments), which were not available at the time the previous studies were completed, and (3) the use of more flexible and appropriate three-parameter distributions rather than the two-parameter Gumbel distribution used in previous studies.

SUMMARY

The estimation of precipitation depths for various durations and frequencies, referred to as depth-duration frequency (DDF), has many uses. A common use of DDF is for the design of structures that control and route localized runoff—such as parking lots, storm drains, and culverts. Another use of DDF is to drive river-flow models that incorporate precipitation characteristics. Accurate DDF estimates are important for cost-effective structural designs at stream crossings and for developing reliable flood prediction models.

The durations investigated during a USGS study of DDF for Texas are 15, 30, and 60 minutes; 1, 2, 3, 6, 12, and 24 hours; and 1, 2, 3, 5, and 7 days. The frequencies in terms of recurrence interval range from 2 to 500 years. The basis of DDF is the time series of annual maxima of precipitation for each identified duration from 173 fifteen-minute, 274 hourly, and 865 daily National Weather Service precipitation stations with at least 10 years of data in Texas. About 3,030; 10,160; and 38,120 cumulative years of record are available for the 15-minute, hourly, and daily stations, respectively. The areal densities, in stations per 1,000 mi^2, are 0.646, 1.02, and 3.23 for the 15-minute, hourly, and daily stations, respectively.

L-moment statistics of the precipitation annual maxima were calculated for each duration and for each station using unbiased L-moment estimators. The statistics calculated were the mean, L-scale, L-coefficient of variation (L–CV), L-skew, and L-kurtosis. These statistics were calculated for each duration and for each station using unbiased L-moment estimators. The mean for each station and duration was corrected for the bias associated with fixed-interval recording of precipitation. L-skew, L-kurtosis, and L-moment ratio diagrams were used to determine that the three-parameter generalized logistic (GLO) distribution is an appropriate probability distribution for modeling the frequency of annual maxima for durations of 15 minutes to 24 hours. The three-parameter generalized extreme-value (GEV) distribution was determined as appropriate for durations of 1 to 7 days.

Spatial averaging of L–CV and L-skew was used to (1) reduce the random component in their values

and (2) improve the accuracy of L–CV and L-skew estimates. A corrected L-scale subsequently was estimated using the corrected mean and the spatially averaged L–CV for each duration and for each station. Finally, the corrected mean, the corrected L–scale, and the averaged L-skew for each station and duration were transformed into the location, scale, and shape parameters for both the GLO or GEV distributions.

The location, scale, and shape parameters of the GLO and GEV distributions for each station and duration were contoured using an interpolation scheme based on the geostatistical method of kriging to produce 37 maps depicting the spatial variation and magnitude of each parameter. Contour maps of the shape parameter for the GEV distribution for durations of 1 to 7 days are not presented; the root mean square errors of preliminary maps for 1- to 7-day shape parameters were not appreciably smaller than the statewide standard deviation. Therefore, a single statewide mean shape parameter was used for 1- to 7-day durations. The DDF for any location in Texas can be estimated using the appropriate maps and distribution function.

To reduce the effects of potential errors associated with the maps, precipitation intensity-duration frequency curves, known as IDF curves, were developed on the basis of the relation between precipitation intensities (inches per hour) and duration. The IDF curves for selected localities in the State are presented. The relatively smooth transition of the IDF curve for the selected localities from short to long durations is notable and encouraging. In other words, the parameter maps produce consistent precipitation depths. IDF or DDF estimates or curves derived from this report are considered more accurate than estimates from previous studies because of (1) the greater number of stations and longer record available for this study, (2) the use of more powerful statistics (L-moments), which were not available at the time the other studies were completed, and (3) the use of more flexible and appropriate three-parameter distributions than the two-parameter Gumbel distribution used in previous studies.

SELECTED REFERENCES

Bomar, G.W., 1995, Texas weather: Austin, University of Texas Press, 275 p.

Carr, J.R., 1995, Numerical analysis for the geological sciences: Englewood Cliff, N.J., Prentice-Hall, 592 p.

Carr, J.T., Jr., 1967, The climate and physiography of Texas: Texas Water Development Board Report 53, 27 p.

Dalrymple, Tate, 1960, Flood-frequency analyses: U.S. Geological Survey Water-Supply Paper 1543–A, 80 p.

Davis, J.C., 1986, Statistics and data analysis in geology: New York, Wiley, 646 p.

Deutsch, C.V., and Journel, A.G., 1992, Geostatistical software library and user's guide: New York, Oxford University Press, 340 p.

Fischer, R.A., 1929, Moments and product moments of sampling distributions: Journal of London Mathematical Society, 2(30), 199 p.

Frederick, R.H., Meyers, V.A., and Auciello, E.P., 1977, Five- to 60-minute precipitation frequency for the eastern and central United States: Washington, D.C., National Oceanic and Atmospheric Administration Technical Memorandum NWS HYDRO–35, 36 p.

Greenwood, J.A., Landwehr, J.M., Matalas, N.C., and Wallis, J.R., 1979, Probability weighted moments—Definition and relation to parameters of several distributions expressible in inverse form: Water Resources Research, v. 15, no. 5, p. 1,049–1,054.

Hershfield, D.M., 1962, Rainfall frequency atlas of the United States for durations from 30 minutes to 24 hours and return periods from 1 to 100 years: Washington, D.C., U.S. Weather Bureau Technical Paper 40, 61 p.

Hosking, J.R.M., 1986, The theory of probability weighted moments: Yorktown Heights, N.Y., IBM Research Division, T.J. Watson Research Center, Research Report RC–12210, 160 p.

_____1990, L-moments—Analysis and estimation of distributions using linear combinations of order statistics: Journal Royal Statistical Society B, v. 52, no. 1, p. 105–124.

_____1991a, Approximations for use in constructing L-moment ratio diagrams: Yorktown Heights, N.Y., IBM Research Division, T.J. Watson Research Center, Research Report RC–16635, 3 p.

_____1991b, FORTRAN routines for use with the method of L-moments, Version 2: Yorktown Heights, N.Y., IBM Research Division, T.J. Watson Research Center, Research Report RC–17097, 117 p.

_____1992, Moments or L moments? An example comparing two measures of distributional shape: The American Statistician, v. 46, no. 3, p. 186–189.

_____1994, The four-parameter kappa distribution: IBM Journal of Research and Development, v. 38, no. 3, p. 251–258.

Hosking, J.R.M., and Wallis, J.R., 1993, Some statistics useful in regional frequency analysis: Water Resources Research, v. 29, no. 2, p. 271–281.

_____1995, A comparison of unbiased and plotting-position estimators of L-moments: Water Resources Research, v. 31, no. 8, p. 2,019–2,025.

_____1997, Regional frequency analysis—An approach based on L-moments: Cambridge University Press, 224 p.

Huff, F.A., and Angel, J.R., 1992, Rainfall frequency atlas of the midwest: Illinois State Water Survey Bulletin 17, 141 p.

Hydrosphere Data Products, Inc., 1996, Custom storm data for Texas: Boulder, Colo., Hydrosphere Data Products, Inc., 1 diskette.

Jones, B.D., 1991, Floods and droughts—Texas, *in* U.S. Geological Survey, National water summary 1988–89—Hydrologic events and floods and droughts: U.S. Geological Survey Water-Supply Paper 2375, p. 513–520.

Kirby, W.H., 1974, Algebraic boundness of sample statistics: Water Resources Research, v. 10, no. 2, p. 220–222.

Landwehr, J.M., Matalas, N.C., and Wallis, J.R., 1979, Probability weighted moments compared with some traditional techniques in estimating Gumbel parameters and quantiles: Water Resources Research, v. 15, no. 5, p. 1,055–1,064.

McCuen, R.H., 1985, Statistical methods for engineers: Englewood Cliffs, N.J., Prentice-Hall, p. 61–63.

McKay, Megan, and Wilks, D.S., 1995, Atlas of short-duration precipitation extremes for the northeastern United States and southeastern Canada: Northeast Regional Climate Center, Cornell University, Publication RR 95–1, 26 p.

Miller, J.F., Frederick, R.H., and Tracey, R.J., 1973, NOAA Atlas 2, Precipitation frequency atlas of the western United States (by states): Silver Spring, Md., U.S. Department of Commerce, National Weather Service, National Oceanic and Atmospheric Administration, 11 v.

Norwine, Jim, Giardino, J.R., North, G.R., and Valdes, J.B., 1995, The changing climate of Texas—Predictability and implications for the future: College Station, Tex., Texas A&M University, 348 p.

Office of the State Climatologist, 1987, The climates of Texas counties: College Station, Tex., Texas A&M University, Monograph 2.

Parrett, C.P., 1997, Regional analysis of annual precipitation maxima in Montana: U.S. Geological Survey Water-Resources Investigations Report 97–4004, 51 p.

Schaefer, M.G., 1990, Regional analyses of precipitation annual maxima in Washington State: Water Resources Research, v. 26, no. 1, p. 119–131.

_____1993, Dam safety guidelines, Technical note 3—Design storm construction: Olympia, Wash., Washington State Department of Ecology, Dam Safety Section [variously paged].

Slade, R.M., Jr., 1986, Large rainstorms along the Balcones escarpment in central Texas *in* Abbott, P.L., and Woodruff, C.M., Jr., eds., The Balcones escarpment—Geology, hydrology, ecology and social development in Central Texas: Geological Society of America, p. 15–20.

Stedinger, J.R., Vogel, R.M., and Foufoula-Georgiou, Efi, 1993, Frequency analysis of extreme events, *in* Maidment, D.A., ed., Handbook of applied hydrology, chap. 18: New York, McGraw-Hill, p. 18.1–66.

Vogel, J.L., and Lin, Bingzhang, 1992, Precipitation return frequencies and L-moment statistics, *in* 12th Conference on Probability and Statistics in the Atmospheric Sciences, Toronto, Ont., Canada, 1992: American Meteorological Society, p. 251–254.

Vogel, R.M., and Fennessey, N.M., 1993, L-moment diagrams should replace product moment diagrams: Water Resources Research, v. 29, no. 6, p. 1,745–1,752.

Wallis, J.R., 1989, Regional frequency studies using L-moments: Yorktown Heights, N.Y., IBM Research Division, T.J. Watson Research Center, Research Report RC–14597, 17 p.

Wallis, J.R., Matalas, N.C., and Slack, J.R., 1974, Just a moment: Water Resources Research, v. 10, no. 2, p. 211–219.

Weiss, L.L., 1964, Ratio of true to fixed-interval maximum rainfall: American Society of Civil Engineers, Journal of the Hydraulics Division, v. 90, HY–1, p. 77–82.

Wilks, D.S., and Cember, R.P., 1993, Atlas of precipitation extremes for the northeastern United States and southeastern Canada: Northeast Regional Climate Center, Cornell University, Publication RR 93–5, 26 p.

World Meteorological Organization, 1986, Manual for estimation of probable maximum precipitation (2d ed.): Geneva, Switzerland, Secretariat of the World Meteorological Organization, Operational Hydrology Report 1, WMO 332.

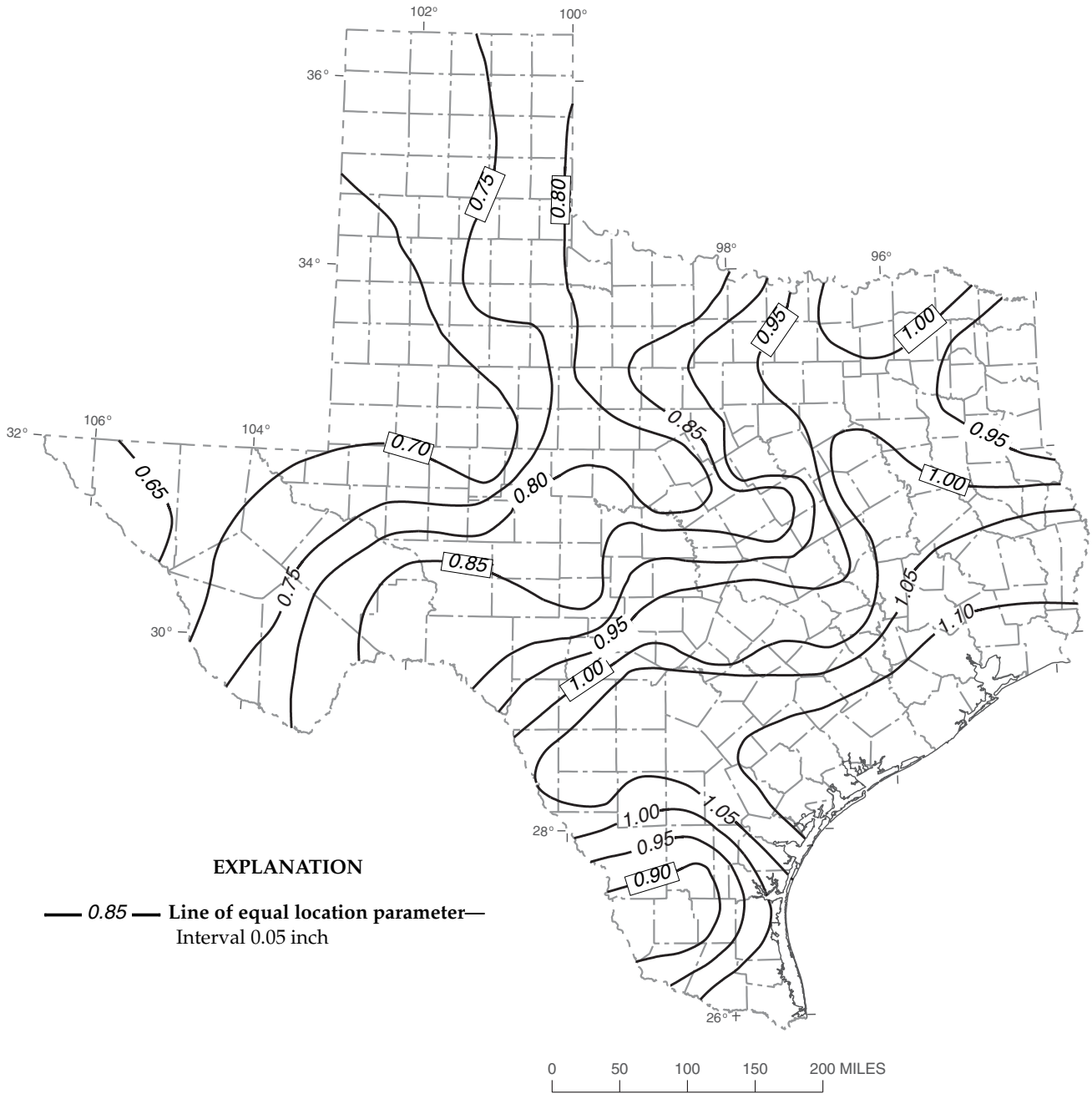

Figure 10. Location (ξ) parameter of generalized logistic (GLO) distribution for 15-minute precipitation duration in Texas.

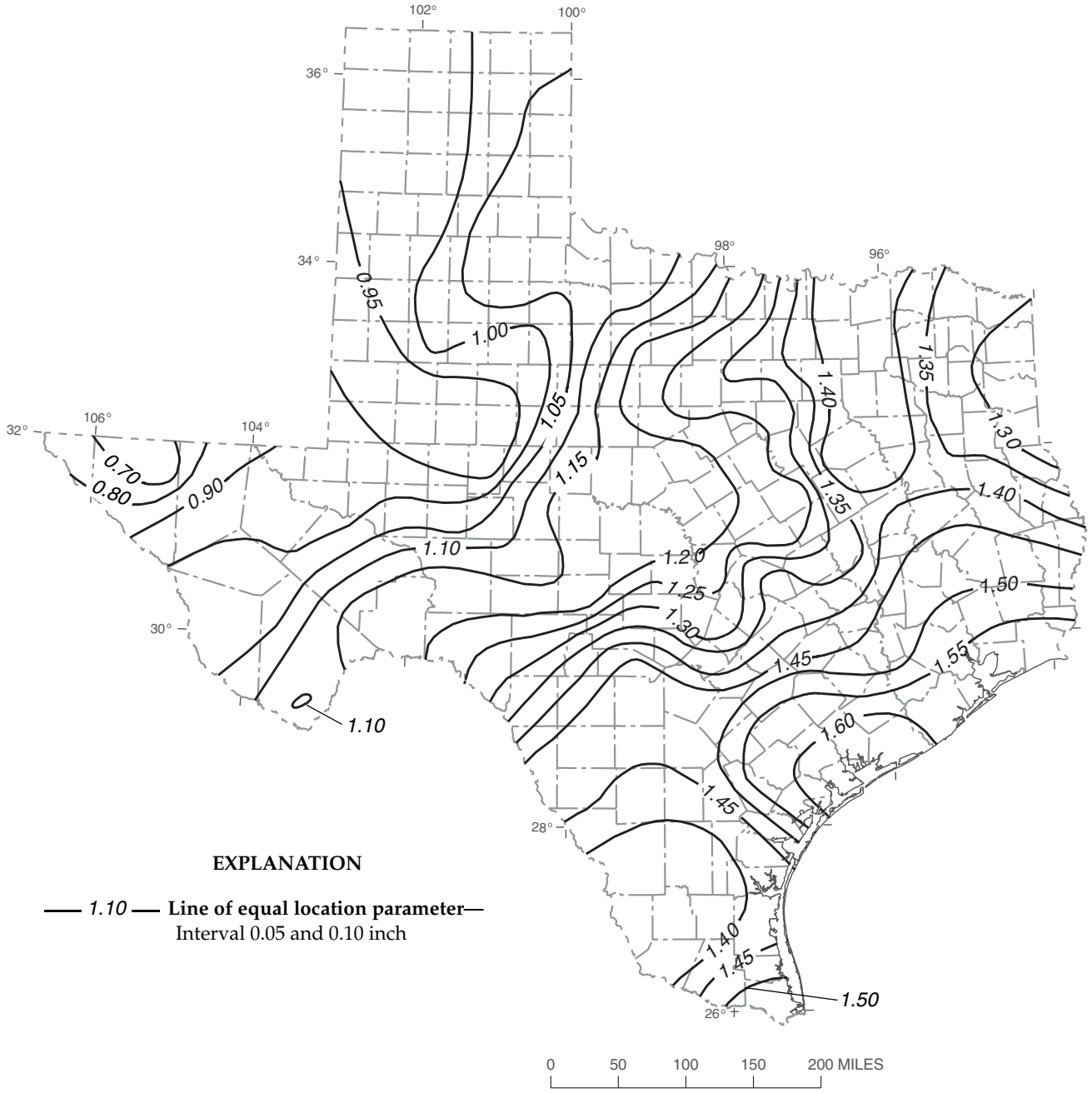

Figure 11. Location (ξ) parameter of generalized logistic (GLO) distribution for 30-minute precipitation duration in Texas.

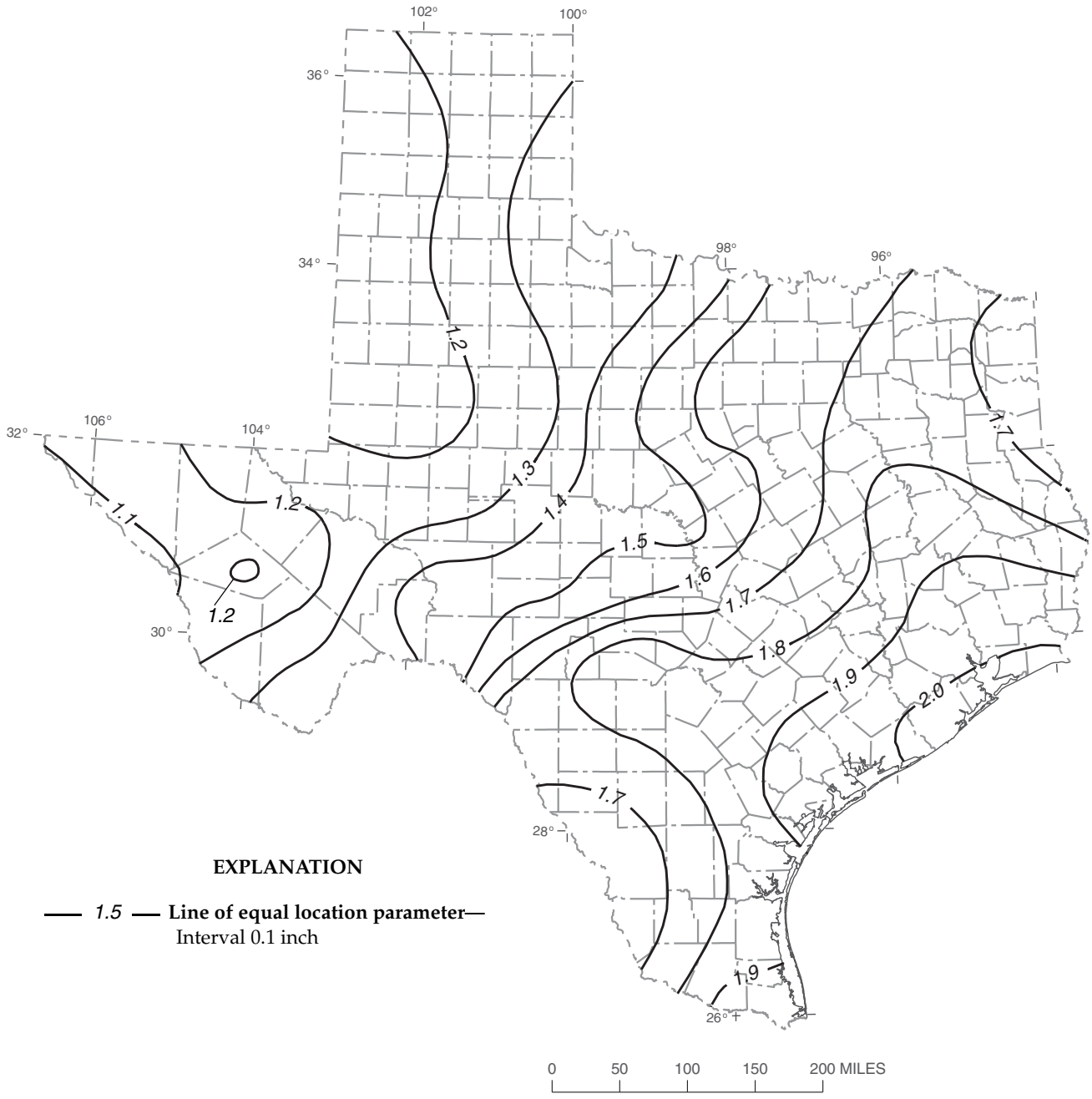

Figure 12. Location (ξ) parameter of generalized logistic (GLO) distribution for 60-minute precipitation duration in Texas.

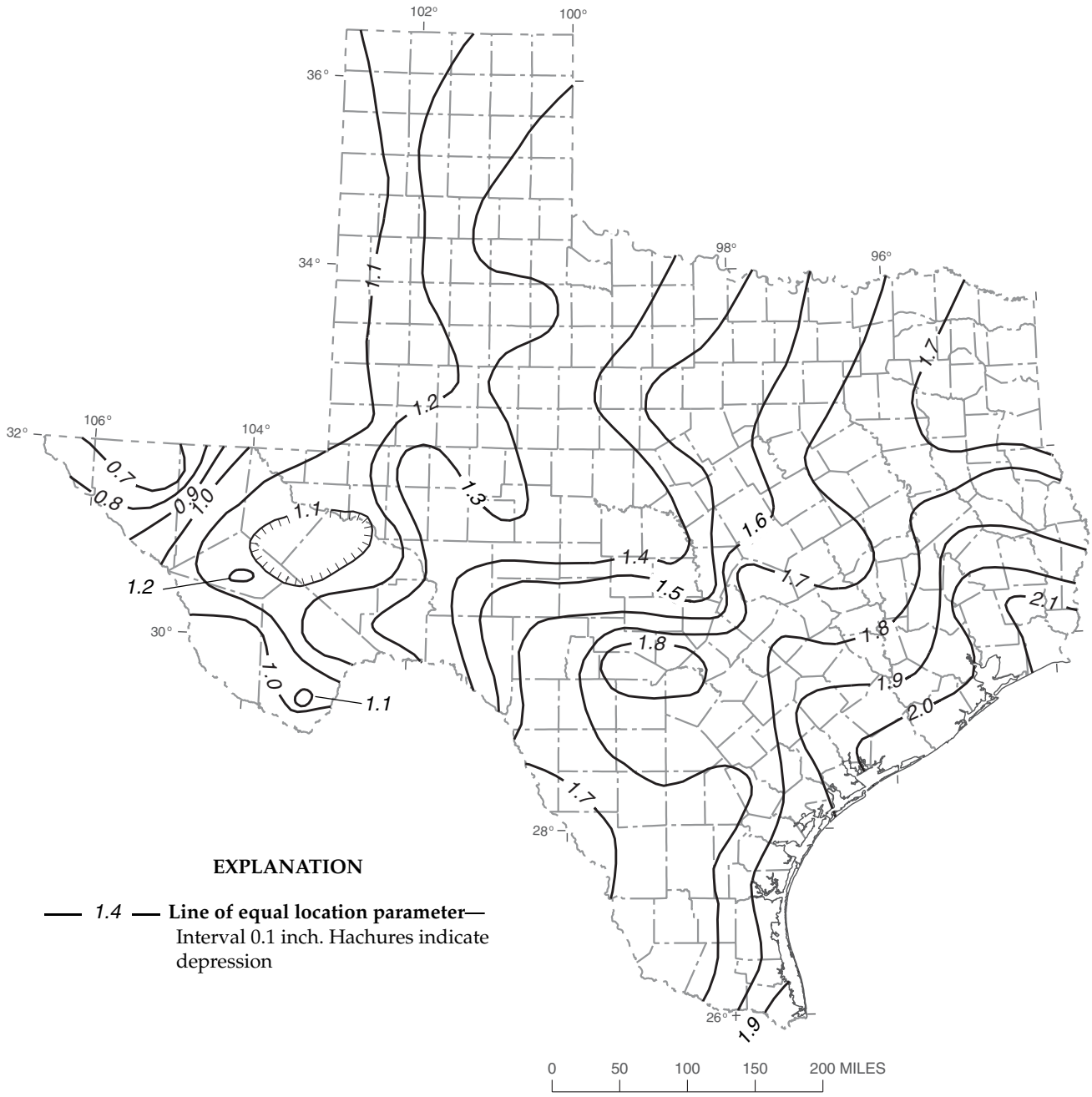

Figure 13. Location (ξ) parameter of generalized logistic (GLO) distribution for 1-hour precipitation duration in Texas.

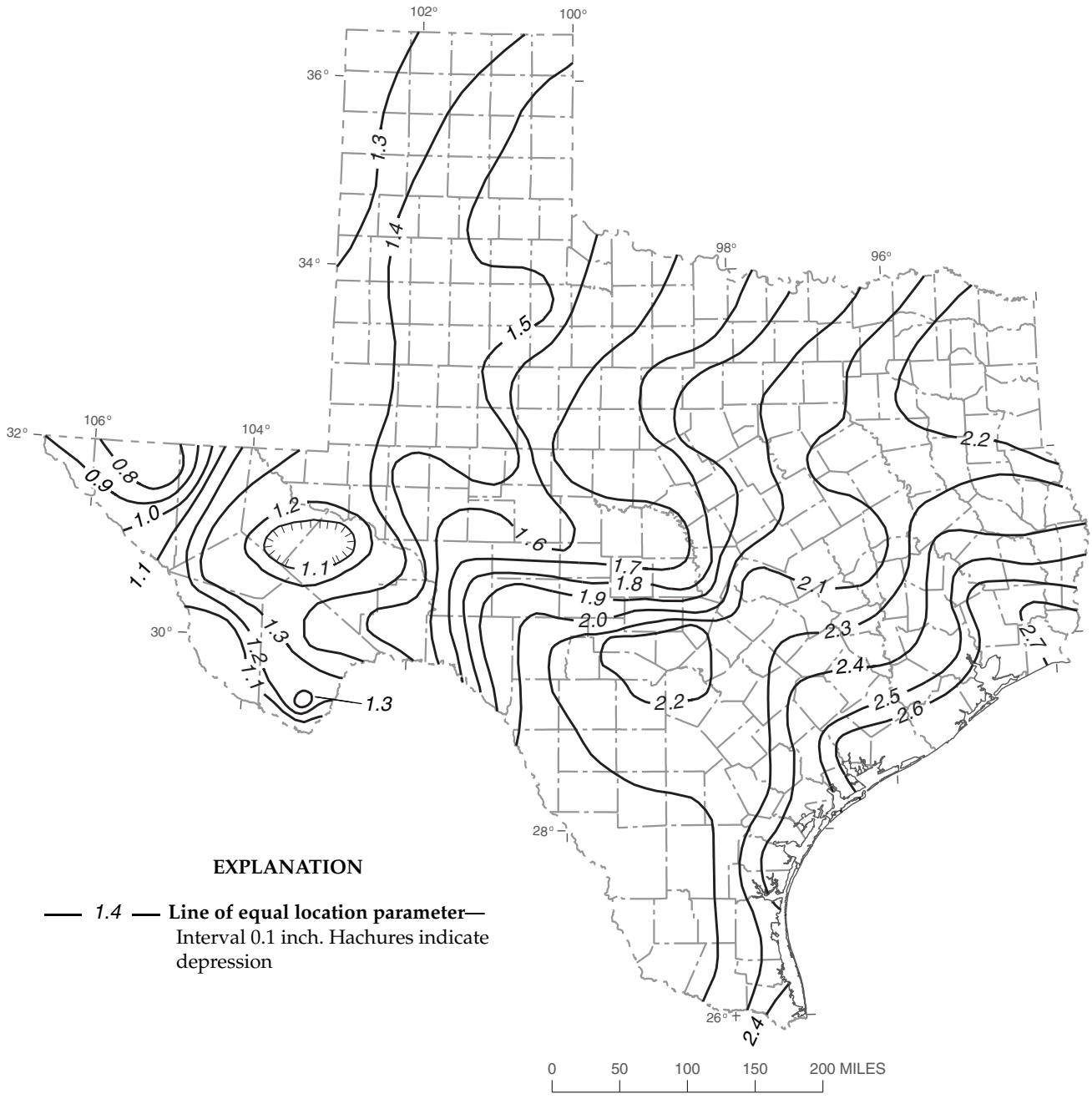

Figure 14. Location (ξ) parameter of generalized logistic (GLO) distribution for 2-hour precipitation duration in Texas.

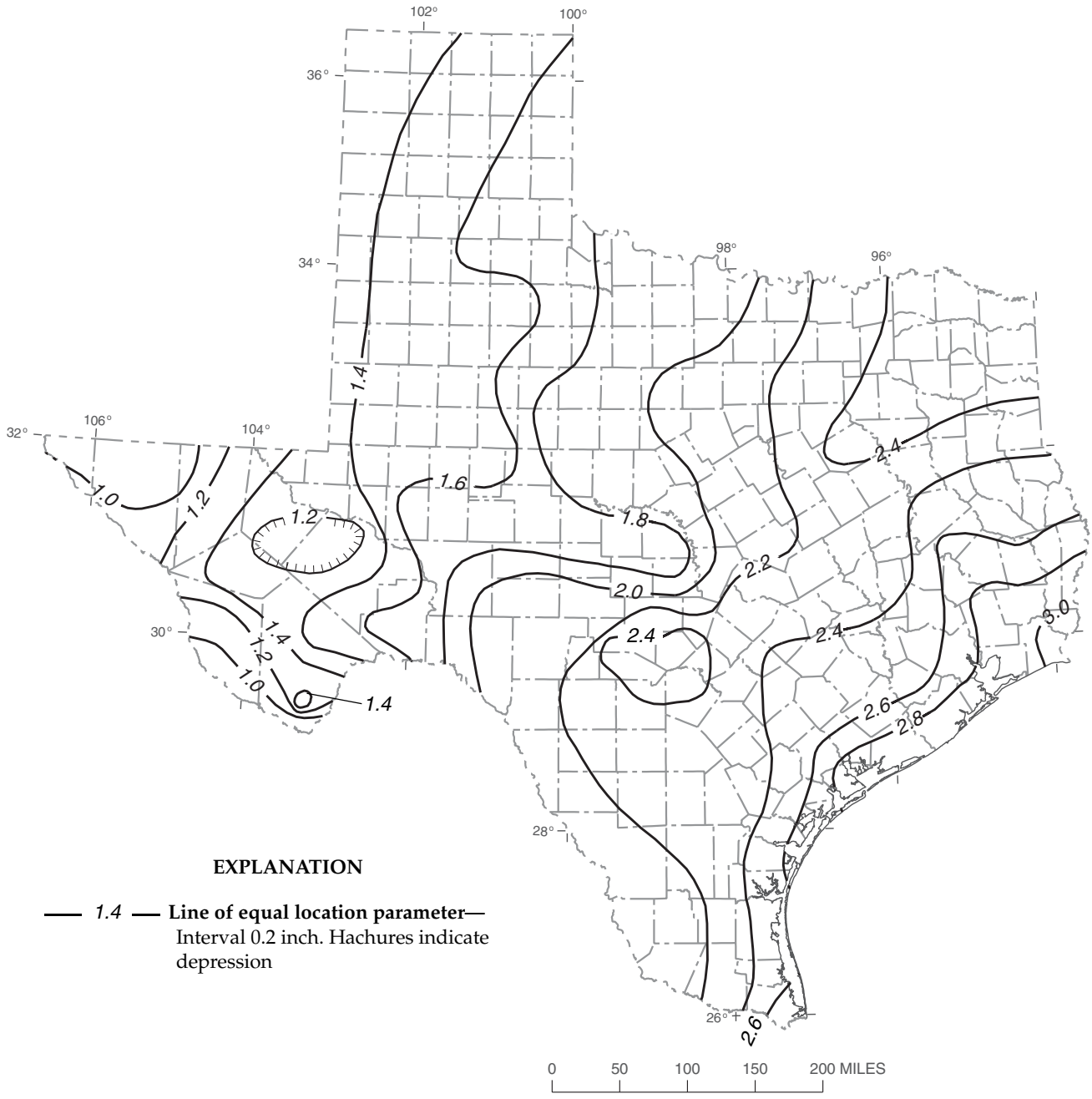

Figure 15. Location (ξ) parameter of generalized logistic (GLO) distribution for 3-hour precipitation duration in Texas.

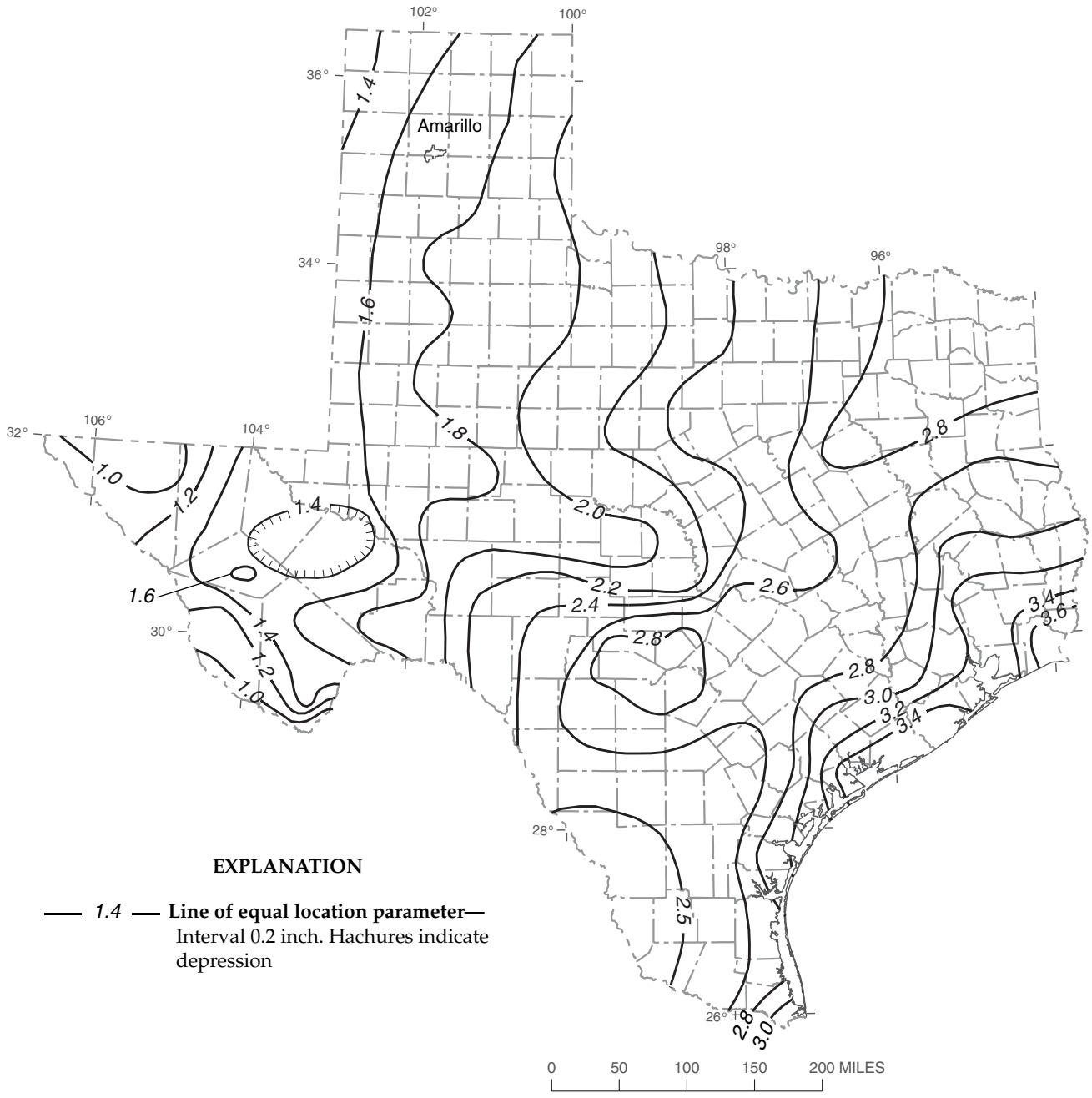

Figure 16. Location (ξ) parameter of generalized logistic (GLO) distribution for 6-hour precipitation duration in Texas.

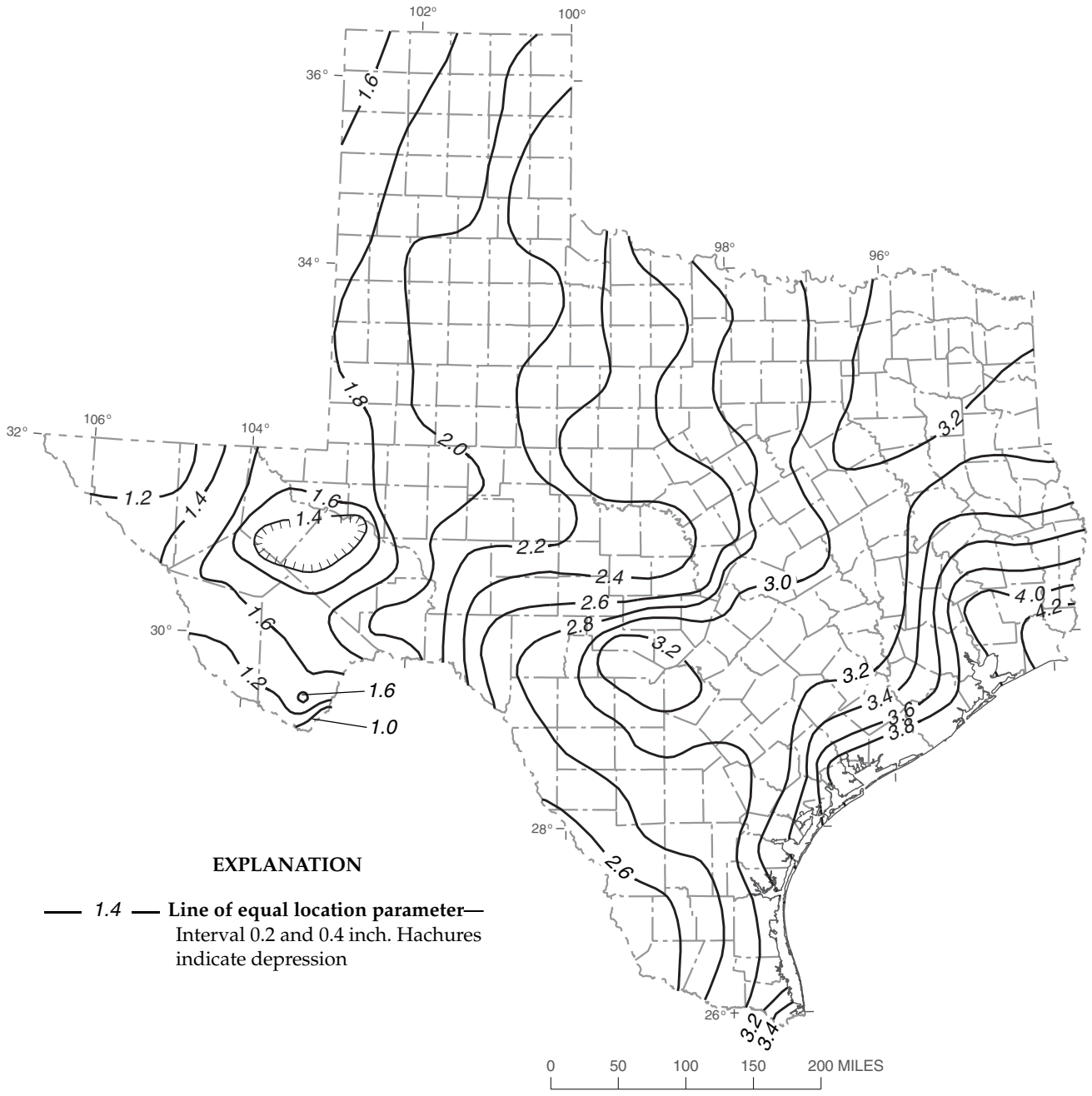

Figure 17. Location (ξ) parameter of generalized logistic (GLO) distribution for 12-hour precipitation duration in Texas.

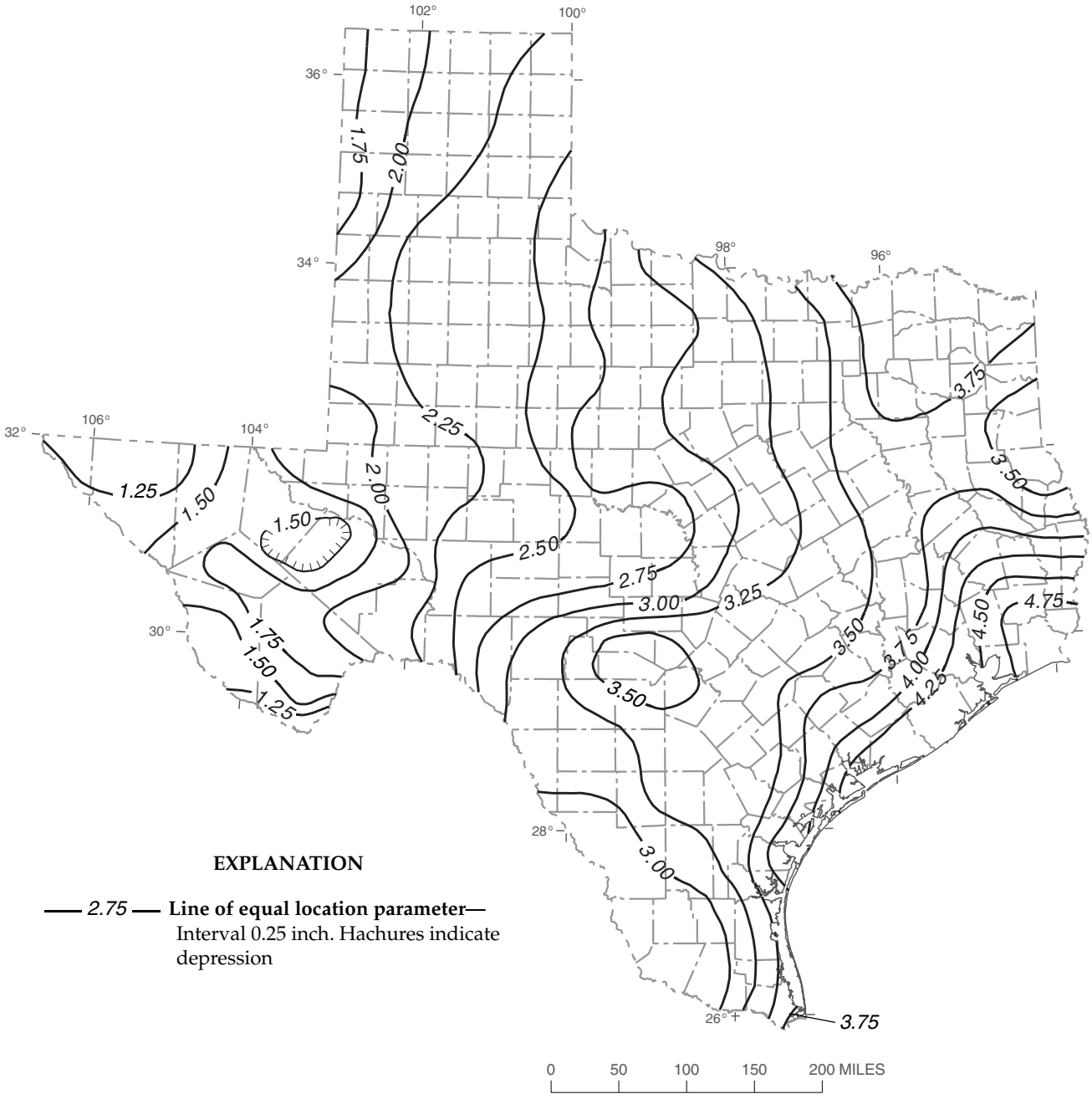

Figure 18. Location (ξ) parameter of generalized logistic (GLO) distribution for 24-hour precipitation duration in Texas.

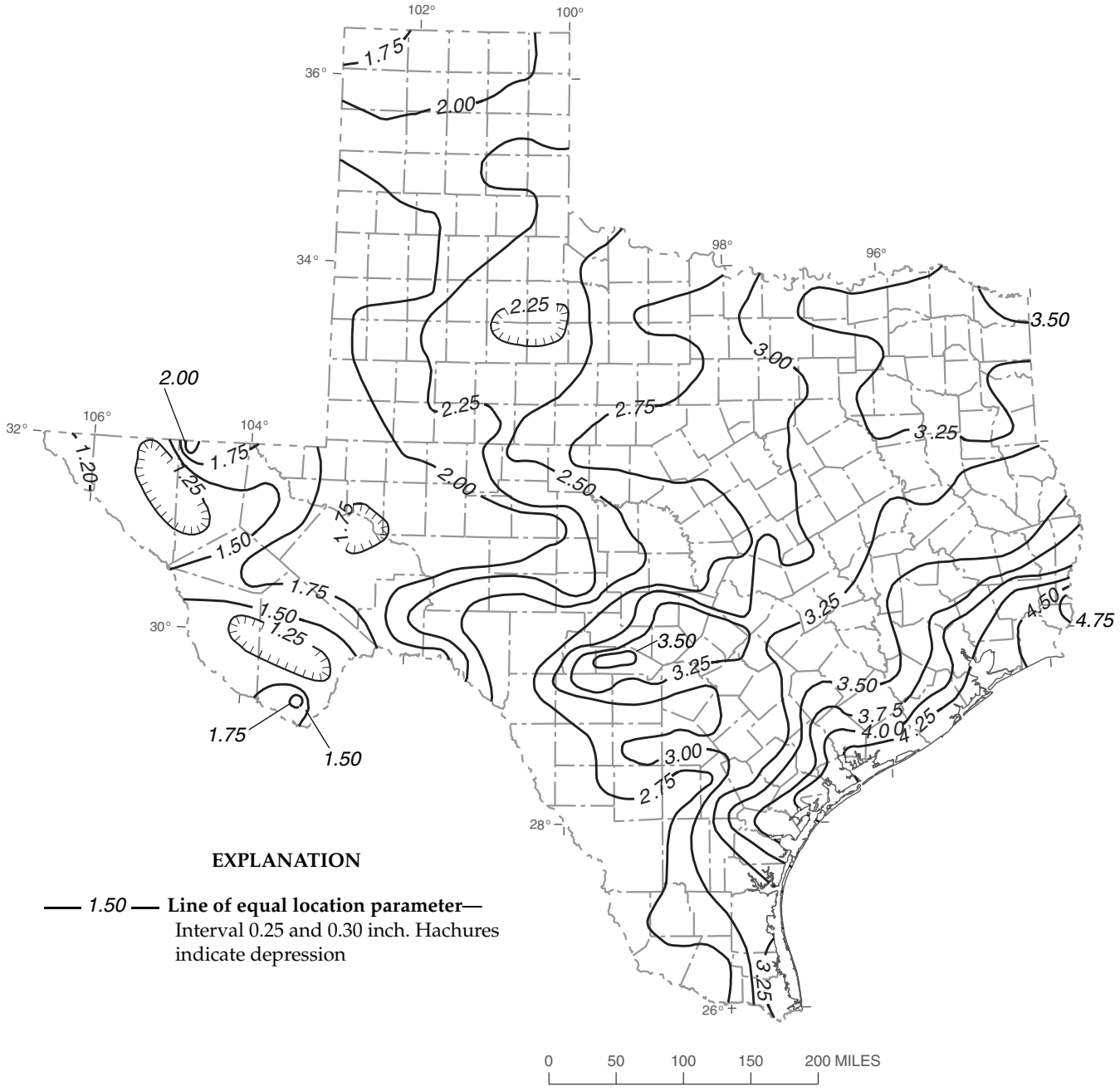

Figure 19. Location (ξ) parameter of generalized extreme-value (GEV) distribution for 1-day precipitation duration in Texas.

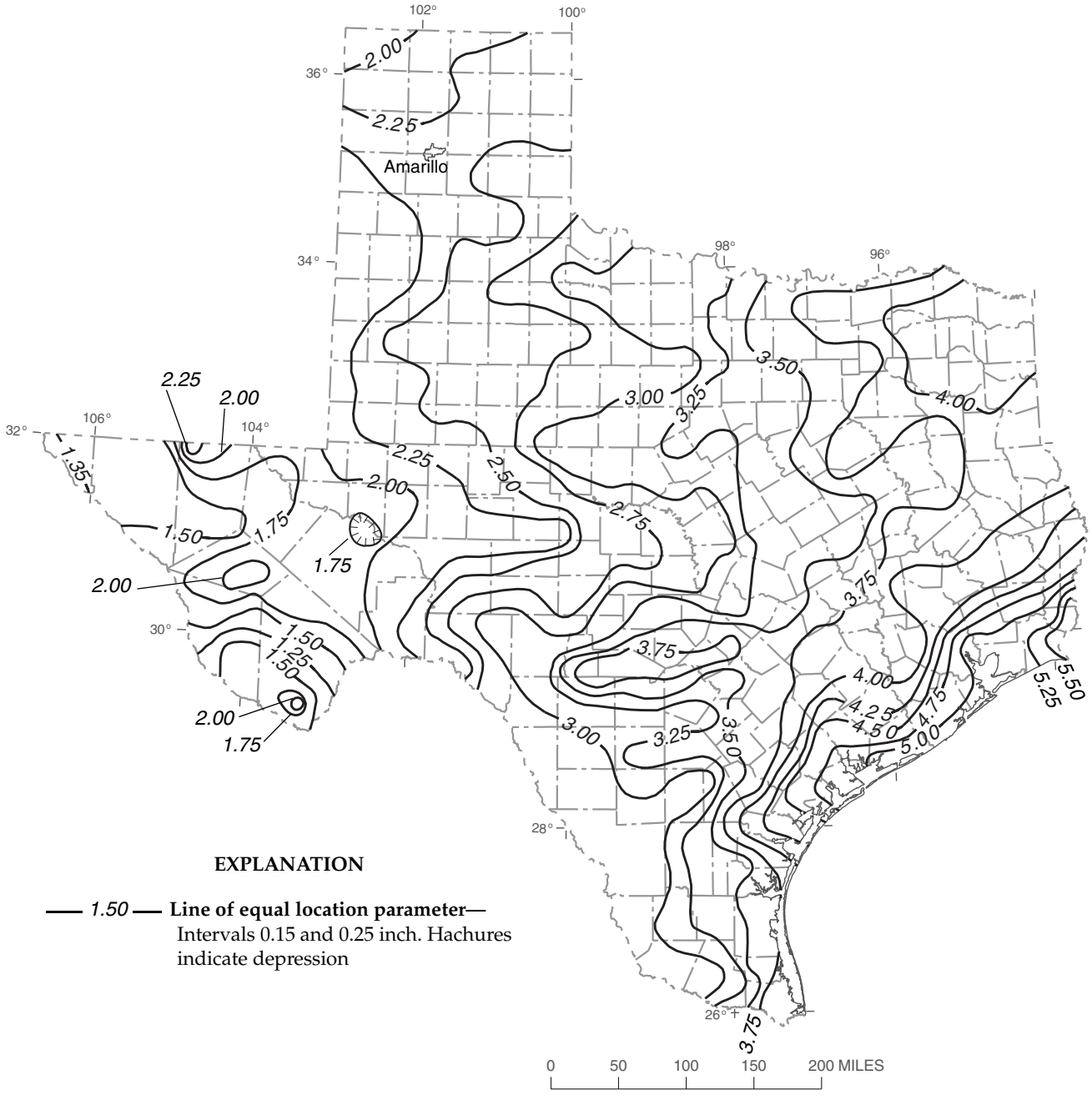

Figure 20. Location (ξ) parameter of generalized extreme-value (GEV) distribution for 2-day precipitation duration in Texas.

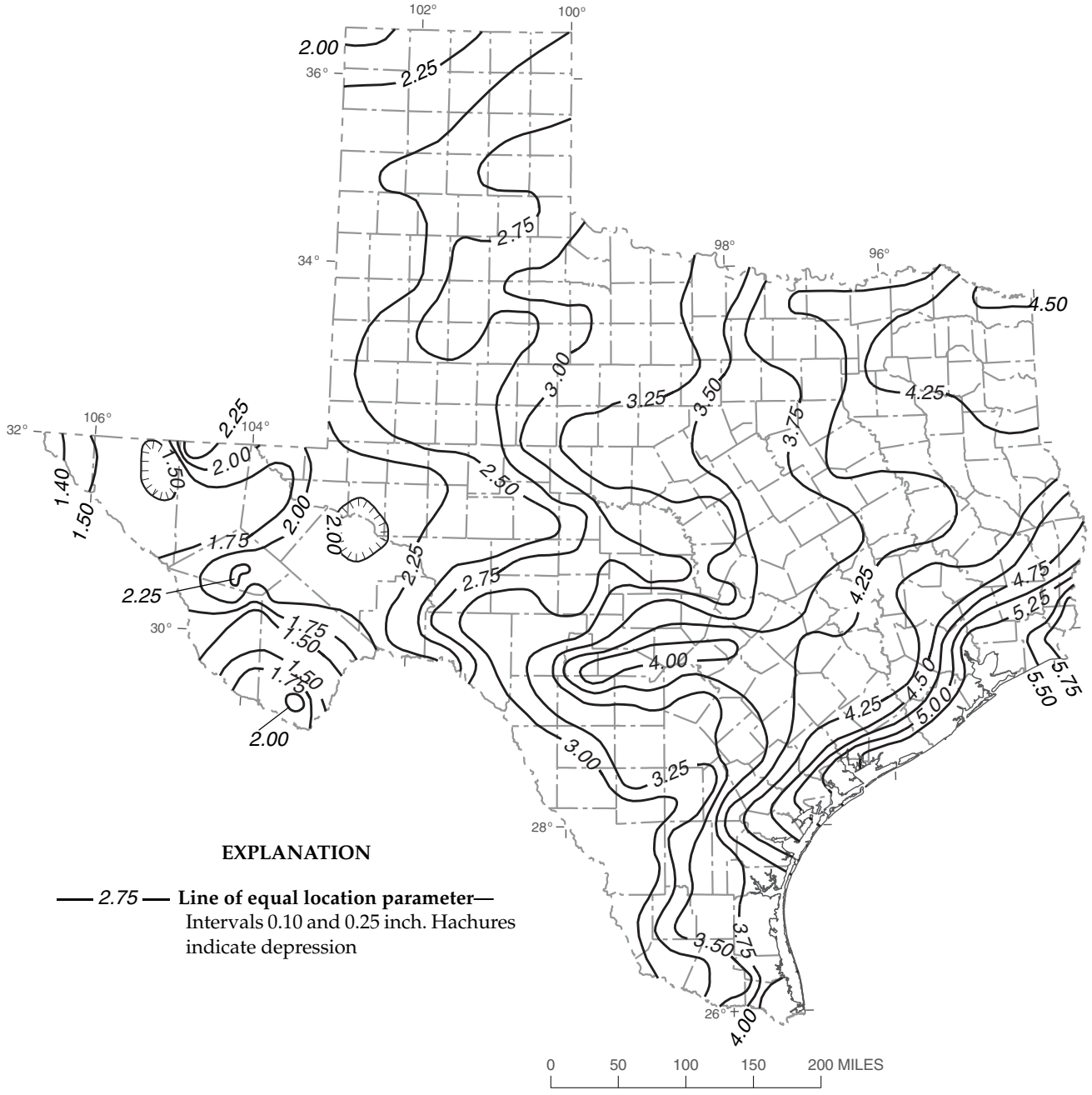

Figure 21. Location (ξ) parameter of generalized extreme-value (GEV) distribution for 3-day precipitation duration in Texas.

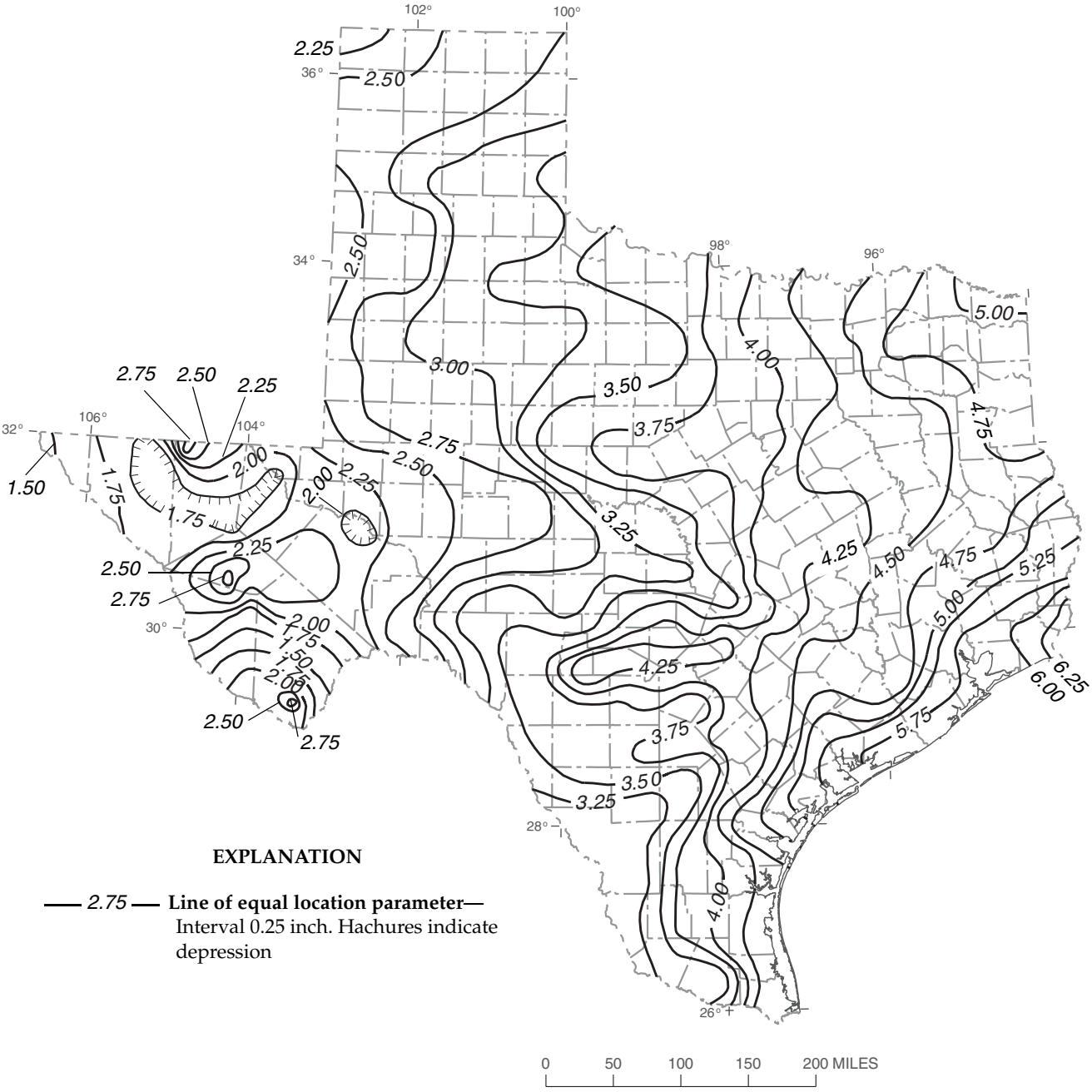

Figure 22. Location (ξ) parameter of generalized extreme-value (GEV) distribution for 5-day precipitation duration in Texas.

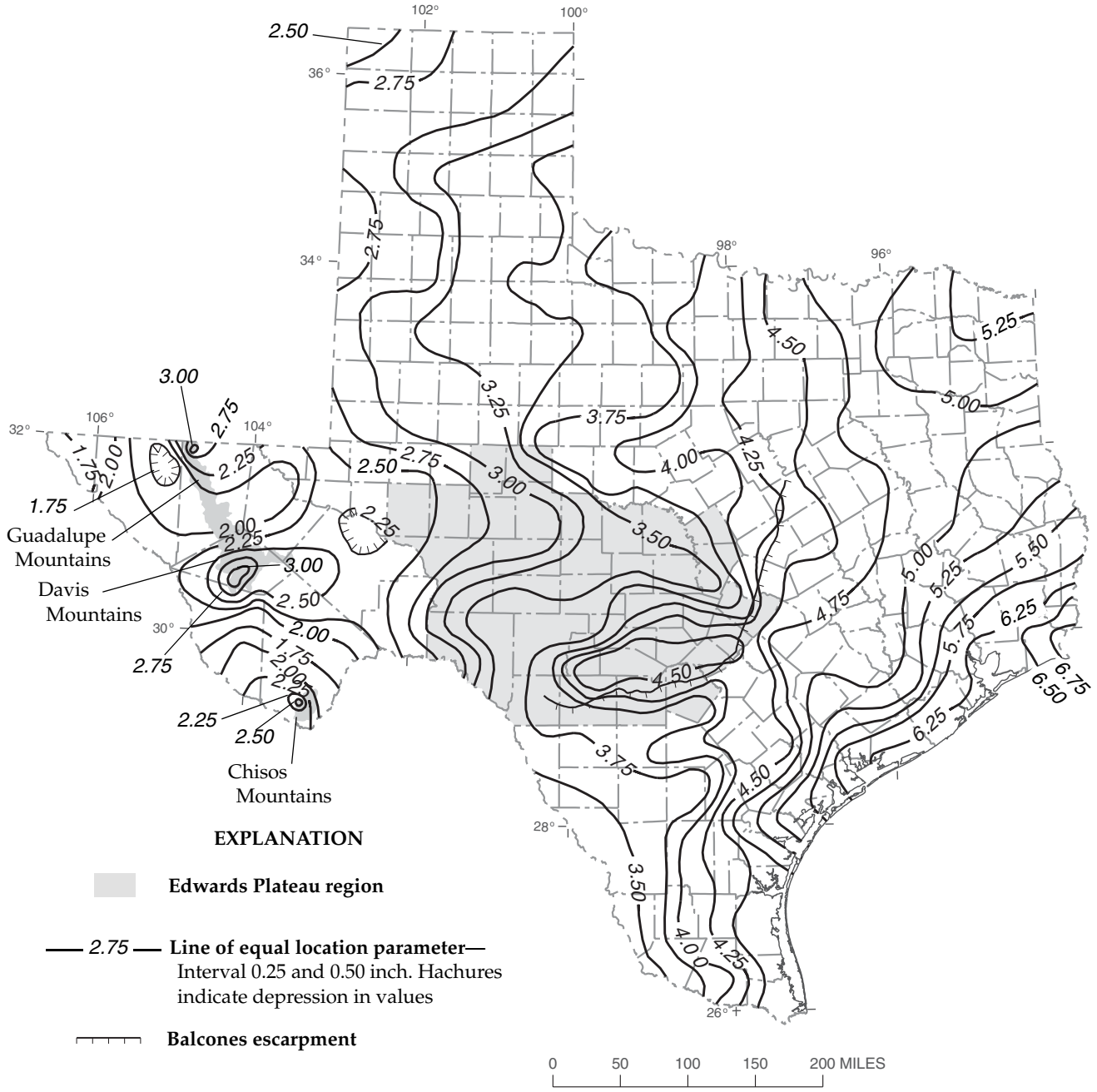

Figure 23. Location (ξ) parameter of generalized extreme-value (GEV) distribution for 7-day precipitation duration in Texas.

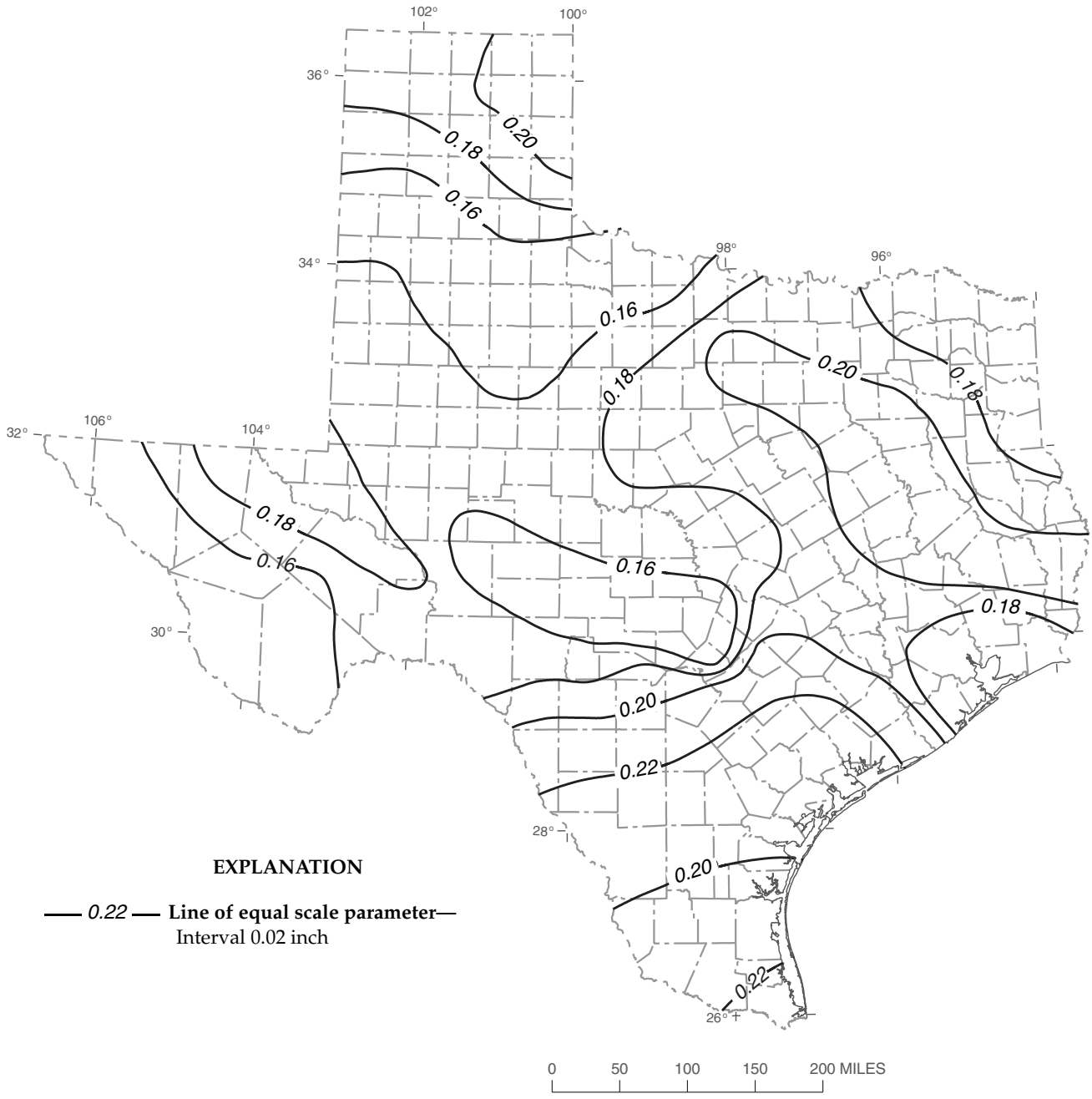

Figure 24. Scale (α) parameter of generalized logistic (GLO) distribution for 15-minute precipitation duration in Texas.

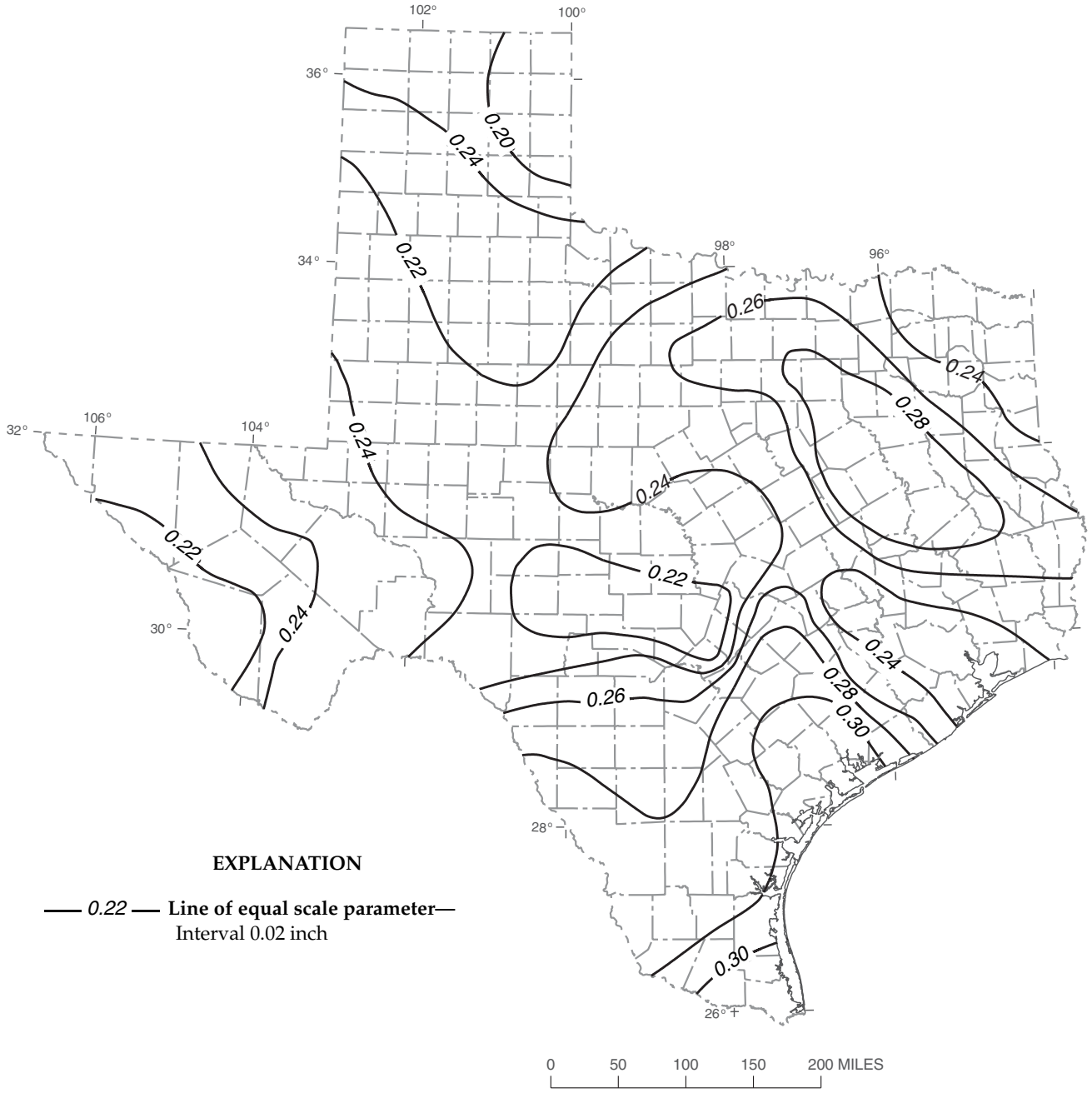

Figure 25. Scale (α) parameter of generalized logistic (GLO) distribution for 30-minute precipitation duration in Texas.

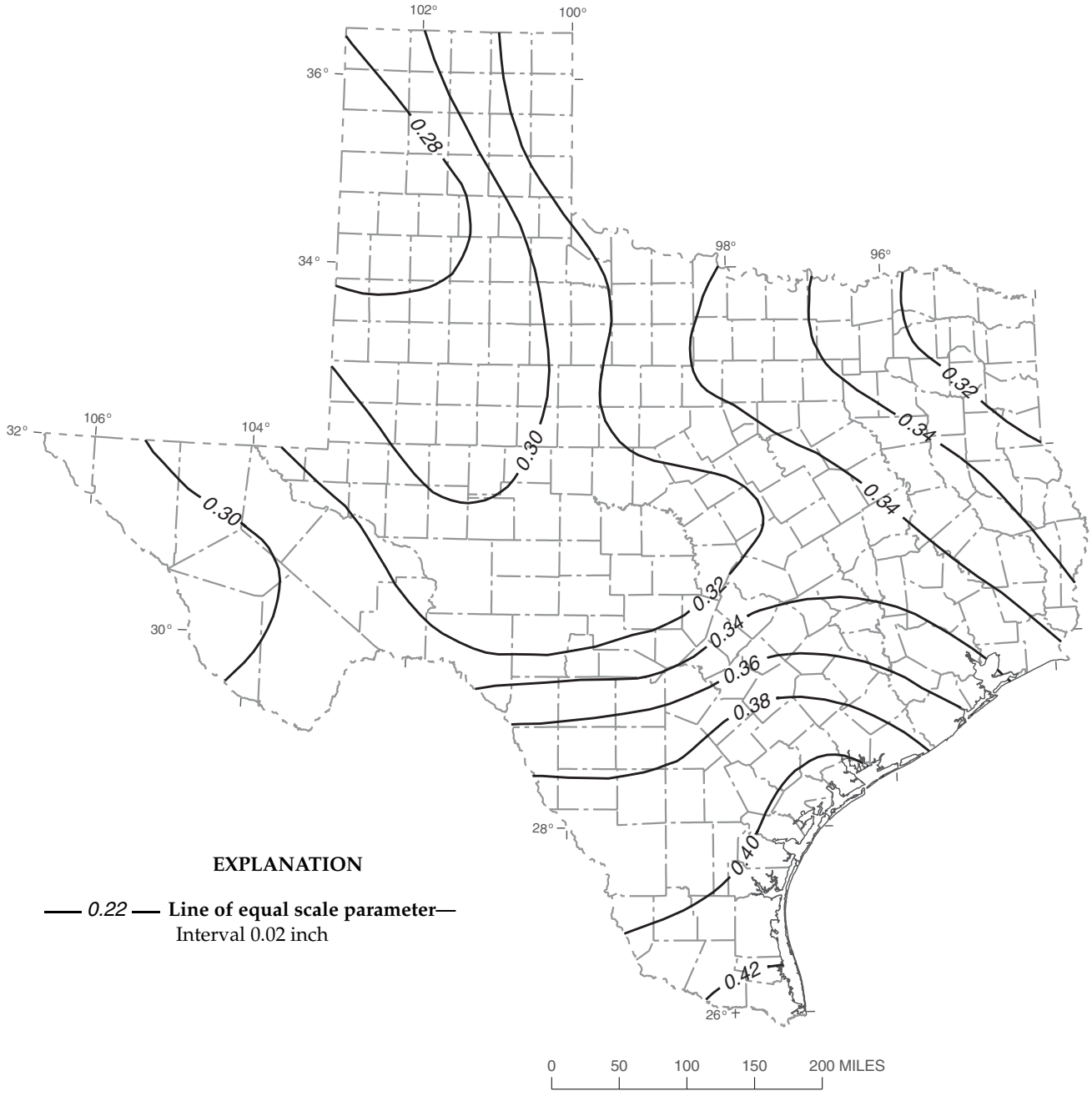

Figure 26. Scale (α) parameter of generalized logistic (GLO) distribution for 60-minute precipitation duration in Texas.

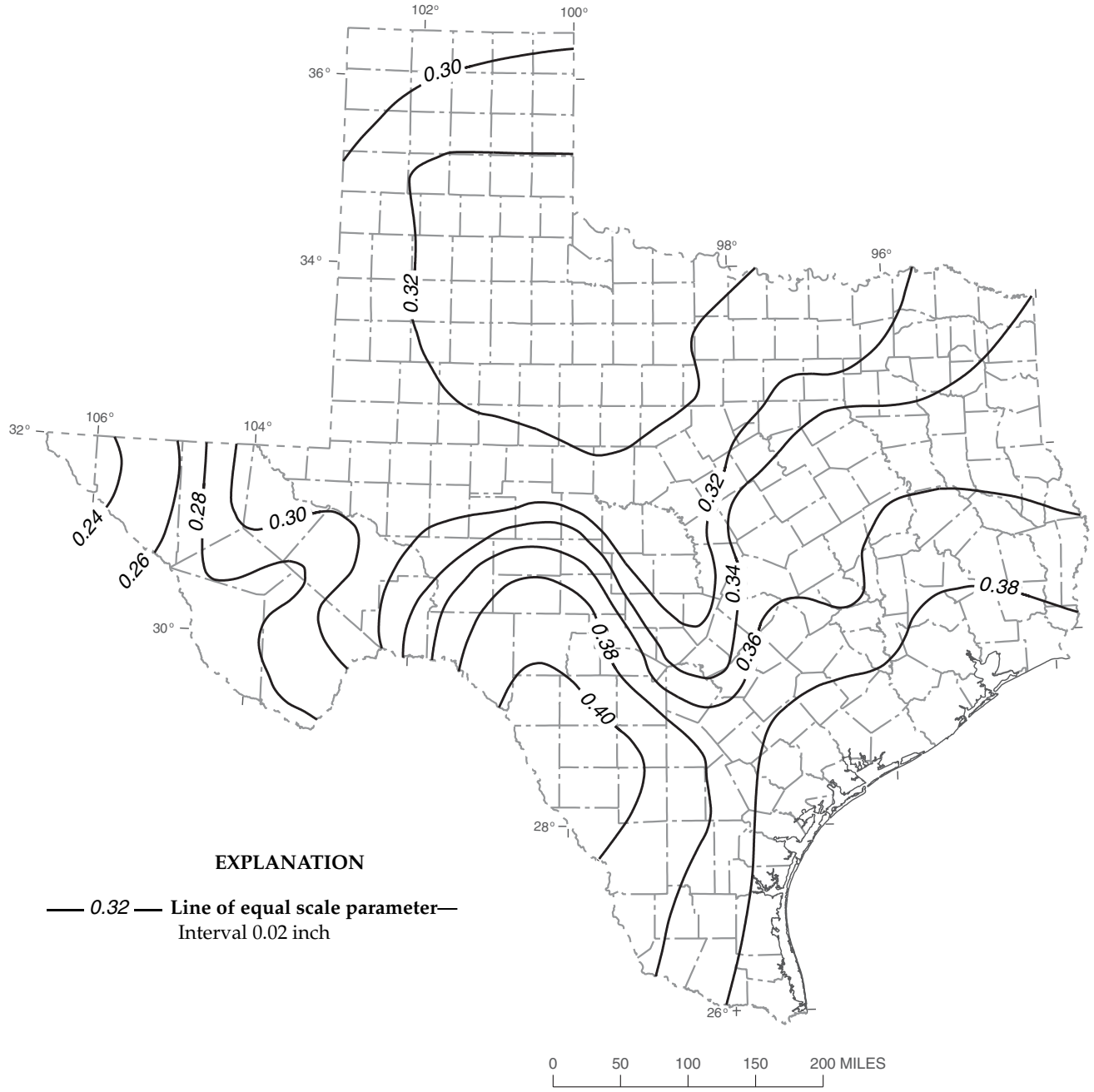

Figure 27. Scale (α) parameter of generalized logistic (GLO) distribution for 1-hour precipitation duration in Texas.

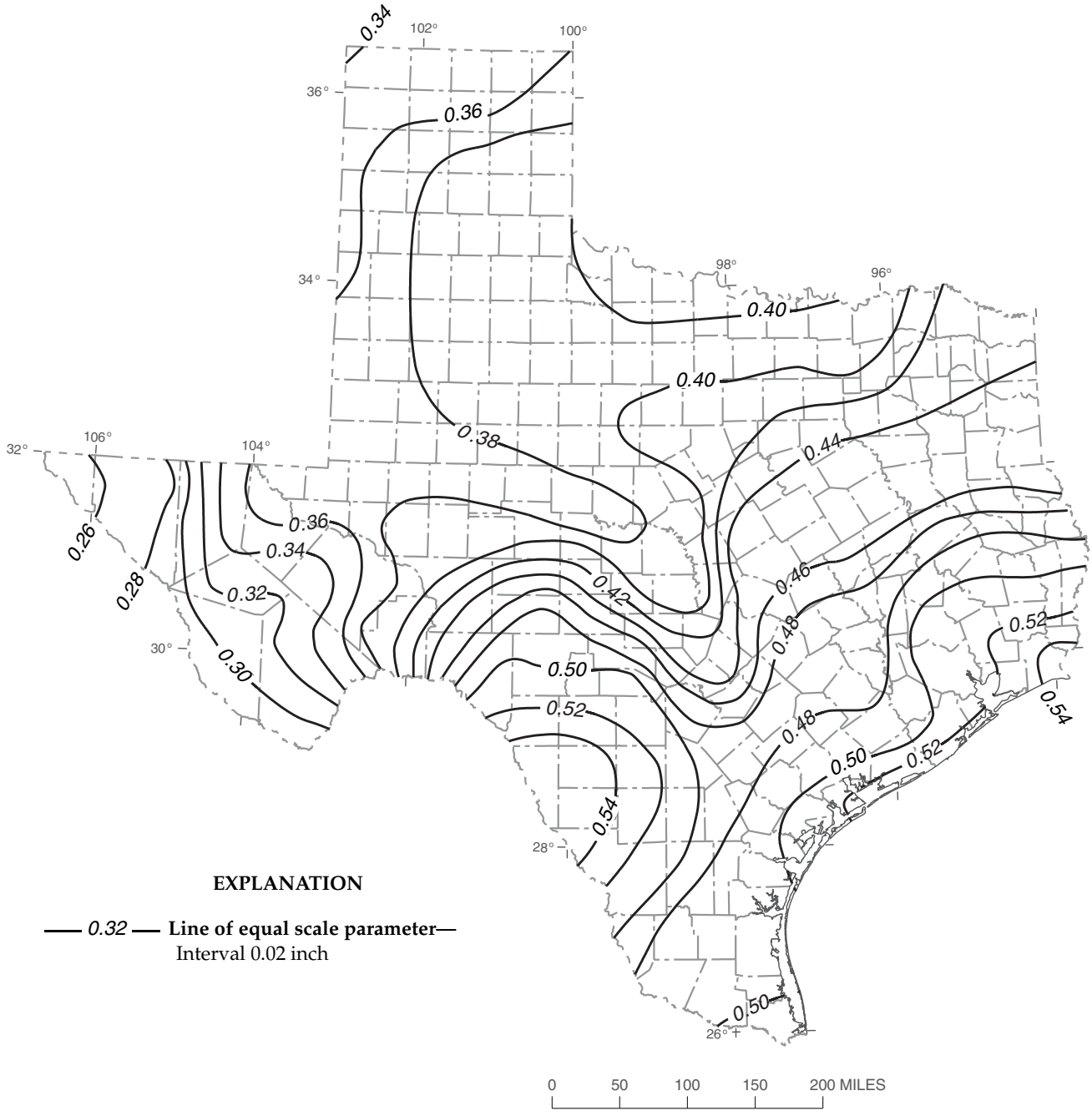

Figure 28. Scale (α) parameter of generalized logistic (GLO) distribution for 2-hour precipitation duration in Texas.

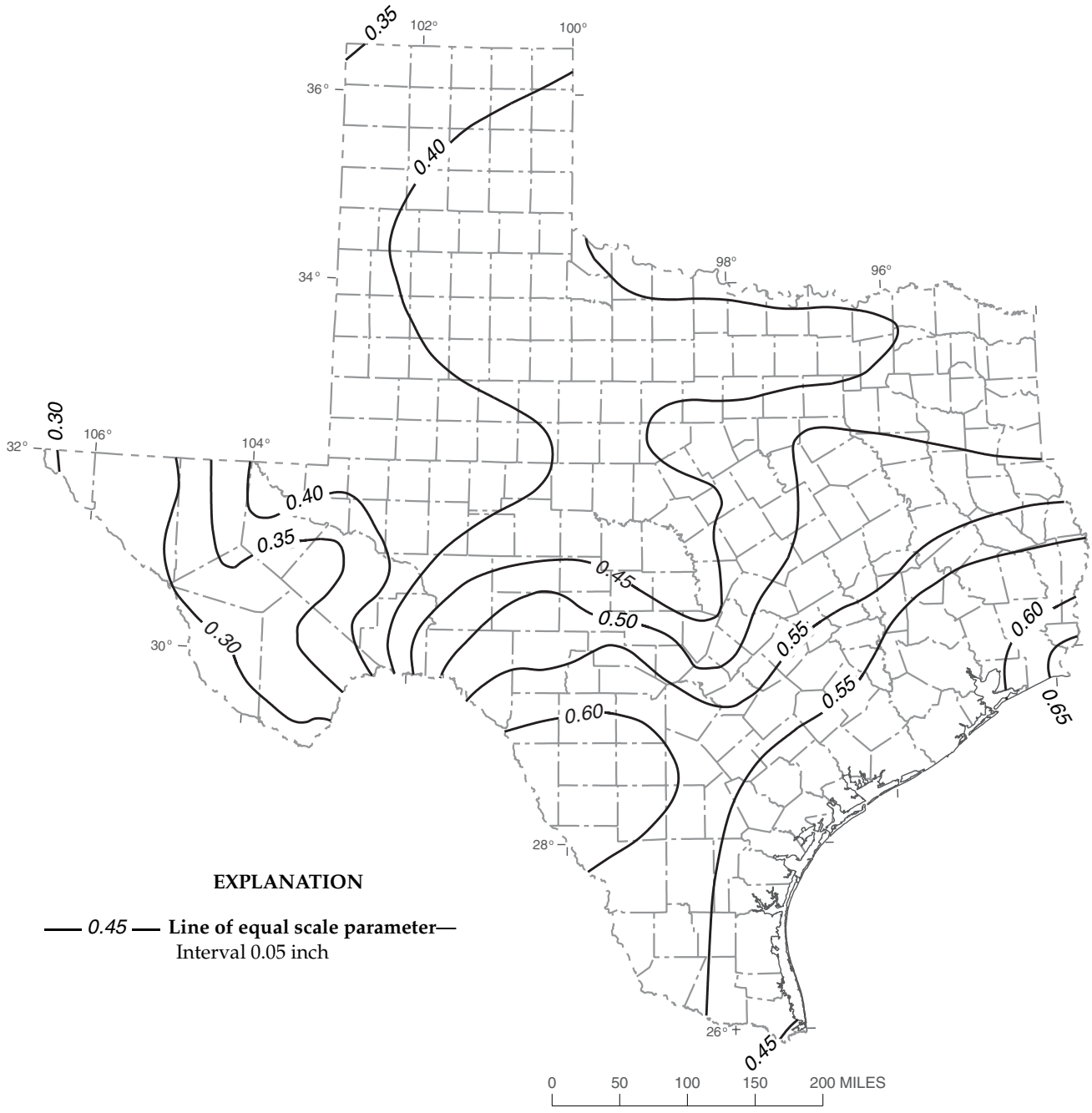

Figure 29. Scale (α) parameter of generalized logistic (GLO) distribution for 3-hour precipitation duration in Texas.

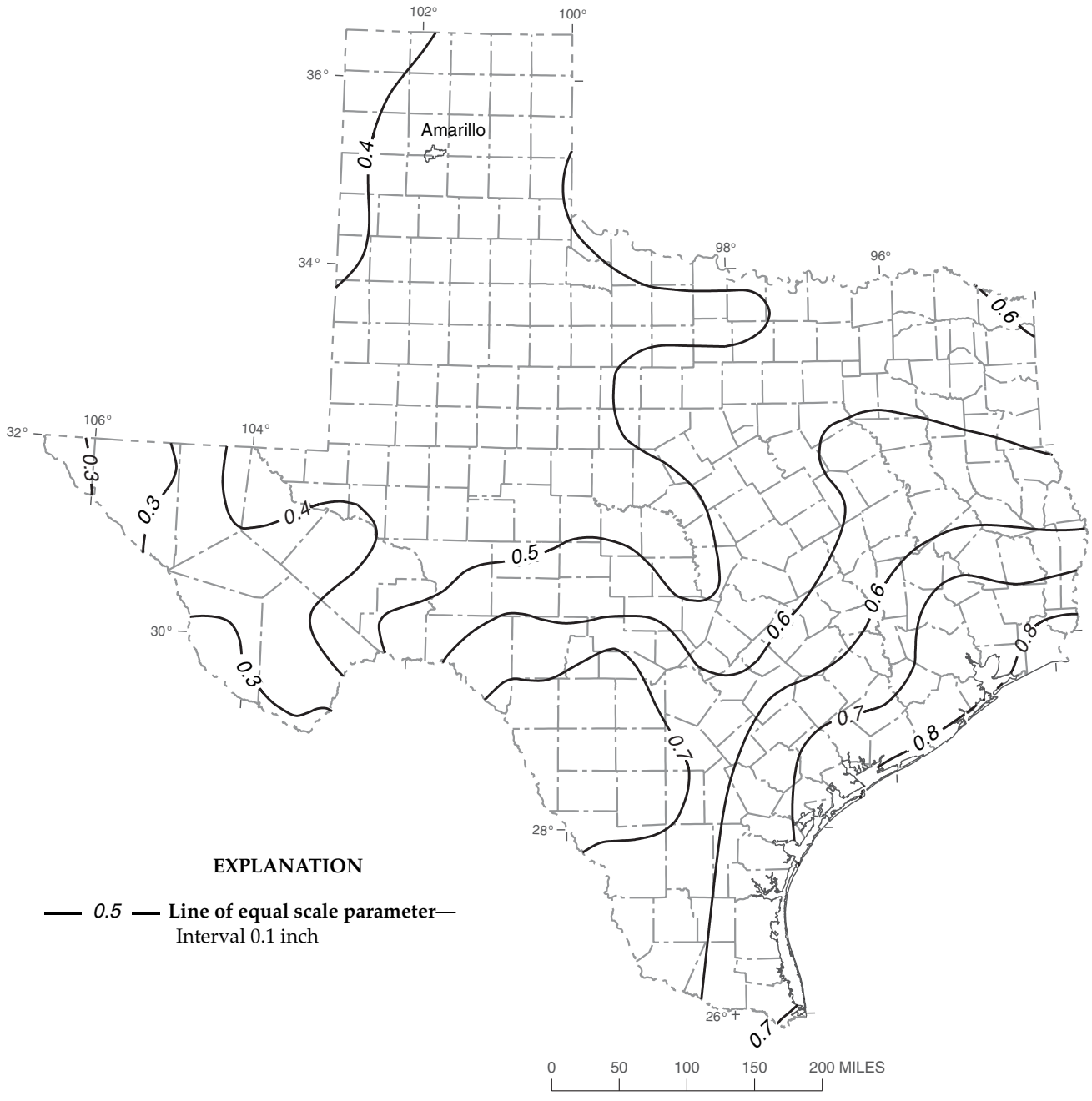

Figure 30. Scale (α) parameter of generalized logistic (GLO) distribution for 6-hour precipitation duration in Texas.

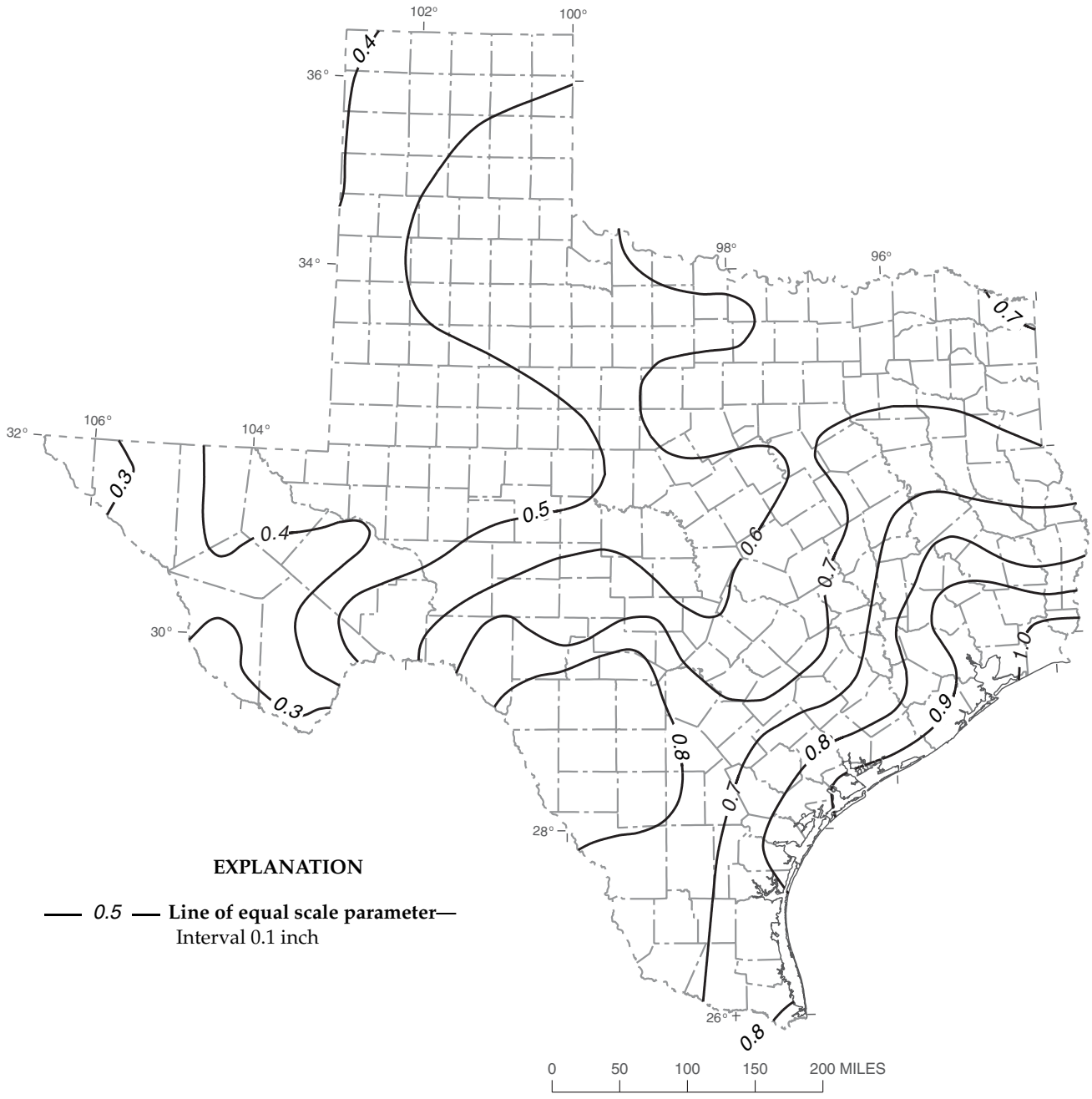

Figure 31. Scale (α) parameter of generalized logistic (GLO) distribution for 12-hour precipitation duration in Texas.

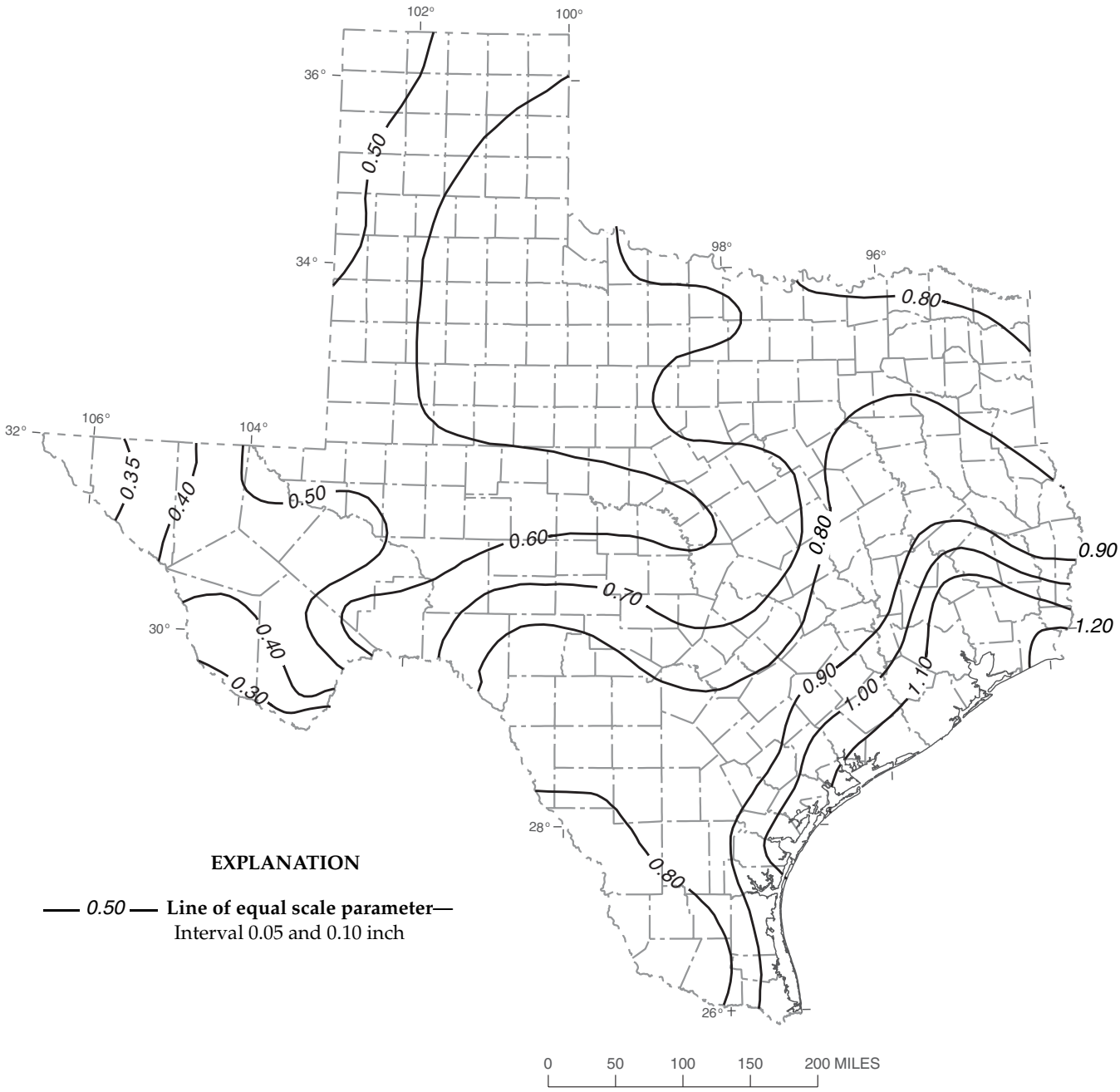

Figure 32. Scale (α) parameter of generalized logistic (GLO) distribution for 24-hour precipitation duration in Texas.

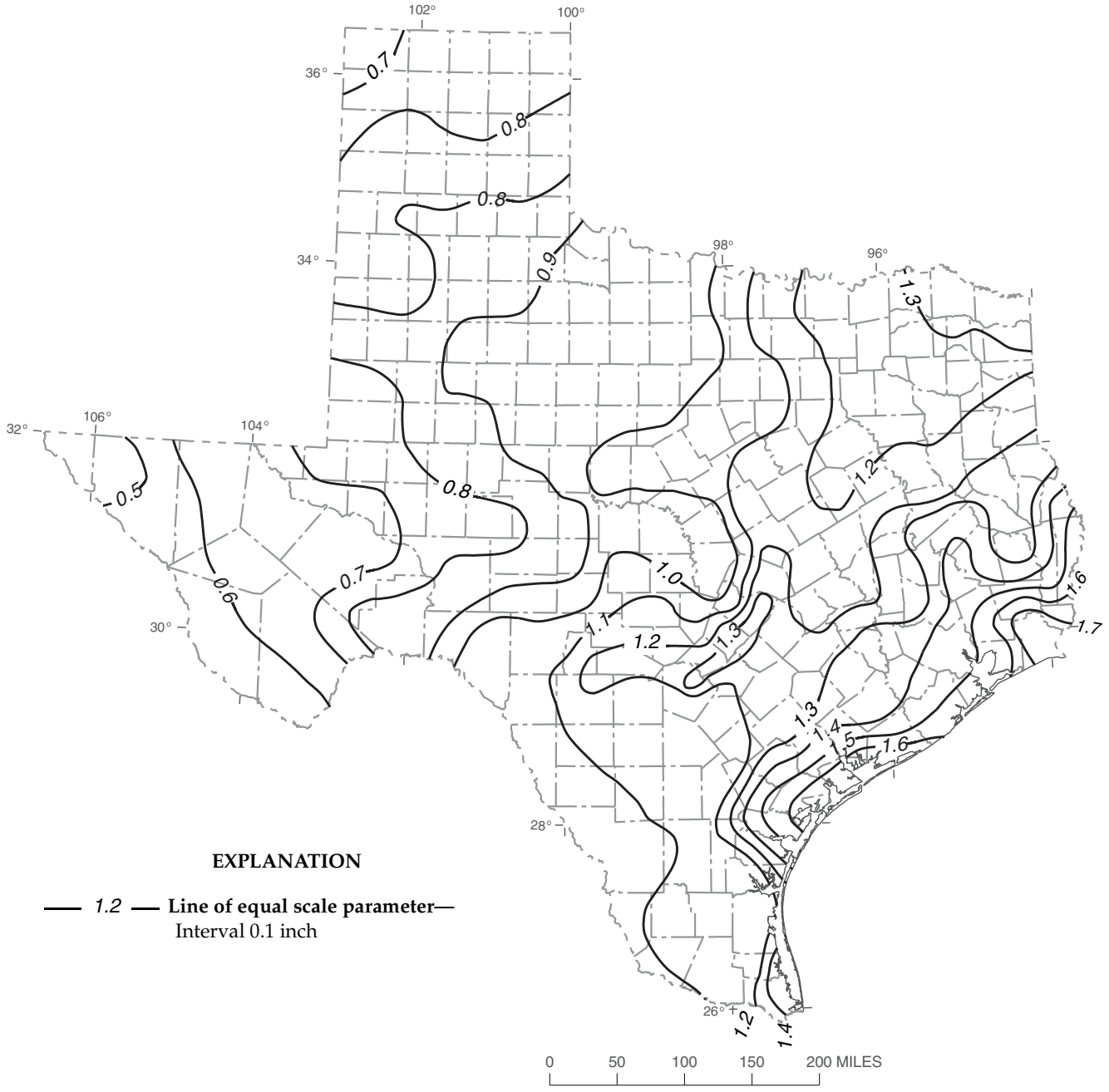

Figure 33. Scale (α) parameter of generalized extreme-value (GEV) distribution for 1-day precipitation duration in Texas.

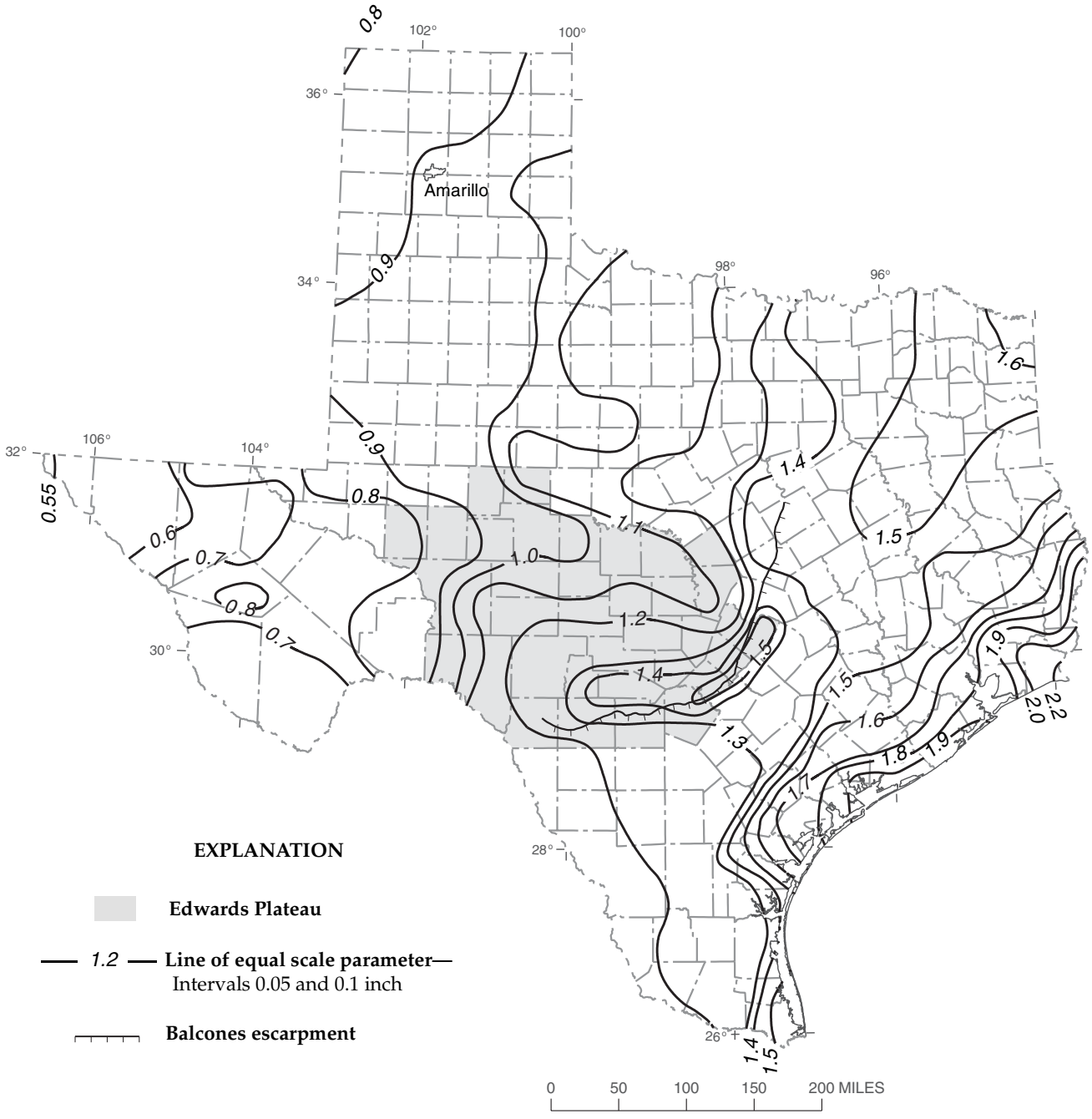

Figure 34. Scale (α) parameter of generalized extreme-value (GEV) distribution for 2-day precipitation duration in Texas.

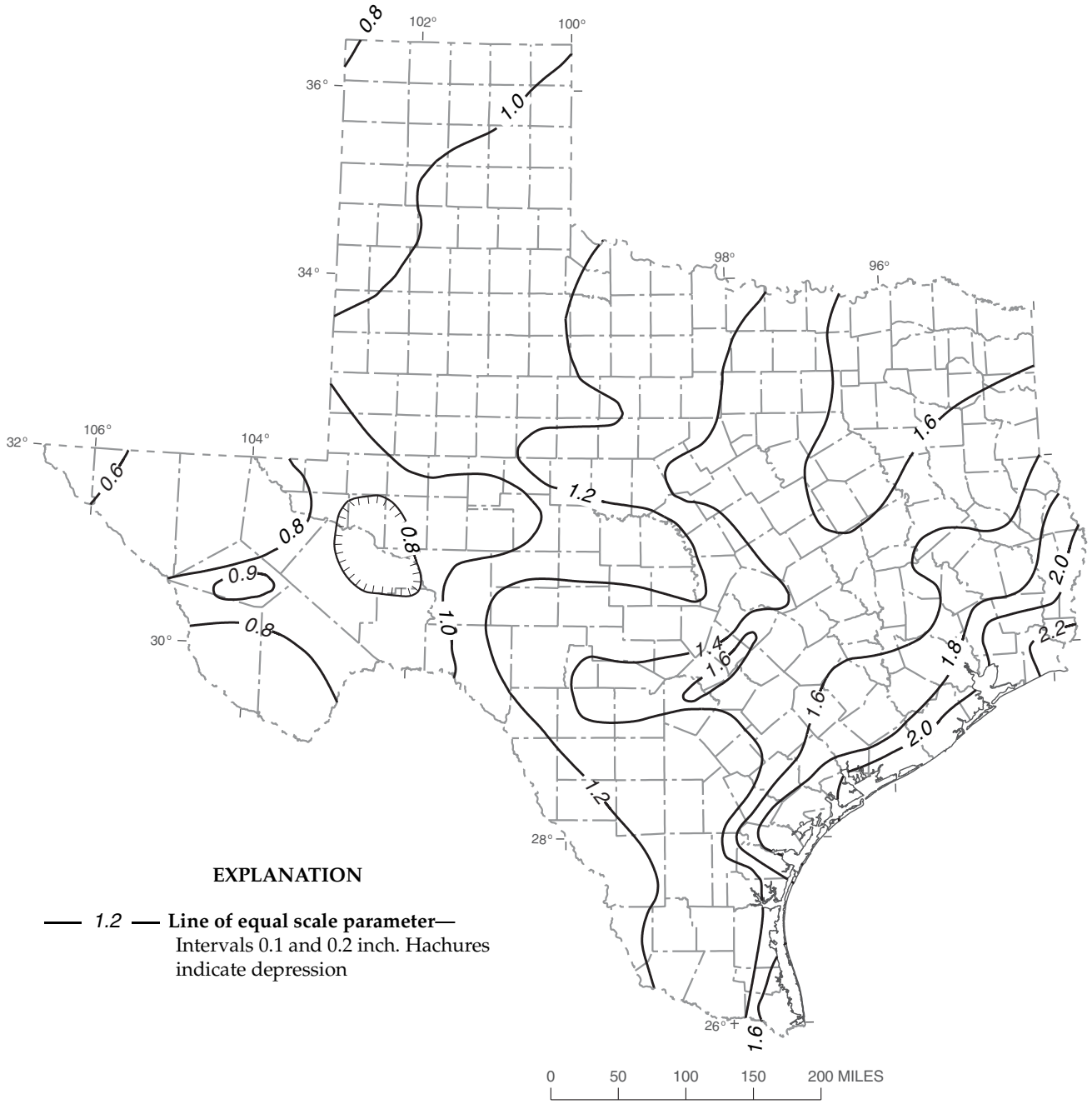

Figure 35. Scale (α) parameter of generalized extreme-value (GEV) distribution for 3-day precipitation duration in Texas.

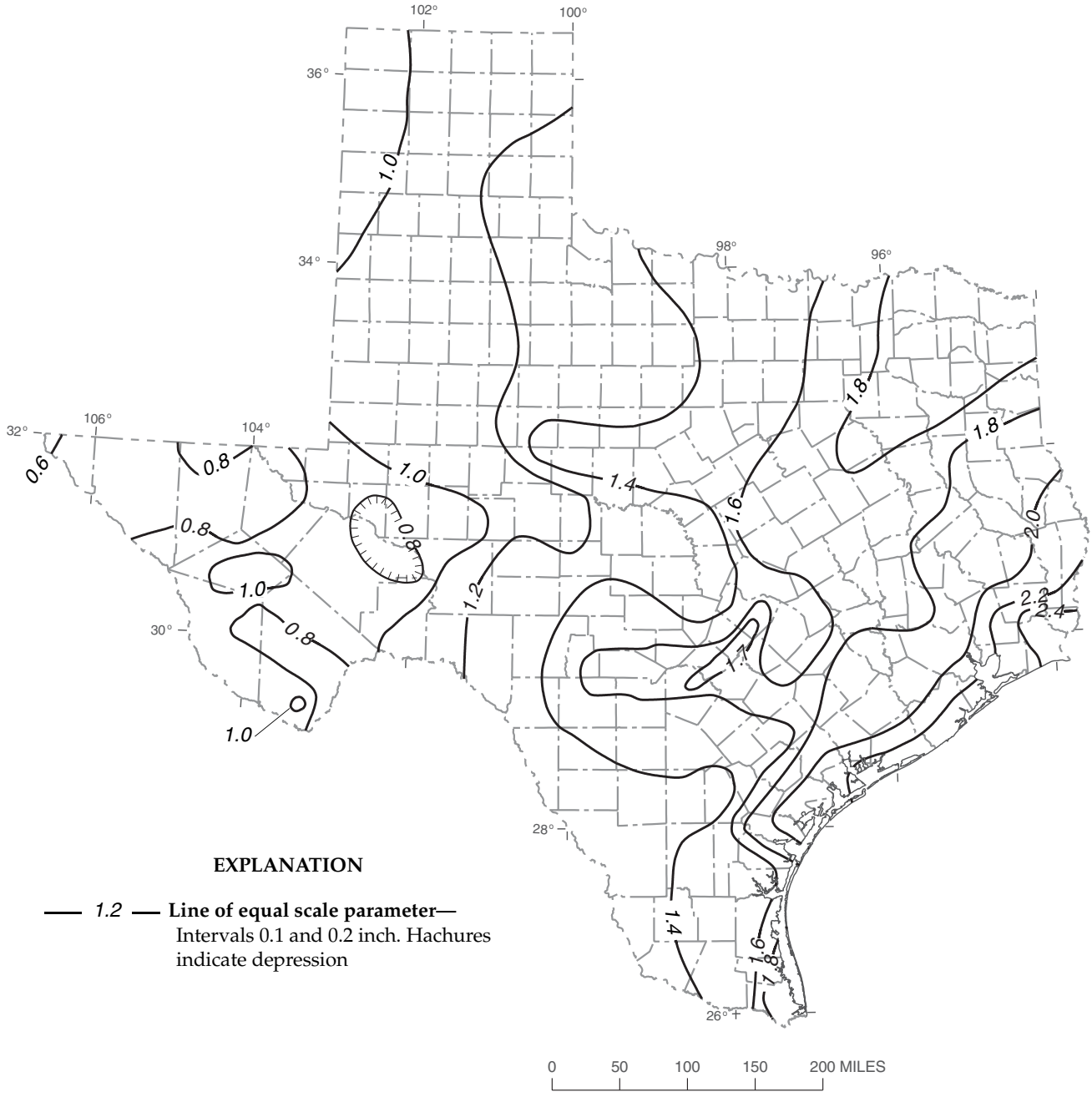

Figure 36. Scale (α) parameter of generalized extreme-value (GEV) distribution for 5-day precipitation duration in Texas.

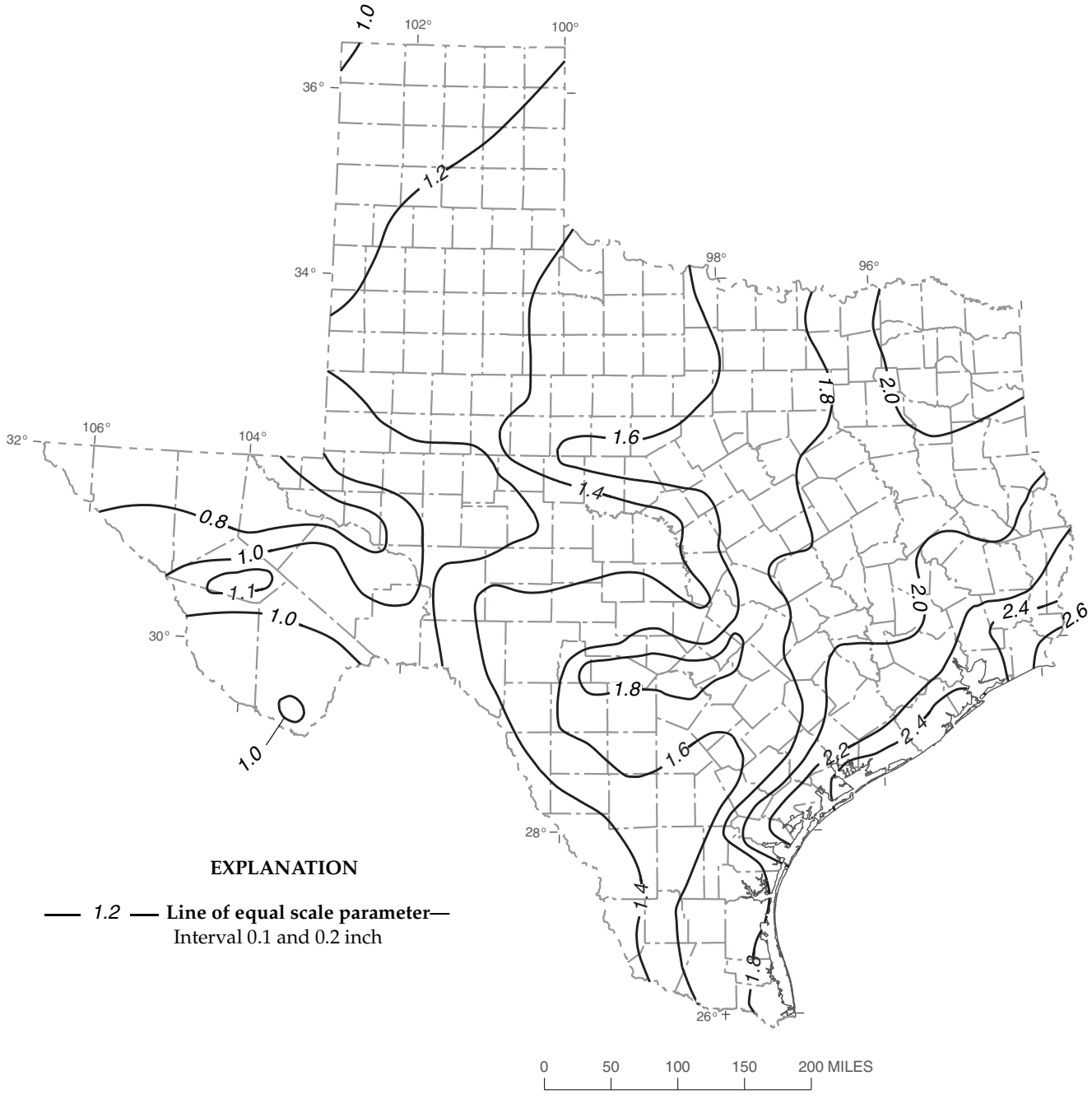

Figure 37. Scale (α) parameter of generalized extreme-value (GEV) distribution for 7-day precipitation duration in Texas.

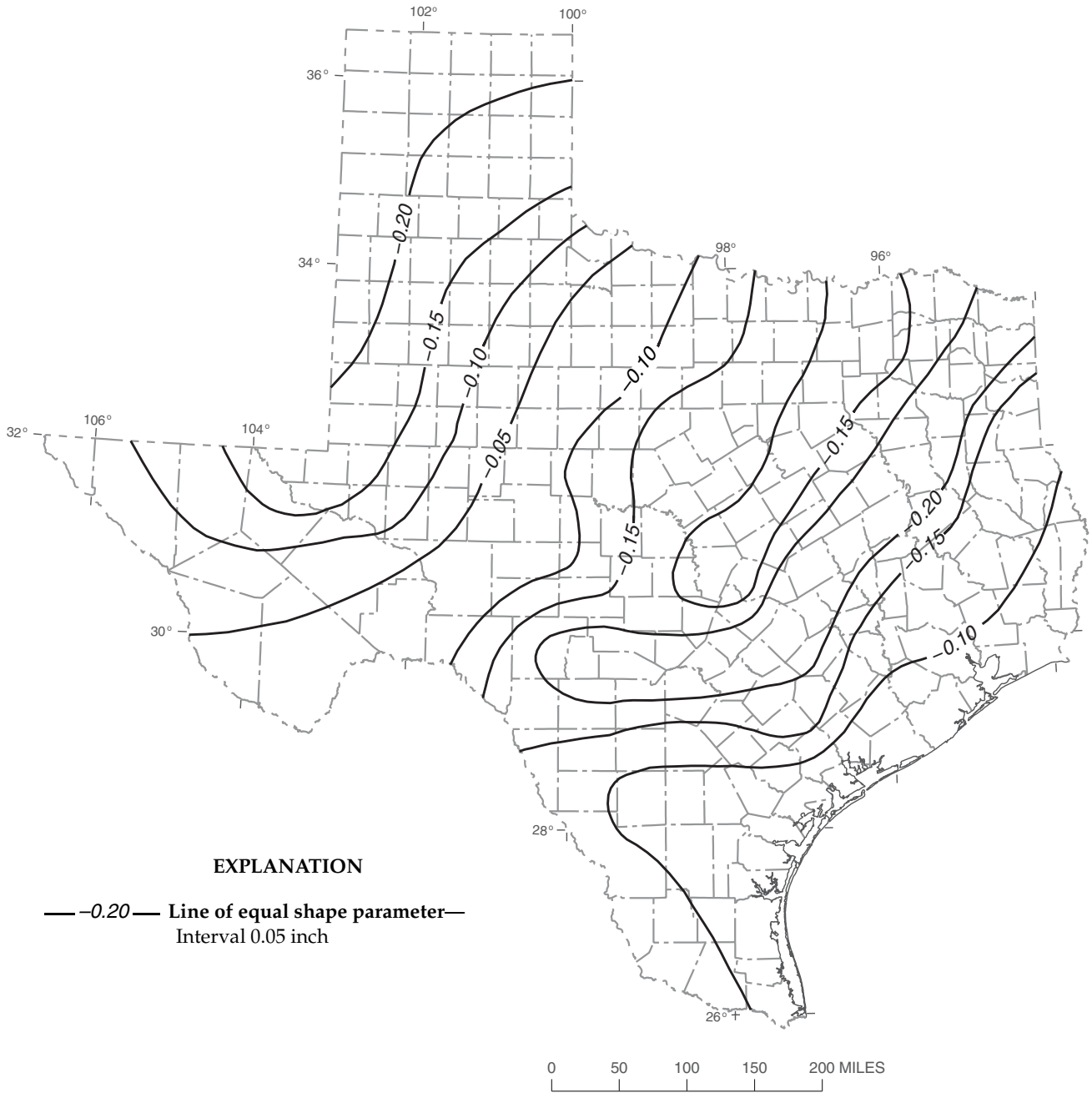

Figure 38. Shape (κ) parameter of generalized logistic (GLO) distribution for 15-minute precipitation duration in Texas.

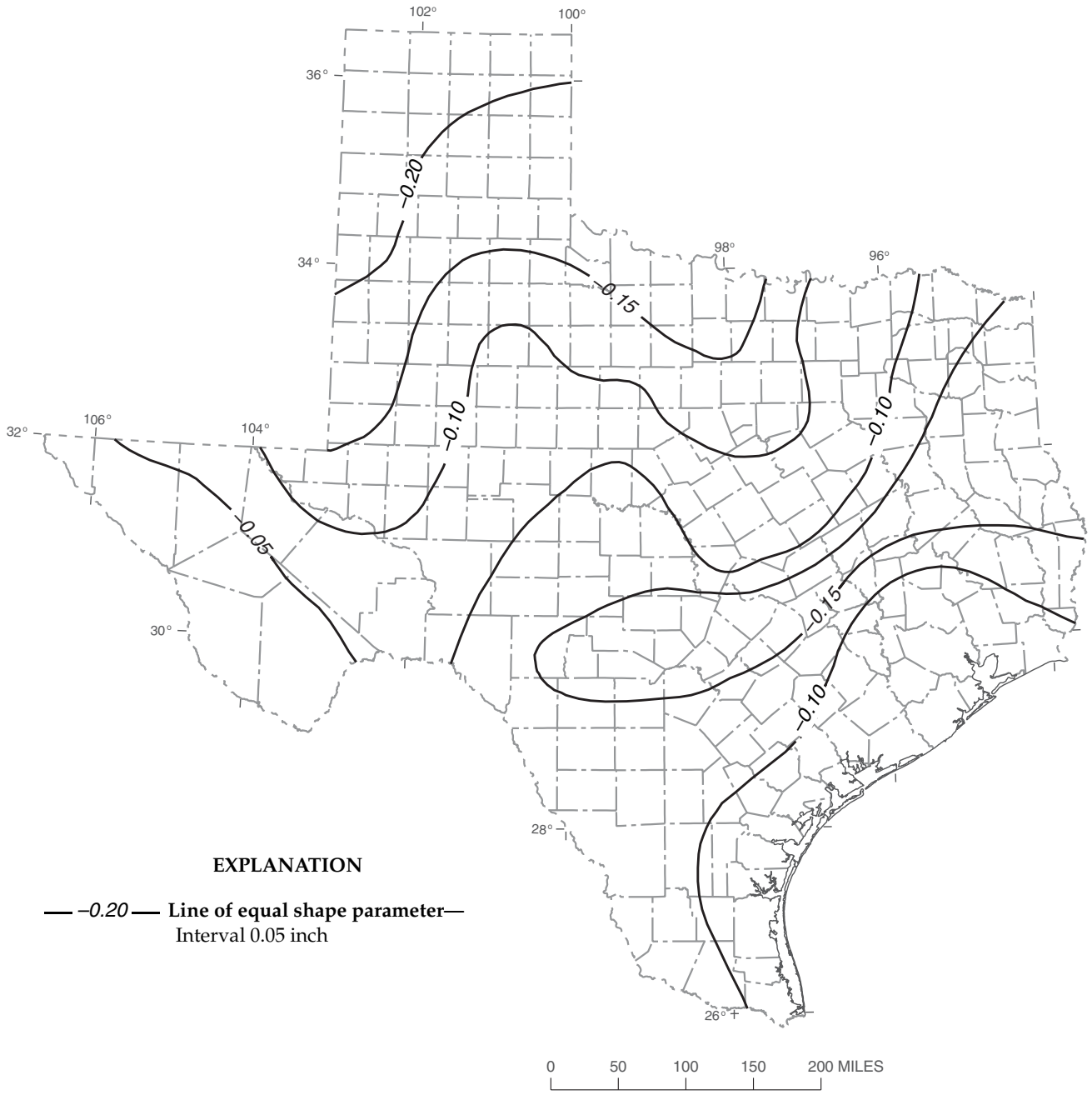

Figure 39. Shape (κ) parameter of generalized logistic (GLO) distribution for 30-minute precipitation duration in Texas.

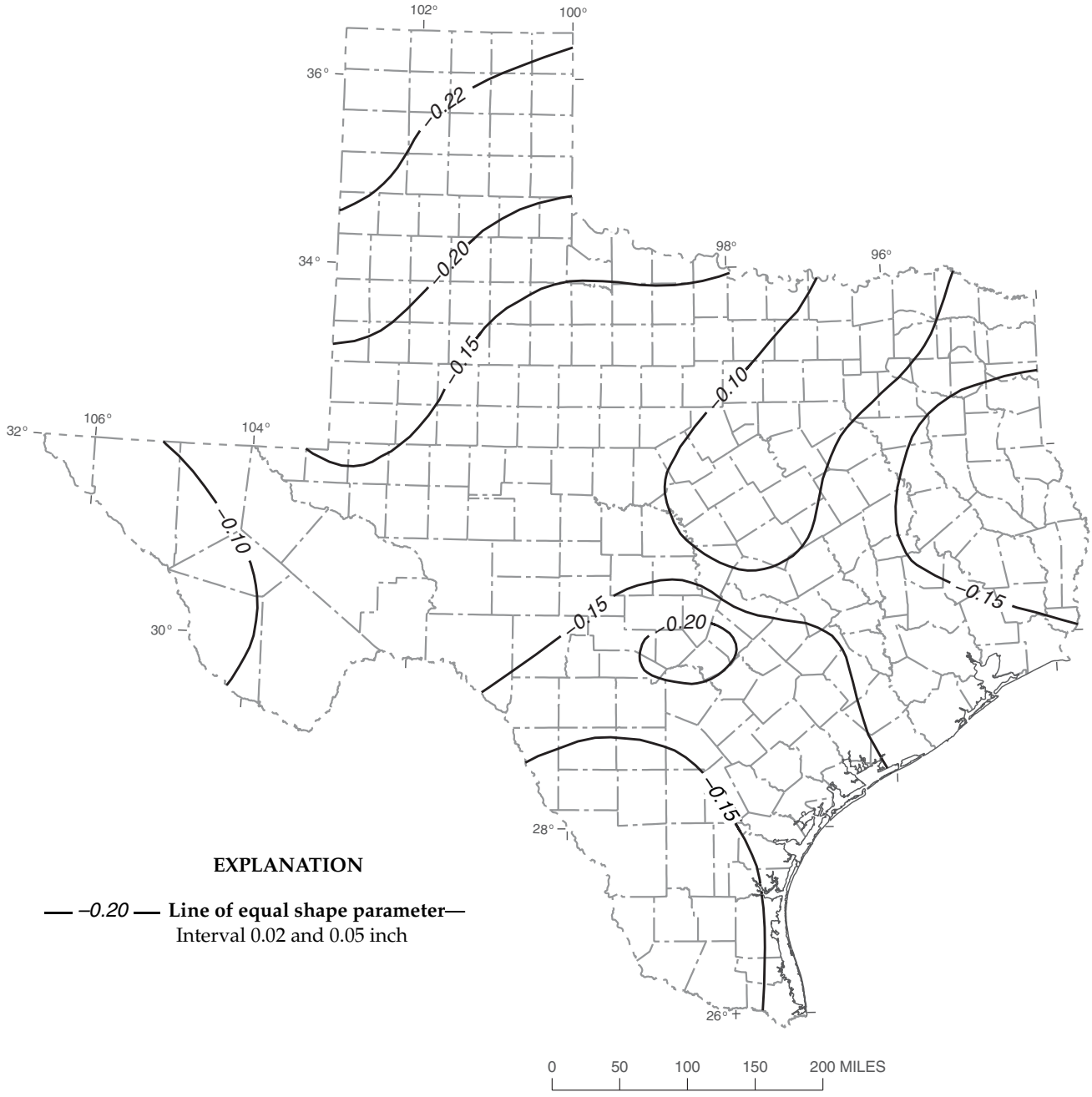

Figure 40. Shape (κ) parameter of generalized logistic (GLO) distribution for 60-minute precipitation duration in Texas.

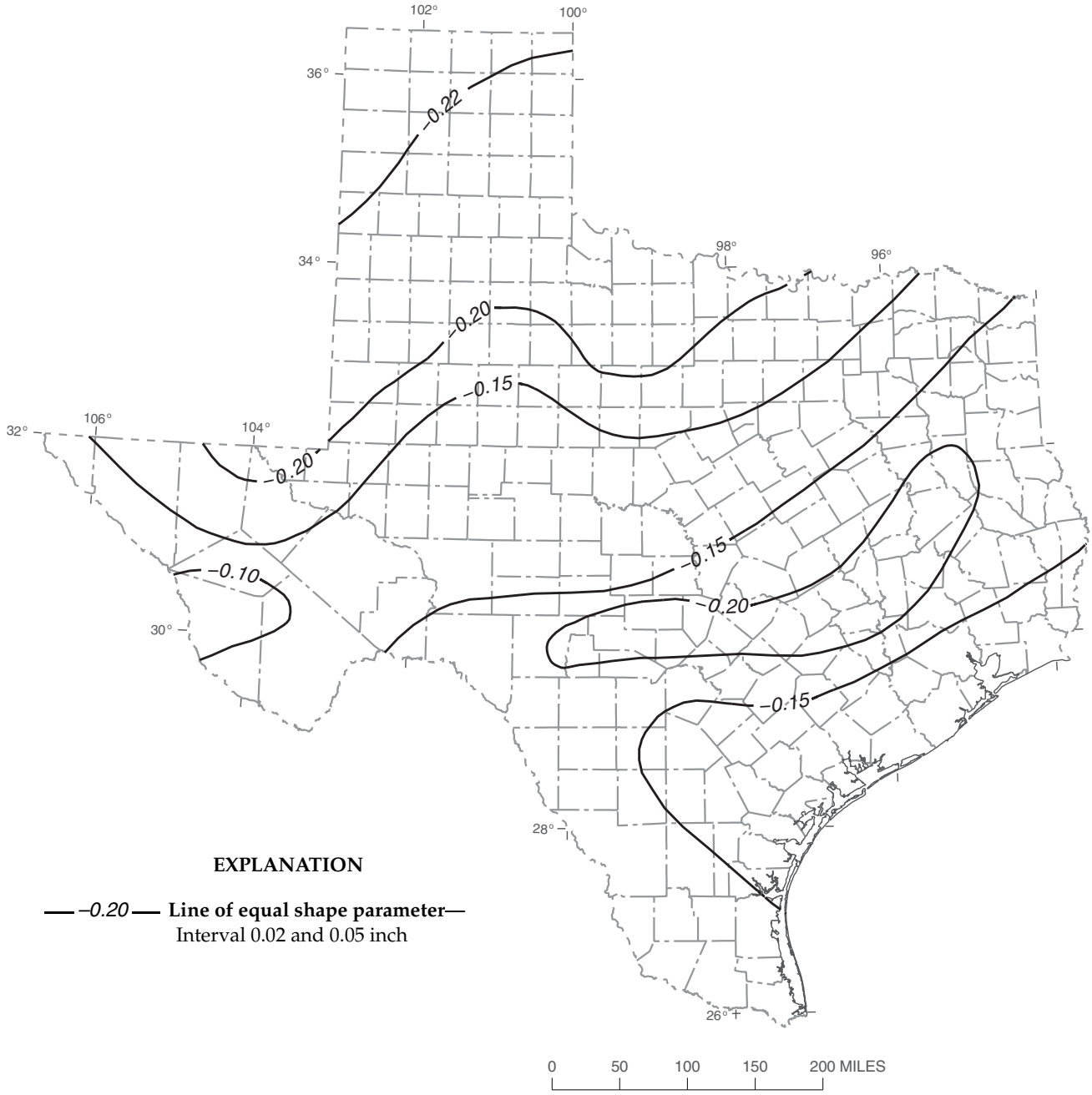

Figure 41. Shape (κ) parameter of generalized logistic (GLO) distribution for 1-hour precipitation duration in Texas.

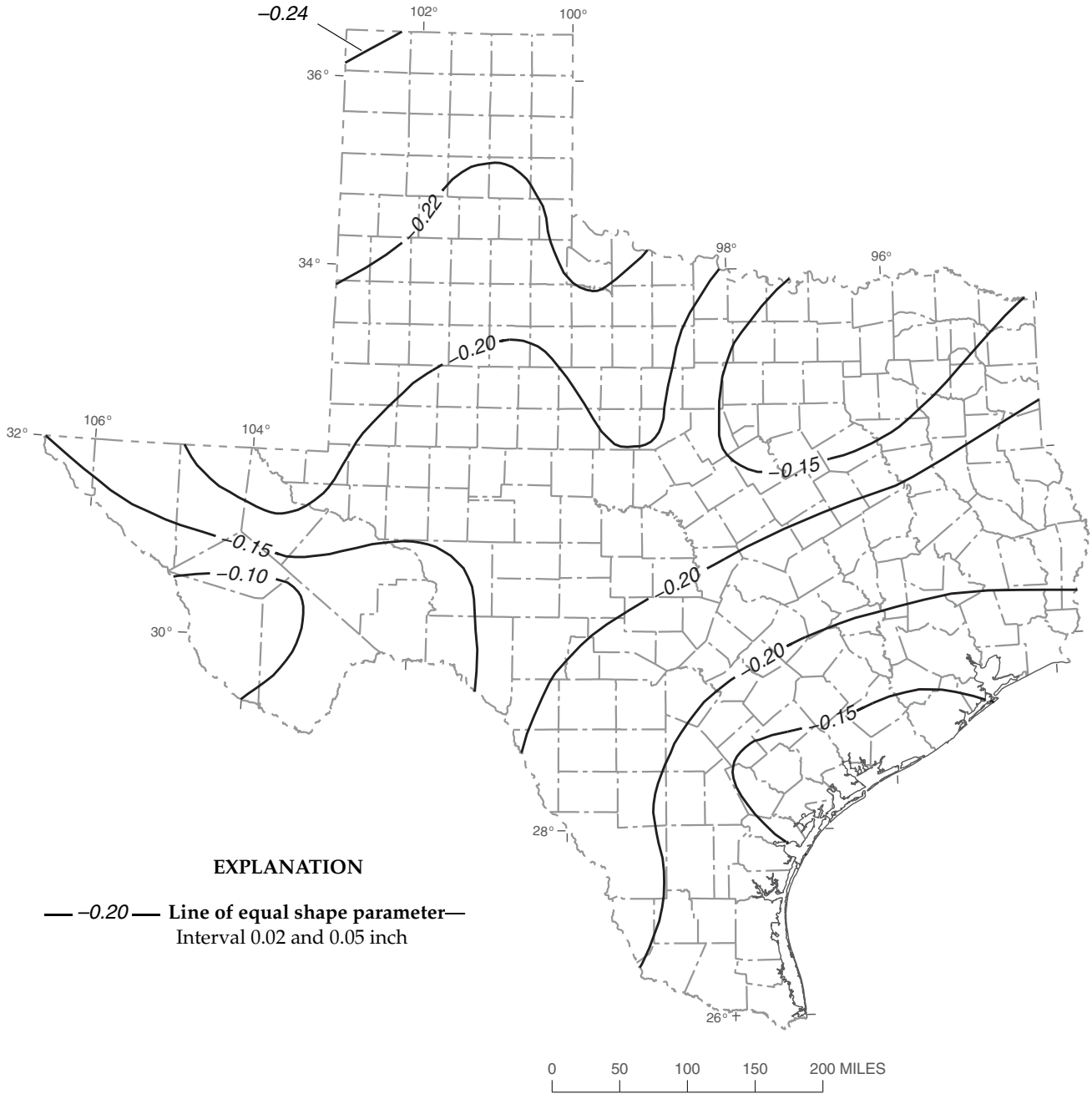

Figure 42. Shape (κ) parameter of generalized logistic (GLO) distribution for 2-hour precipitation duration in Texas.

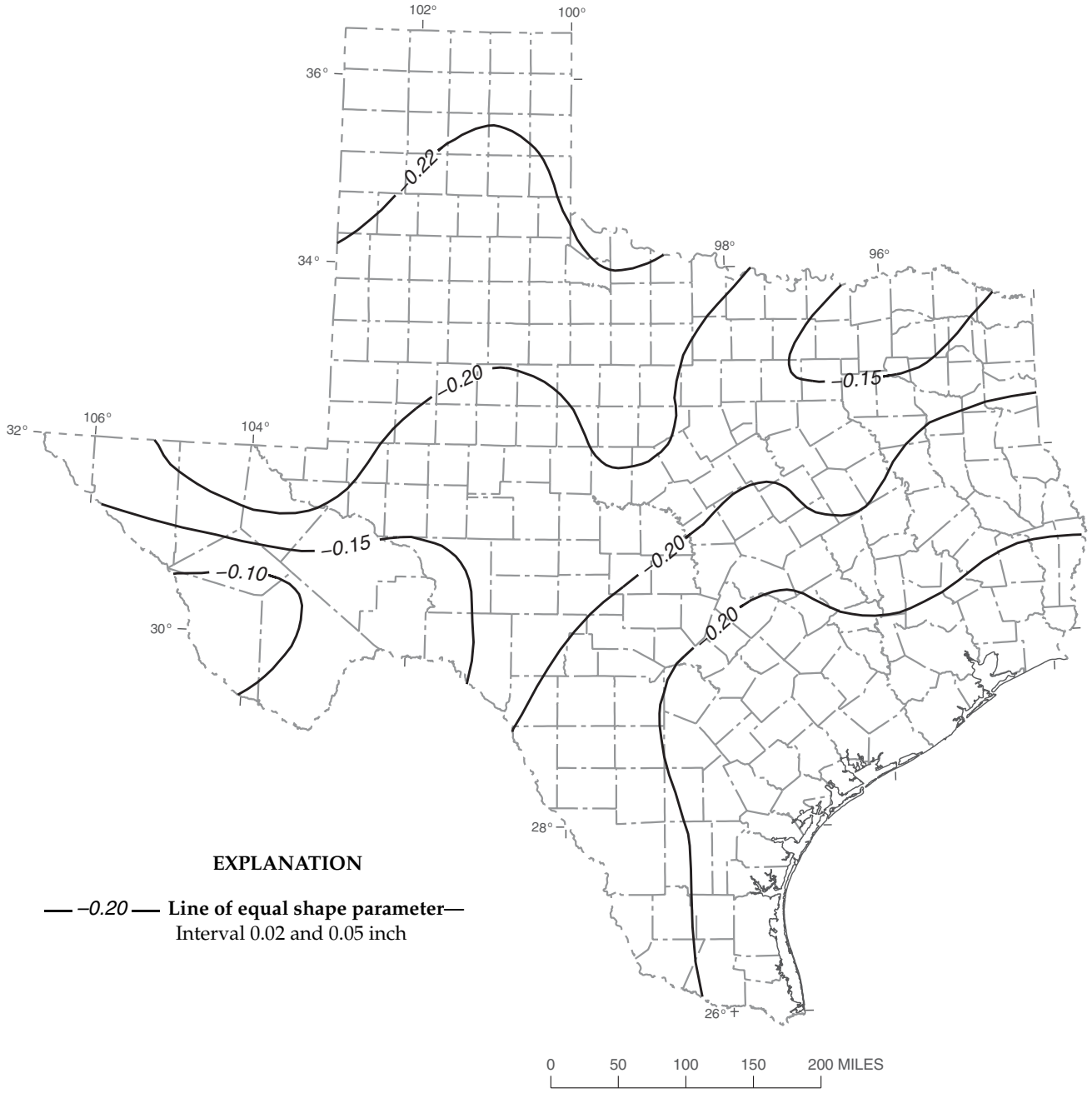

Figure 43. Shape (κ) parameter of generalized logistic (GLO) distribution for 3-hour precipitation duration in Texas.

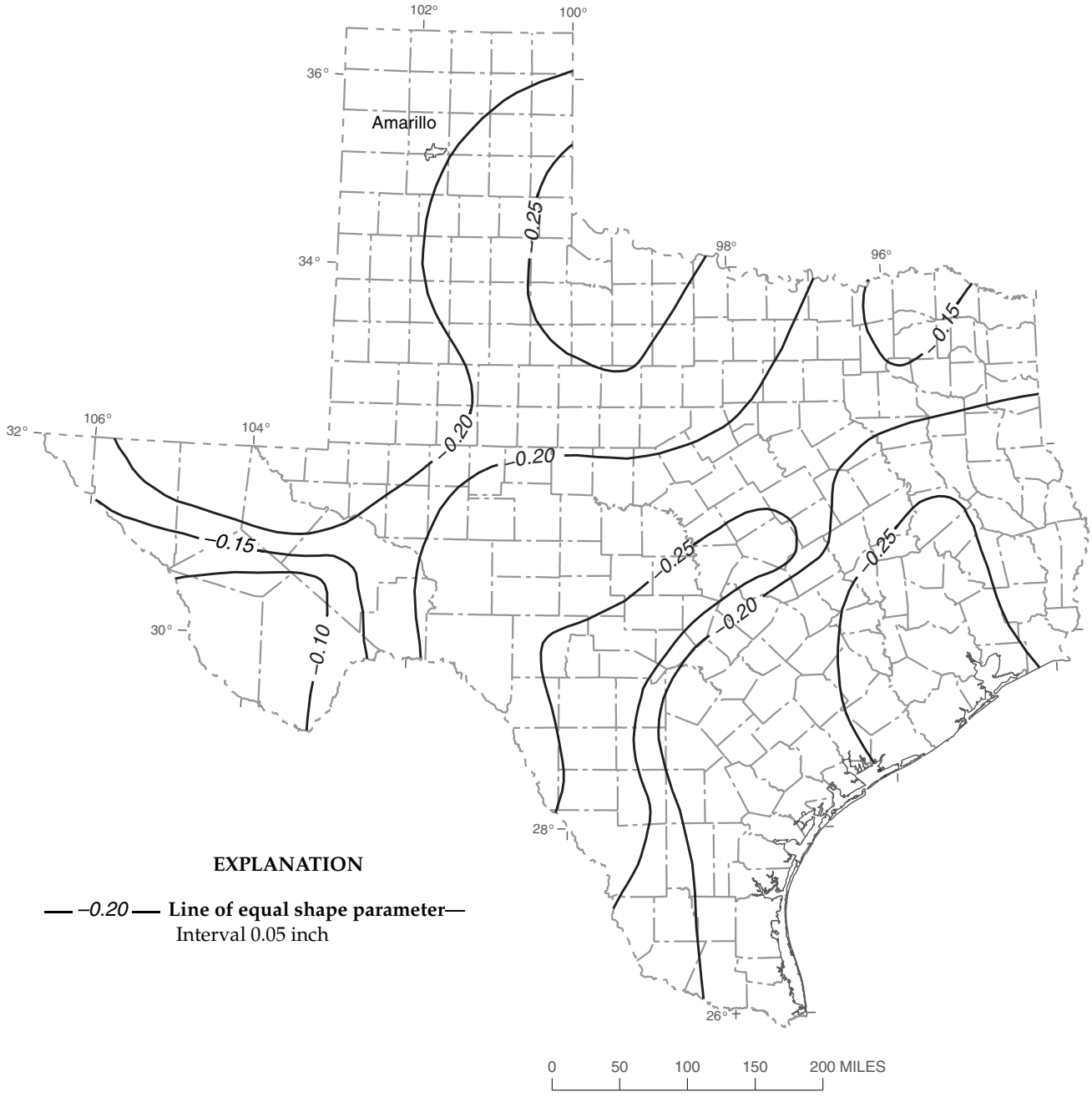

Figure 44. Shape (κ) parameter of generalized logistic (GLO) distribution for 6-hour precipitation duration in Texas.

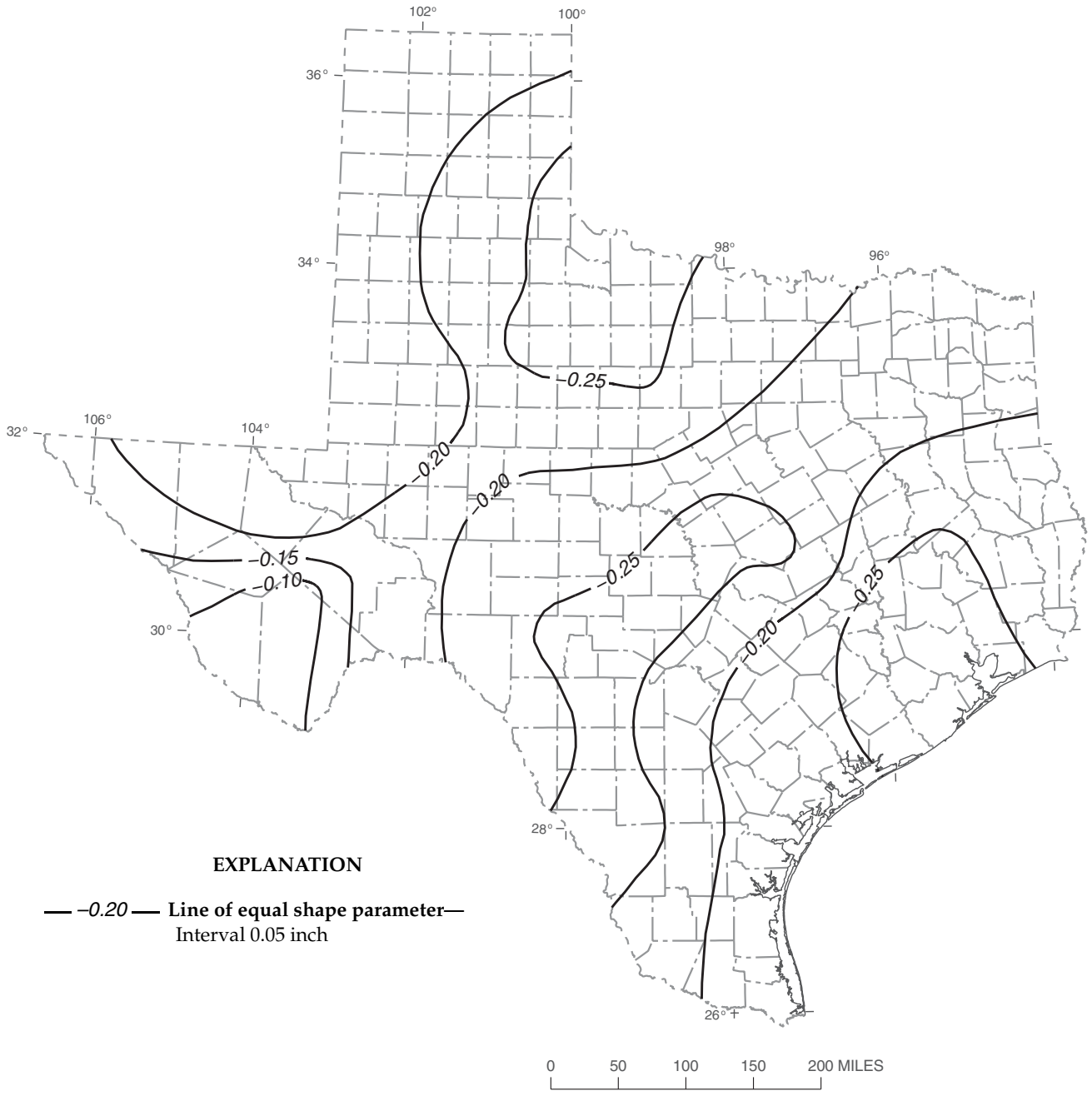

Figure 45. Shape (κ) parameter of generalized logistic (GLO) distribution for 12-hour precipitation duration in Texas.

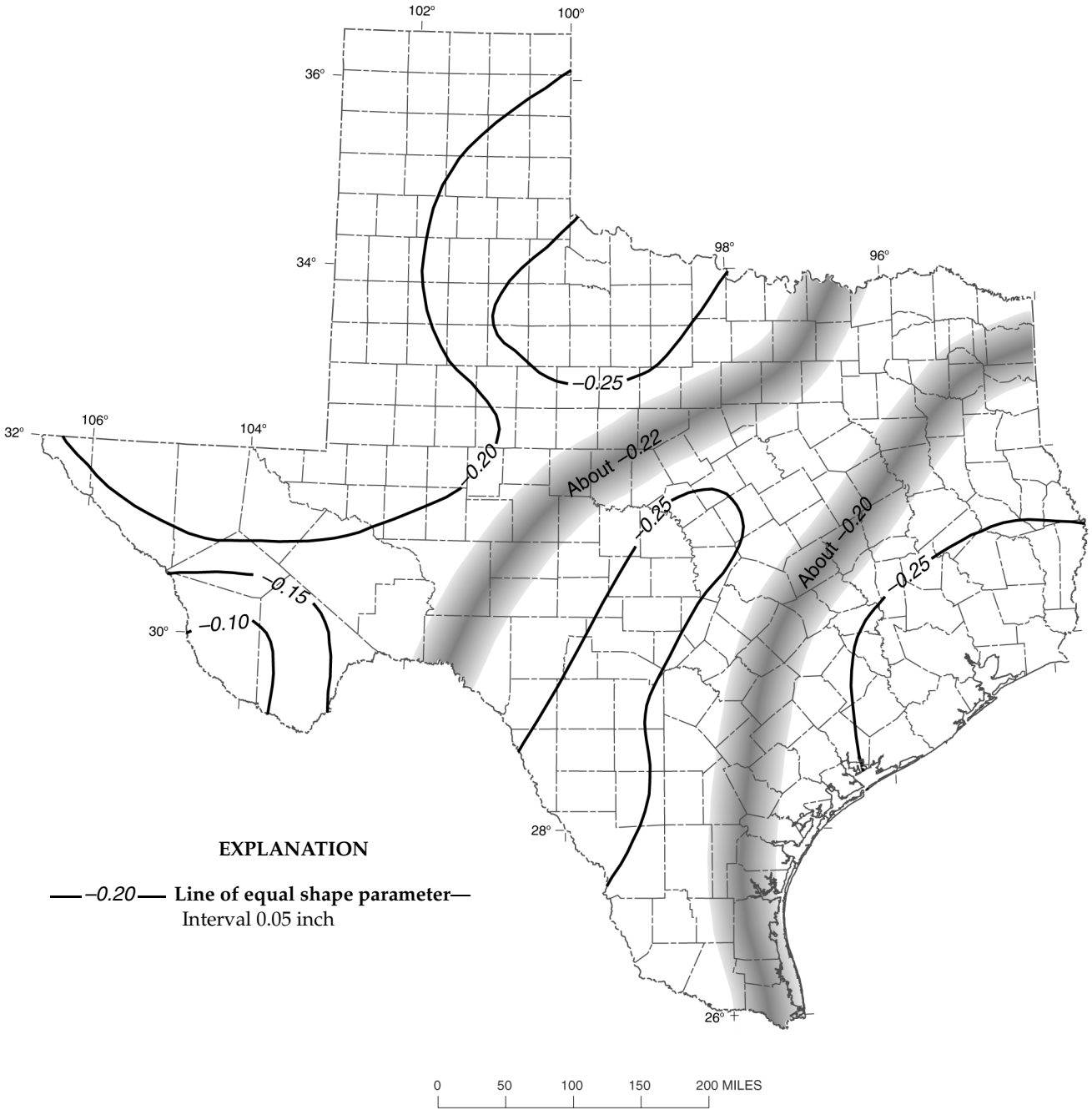

Figure 46. Shape (κ) parameter of generalized logistic (GLO) distribution for 24-hour precipitation duration in Texas.

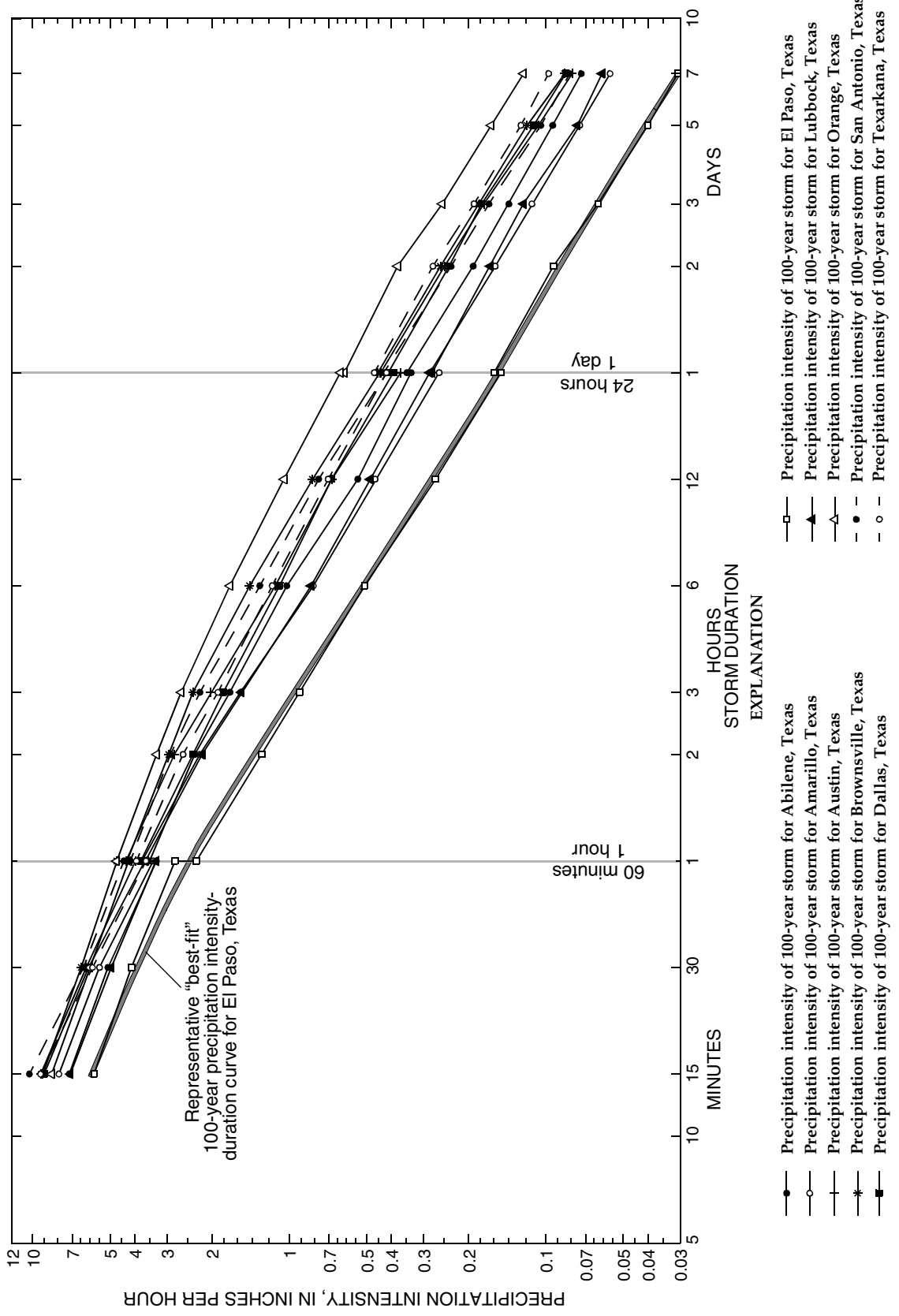

Figure 47. Precipitation intensity-duration curves of 100-year storm for selected localities in Texas.

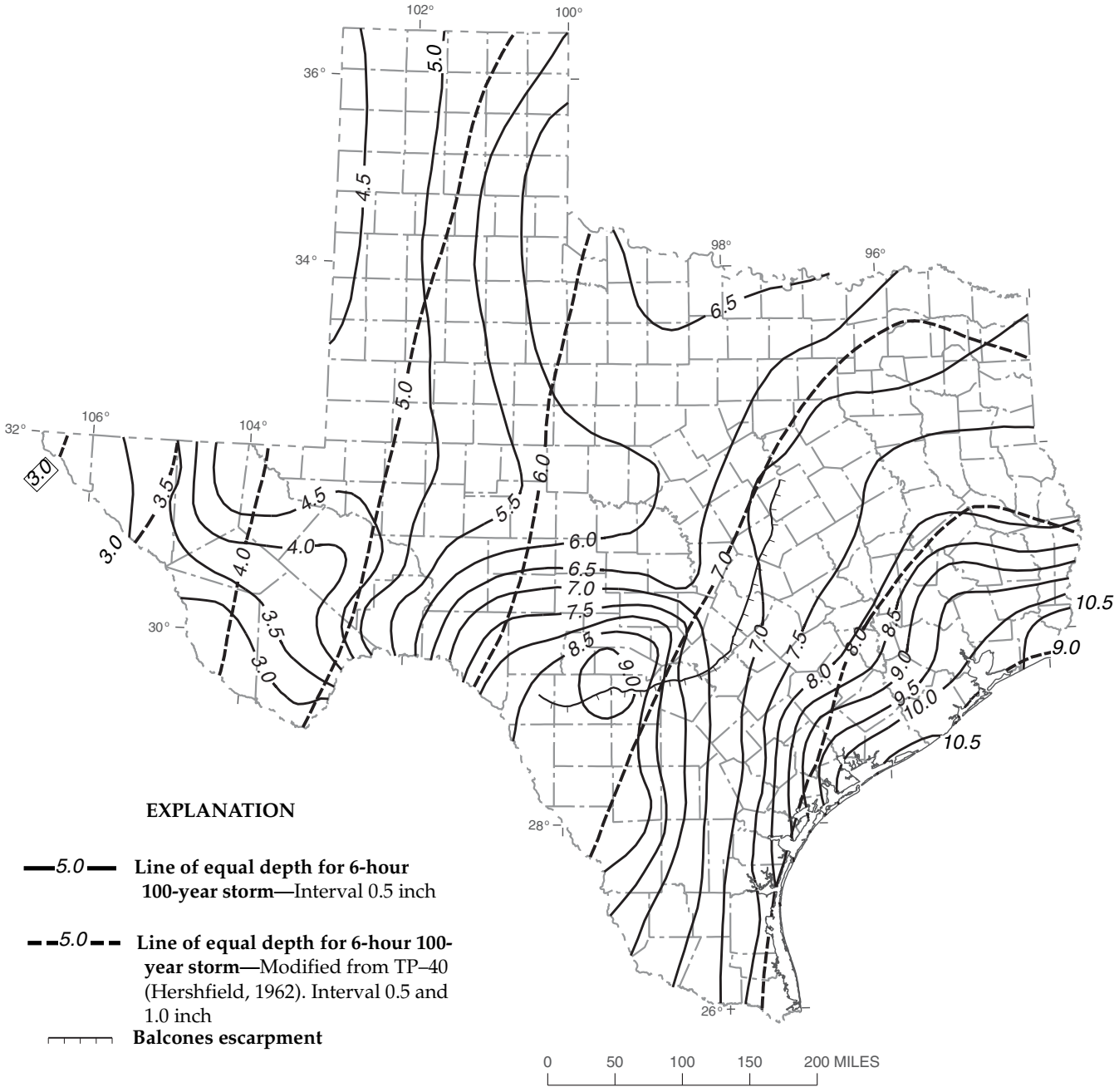

Figure 48. Depth of 100-year storm for 6-hour precipitation duration in Texas.

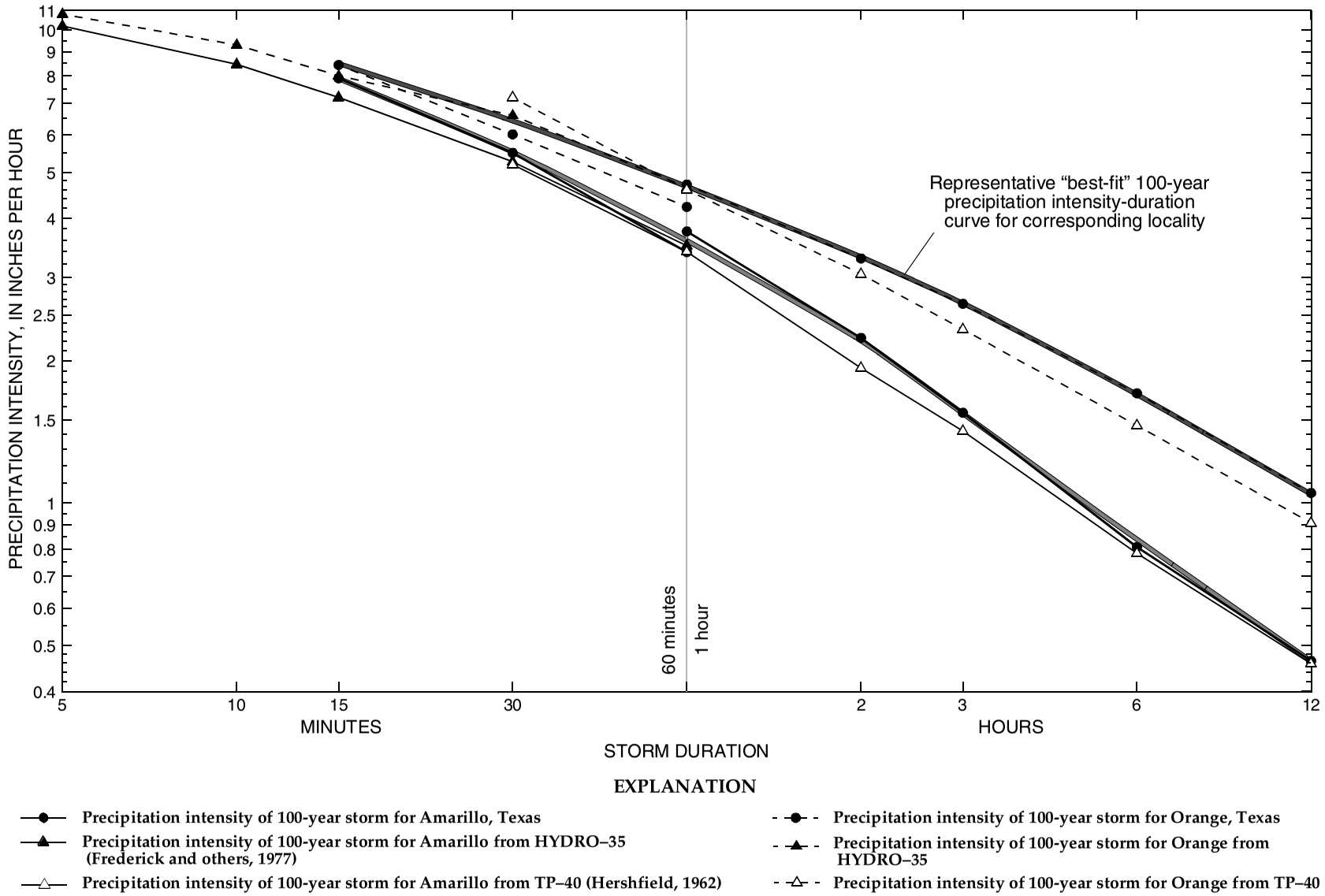

Figure 49

Figure 49. Precipitation intensity-duration curves of 100-year storm for Amarillo and Orange, Texas.

APPENDICES

Appendix 1. Fifteen-minute precipitation stations in Texas with at least 10 years of annual maxima data through 1994

[Station name: LCRA, Lower Colorado River Authority; FAA, Federal Aviation Administration; WSO, Weather Service Office; WSMO, Weather Service Meteorological Observatory.

Climatic region: TP, Trans-Pecos; NC, North Central; HP, High Plains; EP, Edwards Plateau; UC, Upper Coast; SC, South Central; ST, South Texas; LRP, Low Rolling Plains; ET, East Texas.]

Station no.	Station name	Latitude and longitude		Climatic region	Years of record	Beginning year of record	Ending year of record
0174	Alpine	30°22'	103°40'	TP	17	1978	1994
0206	Alvord 4 NE	33°23'	97°39'	NC	23	1971	1994
0248	Andrews	32°19'	102°32'	HP	23	1972	1994
0262	Anna	33°21'	96°31'	NC	16	1979	1994
0509	Bankersmith	30°08'	98°49'	EP	19	1976	1994
0518	Bardwell Dam	32°16'	96°38'	NC	20	1975	1994
0569	Bay City Waterworks	28°59'	95°59'	UC	18	1977	1994
0639	Beeville 5 NE	28°27'	97°42'	SC	24	1971	1994
0689	Benavides and 0690[1]	27°36'	98°25'	ST	19	1976	1994
0691	Benbrook Dam	32°39'	97°27'	NC	11	1984	1994
0738	Bertram 3 ENE	30°45'	98°01'	EP	11	1984	1994
0776	Big Lake (LCRA 140)	31°12'	101°28'	EP	20	1975	1994
0784	Big Spring Field Station	32°16'	101°29'	HP	24	1971	1994
0926	Bonita	33°46'	97°36'	NC	17	1978	1994
1017	Brady	31°07'	99°20'	EP	22	1973	1994
1068	Briggs	30°53'	97°56'	EP	18	1977	1994
1246	Burleson 3 SSE	32°30'	97°18'	NC	13	1982	1994
1429	Canyon Dam	29°52'	98°12'	EP	11	1984	1994
1431	Canyon Dam 1	29°52'	98°18'	EP	11	1984	1994
1433	Canyon Dam 3	29°57'	98°24'	EP	11	1984	1994
1434	Canyon Dam 4	29°55'	98°22'	EP	11	1984	1994
1436	Canyon Dam 6	29°57'	98°18'	EP	11	1984	1994
1438	Canyon Dam 7	29°55'	98°13'	EP	10	1984	1993
1492	Carta Valley	29°48'	100°40'	EP	21	1974	1994
1528	Catarina	28°21'	99°37'	ST	17	1978	1994
1646	Channing	35°41'	102°20'	HP	24	1971	1994
1671	Cheapside	29°16'	97°24'	SC	19	1976	1994
1698	Childress FAA Airport	34°26'	100°17'	LRP	20	1975	1994
1773	Clarksville 1 W	33°37'	95°04'	ET	24	1971	1994
1921	Commerce	33°16'	95°54'	NC	20	1975	1994
1956	Conroe	30°20'	95°29'	ET	17	1978	1994
2024	Coryell City	31°33'	97°37'	NC	12	1977	1988

Footnote at end of table.

Appendix 1. Fifteen-minute precipitation stations in Texas with at least 10 years of annual maxima data through 1994—Continued

Station no.	Station name	Latitude and longitude		Climatic region	Years of record	Beginning year of record	Ending year of record
2048	Cotulla	28°26'	99°15'	ST	20	1975	1994
2082	Crane	31°23'	102°20'	TP	20	1975	1994
2086	Cranfills Gap	31°46'	97°50'	NC	19	1975	1994
2096	Cresson	32°32'	97°37'	NC	15	1980	1994
2131	Cross Plains 2	32°08'	99°01'	NC	24	1971	1994
2244	Dallas FAA Airport	32°51'	96°51'	NC	20	1975	1994
2312	Deberry	32°18'	94°10'	ET	10	1974	1983
2394	Denison Dam	33°49'	96°34'	NC	11	1984	1994
2404	Denton 2 SE	33°12'	97°06'	NC	11	1984	1994
2415	Deport	33°31'	95°19'	NC	11	1984	1994
2462	Dime Box	30°22'	96°50'	SC	11	1984	1994
2621	Dumont	33°48'	100°31'	LRP	11	1984	1994
2675	Eagle Lake and 2676[1]	29°36'	96°20'	SC	19	1976	1994
2679	Eagle Pass	28°42'	100°29'	ST	24	1971	1994
2715	Eastland	32°24'	98°51'	NC	11	1984	1994
2744	Eden 2	31°13'	99°51'	EP	15	1972	1986
2811	Eldorado 1 N	30°53'	100°36'	EP	24	1971	1994
3005	Evant 4 SW	31°27'	98°13'	NC	18	1977	1994
3133	Ferris	32°32'	96°40'	NC	11	1984	1994
3171	Flat	31°19'	97°38'	NC	11	1984	1994
3270	Fort McKavett 7 N	30°56'	100°07'	EP	24	1971	1994
3278	Fort Stockton 35 SSW	30°23'	103°02'	TP	10	1978	1987
3284	Fort Worth Meach WSO Airport	32°49'	97°21'	NC	24	1971	1994
3285	Fort Worth Federal Building	32°45'	97°20'	NC	24	1971	1994
3370	Frisco	33°09'	96°50'	NC	11	1984	1994
3410	Gageby 2 NW	35°38'	100°22'	HP	21	1971	1994
3415	Gainesville	33°38'	97°08'	NC	24	1971	1994
3507	Georgetown Lake	30°41'	97°43'	NC	11	1984	1994
3546	Gilmer 2 W	32°44'	94°59'	ET	16	1979	1994
3642	Gordonville	33°48'	96°51'	NC	18	1977	1994
3646	Gorman	32°13'	98°40'	NC	11	1984	1994
3686	Granger Dam	30°42'	97°20'	NC	11	1984	1994
3691	Grapevine Dam	32°58'	97°03'	NC	24	1971	1994
3771	Groesbeck 2	31°32'	96°32'	NC	18	1977	1994
4098	Hereford	34°49'	102°24'	HP	24	1971	1994
4137	Hico	31°59'	98°02'	NC	18	1977	1994

Footnote at end of table.

Appendix 1. Fifteen-minute precipitation stations in Texas with at least 10 years of annual maxima data through 1994—Continued

Station no.	Station name	Latitude and longitude		Climatic region	Years of record	Beginning year of record	Ending year of record
4191	Hindes	28°43'	98°48'	ST	18	1977	1994
4257	Honey Grove	33°35'	95°54'	NC	22	1971	1994
4278	Hords Creek Dam	31°51'	99°34'	LRP	11	1984	1994
4309	Houston Addicks	29°46'	95°39'	UC	11	1984	1994
4311	Houston-Alief	29°43'	95°36'	UC	11	1984	1994
4375	Hunt 10 W	30°03'	99°31'	EP	19	1976	1994
4425	Imperial 2 W	31°16'	102°44'	TP	14	1980	1993
4476	Iredell	31°59'	97°53'	NC	20	1975	1994
4520	Jacksboro 1 NNE	33°14'	98°09'	NC	18	1977	1994
4570	Jayton	33°15'	100°34'	LRP	23	1971	1994
4670	Junction	30°29'	99°47'	EP	23	1971	1993
4679	Justin	33°05'	97°18'	NC	24	1971	1994
4792	Killeen 3 S	31°04'	97°44'	NC	17	1978	1994
4866	Kopperl 5 NNE	32°08'	97°29'	NC	17	1978	1994
4880	Kress	34°22'	101°45'	HP	16	1979	1994
4920	La Pryor	28°57'	99°50'	ST	18	1976	1994
4972	Lake Bridgeport Dam	33°13'	97°50'	NC	19	1976	1994
4974	Lake Colorado City	32°20'	100°55'	LRP	10	1984	1993
4975	Lake Crockett	33°44'	95°55'	NC	22	1973	1994
4982	Lake Kemp	33°45'	99°09'	LRP	11	1984	1994
5048	Langtry	29°48'	101°34'	EP	24	1971	1994
5094	Lavon Dam	33°02'	96°29'	NC	24	1971	1994
5113	Leakey	29°44'	99°46'	EP	20	1975	1994
5192	Lewisville Dam	33°04'	97°01'	NC	11	1984	1994
5193	Lexington	30°25'	97°01'	SC	17	1978	1994
5247	Lipscomb	36°14'	100°16'	HP	24	1971	1994
5312	London	30°40'	99°35'	EP	24	1971	1994
5348	Longview WSMO	32°21'	94°39'	ET	17	1978	1994
5410	Lubbock 9 N	33°42'	101°50'	HP	24	1971	1994
5463	Mabank 4 SW	32°21'	96°07'	ET	18	1977	1994
5528	Malone	31°55'	96°54'	NC	10	1984	1994
5596	Marfa 2	30°18'	104°01'	TP	24	1971	1994
5656	Matador 2	34°01'	100°50'	LRP	24	1971	1994
5695	Maypearl	32°19'	97°01'	NC	11	1984	1994
5770	McLean	35°14'	100°36'	HP	24	1971	1994
5897	Midlothian 2	32°29'	97°00'	NC	19	1976	1994

Footnote at end of table.

Appendix 1. Fifteen-minute precipitation stations in Texas with at least 10 years of annual maxima data through 1994—Continued

Station no.	Station name	Latitude and longitude		Climatic region	Years of record	Beginning year of record	Ending year of record
5957	Mineral Wells 1 SSW	32°47'	98°07'	NC	24	1971	1994
5996	Moline	31°23'	98°19'	NC	17	1978	1994
6104	Mount Locke	30°40'	104°00'	TP	11	1984	1994
6108	Mount Pleasant	33°10'	95°00'	ET	24	1971	1994
6136	Muleshoe 2	34°13'	102°44'	HP	24	1971	1994
6177	Nacogdoches	31°37'	94°38'	ET	20	1974	1994
6210	Navarro Mills Dam	31°57'	96°42'	NC	20	1975	1994
6270	New Boston	33°27'	94°25'	ET	22	1973	1994
6335	New Summerfield 2 W	31°59'	95°08'	ET	11	1984	1994
6504	O'Donnell	32°58'	101°49'	HP	24	1971	1994
6615	Old "8" Camp (6666)	33°34'	100°11'	LRP	15	1974	1994
6736	Ozona 8 WSW	30°41'	101°20'	EP	22	1973	1994
6757	Palestine 2 NE	31°47'	95°36'	ET	11	1984	1994
6776	Pampa 2	35°34'	100°58'	HP	21	1974	1994
6792	Panther Junction	29°19'	103°13'	TP	23	1972	1994
6834	Pat Mayse Dam	33°52'	95°31'	NC	24	1971	1994
6893	Pecos 12 SSW	31°16'	103°36'	TP	18	1977	1994
6935	Pep	33°49'	102°34'	HP	24	1971	1994
7066	Pittsburg 5 S	32°56'	94°58'	ET	18	1977	1994
7074	Plains	33°11'	102°50'	HP	24	1971	1994
7140	Point Comfort	28°40'	96°33'	UC	11	1984	1994
7243	Prairie Mountain	30°35'	98°53'	EP	24	1971	1994
7274	Priddy 3 N	31°43'	98°31'	NC	11	1984	1994
7300	Proctor Reservoir	31°58'	98°30'	NC	11	1984	1994
7422	Randolph Field	29°32'	98°17'	EP	20	1975	1994
7481	Red Bluff Dam	31°54'	103°55'	TP	14	1980	1994
7497	Red Rock and 7498[1]	29°58'	97°27'	SC	24	1971	1994
7499	Red Springs 2 ESE	33°36'	99°23'	LRP	24	1971	1994
7556	Reno	32°57'	97°34'	NC	24	1971	1994
7594	Richmond	29°35'	95°45'	UC	11	1984	1994
7706	Rocksprings	30°01'	100°13'	EP	17	1975	1994
7936	Sam Rayburn Dam	31°04'	94°06'	ET	16	1979	1994
8023	Sanderson 5 NNW	30°13'	102°25'	TP	13	1982	1994
8047	Santa Anna	31°44'	99°19'	LRP	15	1980	1994
8081	Sarita 7 E	27°13'	97°41'	ST	17	1978	1994
8252	Sheffield	30°42'	101°50'	TP	17	1978	1994

Footnote at end of table.

Appendix 1. Fifteen-minute precipitation stations in Texas with at least 10 years of annual maxima data through 1994—Continued

Station no.	Station name	Latitude	Longitude	Climatic region	Years of record	Beginning year of record	Ending year of record
8305	Sierra Blanca	31°11'	105°21'	TP	17	1978	1994
8446	Somerville Dam	30°20'	96°32'	SC	21	1974	1994
8531	Spicewood 1 S	30°27'	98°10'	EP	11	1984	1994
8563	Springtown 4 S	32°54'	97°41'	NC	18	1977	1994
8583	Stamford 1	32°56'	99°47'	LRP	15	1980	1994
8584	Stamford 2	32°57'	99°48'	LRP	10	1971	1980
8623	Stephenville WSMO	32°13'	98°11'	NC	17	1978	1994
8630	Sterling City	31°51'	100°59'	EP	11	1984	1994
8646	Stillhouse Hollow Dam	31°02'	97°32'	NC	11	1984	1994
8647	Stinnett	35°50'	101°27'	HP	18	1975	1992
8743	Sulphur Springs	33°09'	95°38'	ET	17	1978	1994
8761	Sunray 4 SW	35°58'	101°52'	HP	14	1971	1984
8778	Swan 4 NW	32°27'	95°25'	ET	21	1974	1994
8845	Tarpley	29°40'	99°17'	EP	19	1976	1994
8942	Texarkana	33°25'	94°05'	ET	22	1973	1994
8996	Thompsons 3 WSW	29°29'	95°38'	UC	11	1984	1994
9163	Truscott 5 W	33°45'	99°55'	LRP	11	1984	1994
9270	Valentine	30°34'	104°29'	TP	15	1980	1994
9364	Victoria WSO Airport	28°51'	96°55'	UC	10	1984	1993
9417	Waco Dam	31°36'	97°13'	NC	11	1984	1994
9491	Washington State Park	30°20'	96°09'	ET	17	1978	1994
9499	Water Valley	31°40'	100°43'	EP	24	1971	1994
9527	Wayside	34°48'	101°33'	HP	24	1971	1994
9532	Weatherford	32°46'	97°49'	NC	24	1971	1994
9565	Wellington and 9570[1]	34°50'	100°13'	LRP	21	1971	1994
9588	Weslaco 2 E	26°09'	97°58'	ST	20	1975	1994
9665	Wheelock	30°54'	96°23'	ET	15	1979	1993
9715	Whitney Dam	31°51'	97°22'	NC	19	1975	1993
9817	Winchell	31°28'	99°10'	EP	19	1976	1994
9829	Wink	31°46'	103°09'	TP	19	1976	1994
9893	Woodson 5 NNE	33°06'	99°02'	NC	15	1980	1994
9916	Wright Patman Dam and Lake	33°18'	94°10'	ET	11	1984	1994
9976	Zapata	26°53'	99°18'	ST	19	1976	1994

[1] The record of this station was considered auxiliary and therefore combined with the identified station in the table.

Appendix 2. Hourly precipitation stations in Texas with at least 10 years of annual maxima data through 1994

[Station name: WSO, Weather Service Office; LCRA, Lower Colorado River Authority; FAA, Federal Aviation Administration; WSCMO, Weather Service Contract Meteorological Observatory; WB, Weather Bureau; WSMO, Weather Service Meteorological Observatory; WSFO, Weather Service Forecast Office; CAA; Civilian Aeronautics Administration.

Climatic region: LRP, Low Rolling Plains; EP, Edwards Plateau; TP, Trans-Pecos; NC, North Central; HP, High Plains; ST, South Texas; UC, Upper Coast; SC; South Central; ET, East Texas.]

Station no.	Station name	Latitude and longitude		Climatic region	Years of record	Beginning year of record	Ending year of record
0016	Abilene WSO Airport	32°26'	99°41'	LRP	89	1906	1994
0050	Adamsville	31°17'	98°09'	EP	23	1963	1985
0174	Alpine	30°22'	103°40'	TP	24	1971	1994
0206	Alvord 4 NE	33°23'	97°39'	NC	52	1942	1994
0211	Amarillo WSO Airport	35°14'	101°42'	HP	54	1941	1994
0248	Andrews	32°19'	102°32'	HP	53	1942	1994
0262	Anna	33°21'	96°31'	NC	49	1946	1994
0380	Asherton	28°26'	99°45'	ST	19	1941	1959
0428	Austin WSO Airport	30°18'	97°42'	EP	65	1927	1994
0495	Balmorhea	30°59'	103°44'	TP	16	1942	1959
0509	Bankersmith	30°08'	98°49'	EP	55	1940	1994
0518	Bardwell Dam	32°16'	96°38'	NC	30	1965	1994
0569	Bay City Waterworks	28°59'	95°59'	UC	37	1940	1994
0572	Bay City 2 N	29°00'	95°58'	UC	19	1947	1965
0580	Baylor Ranch	28°18'	98°59'	ST	13	1940	1952
0587	Baytown 2	29°45'	95°01'	UC	15	1947	1969
0639	Beeville 5 NE	28°27'	97°42'	SC	42	1953	1994
0665	Belton Dam	31°06'	97°29'	NC	42	1951	1992
0689	Benavides and 0690[1]	27°36'	98°25'	ST	54	1940	1994
0691	Benbrook Dam	32°39'	97°27'	NC	46	1949	1994
0738	Bertram 3 ENE	30°45'	98°01'	EP	27	1968	1994
0776	Big Lake (LCRA 140)	31°12'	101°28'	EP	55	1940	1994
0784	Big Spring Field Station	32°16'	101°29'	HP	55	1940	1994
0917	Bon Wier	30°44'	93°39'	ET	35	1940	1974
0926	Bonita	33°46'	97°36'	NC	55	1940	1994
1017	Brady	31°07'	99°20'	EP	55	1940	1994
1053	Brewers Store 5 SW	30°41'	99°33'	EP	17	1940	1956
1057	Brice 2 S	34°41'	100°54'	LRP	42	1941	1982
1068	Briggs	30°53'	97°56'	EP	55	1940	1994
1081	Britton	32°33'	97°04'	NC	28	1946	1973
1136	Brownsville WSO Airport	25°54'	97°26'	ST	70	1923	1994
1165	Buchanan Dam	30°45'	98°25'	EP	17	1946	1964

Footnote at end of table.

Appendix 2. Hourly precipitation stations in Texas with at least 10 years of annual maxima data through 1994—Continued

Station no.	Station name	Latitude and longitude		Climatic region	Years of record	Beginning year of record	Ending year of record
1185	Buenavista 2 NNW	31°15'	102°40'	TP	22	1942	1963
1246	Burleson 3 SSE	32°30'	97°18'	NC	13	1982	1994
1267	Bushland 1 WSW	35°11'	102°05'	HP	12	1940	1951
1304	Cadiz	28°26'	97°57'	SC	13	1940	1952
1325	Calhoun	29°32'	96°20'	SC	26	1940	1965
1429	Canyon Dam	29°52'	98°12'	EP	17	1978	1994
1431	Canyon Dam 1	29°52'	98°18'	EP	34	1961	1994
1432	Canyon Dam 2	29°50'	98°21'	EP	28	1961	1988
1433	Canyon Dam 3	29°57'	98°24'	EP	34	1961	1994
1434	Canyon Dam 4	29°55'	98°22'	EP	33	1961	1994
1435	Canyon Dam 5	29°55'	98°21'	EP	27	1961	1987
1436	Canyon Dam 6	29°57'	98°18'	EP	34	1961	1994
1438	Canyon Dam 7	29°55'	98°13'	EP	33	1961	1993
1492	Carta Valley	29°48'	100°40'	EP	32	1963	1994
1528	Catarina	28°21'	99°37'	ST	35	1960	1994
1641	Chancellor	30°42'	103°11'	TP	13	1942	1954
1646	Channing	35°41'	102°20'	HP	54	1941	1994
1671	Cheapside	29°16'	97°24'	SC	55	1940	1994
1680	Cherokee	30°59'	98°43'	EP	31	1941	1972
1696	Childress 3 W	34°26'	100°15'	LRP	30	1940	1975
1698	Childress FAA Airport	34°26'	100°17'	LRP	26	1947	1994
1773	Clarksville 1 W	33°37'	95°04'	ET	50	1940	1994
1921	Commerce	33°16'	95°54'	NC	47	1948	1994
1937	Concord	31°55'	94°35'	ET	22	1962	1983
1956	Conroe	30°20'	95°29'	ET	48	1947	1994
2015	Corpus Christi WSO Airport	27°46'	97°30'	SC	84	1903	1994
2024	Coryell City	31°33'	97°37'	NC	45	1944	1988
2048	Cotulla	28°26'	99°15'	ST	39	1956	1994
2073	Crabb 2 W	29°32'	95°45'	UC	17	1948	1964
2082	Crane	31°23'	102°20'	TP	52	1943	1994
2086	Cranfills Gap Airport	31°46'	97°50'	NC	54	1940	1994
2096	Cresson	32°32'	97°37'	NC	49	1946	1994
2131	Cross Plains 2 and 2128[1]	32°08'	99°01'	NC	55	1940	1994
2242	Dallas-Ft. Worth Regional WSCMO Airport	32°54'	97°02'	NC	21	1974	1994
2244	Dallas FAA Airport	32°51'	96°51'	NC	80	1914	1994
2309	Dallas WSO N	31°54'	96°43'	NC	18	1943	1960

Footnote at end of table.

Appendix 2. Hourly precipitation stations in Texas with at least 10 years of annual maxima data through 1994—Continued

Station no.	Station name	Latitude and longitude		Climatic region	Years of record	Beginning year of record	Ending year of record
2312	Deberry	32°18'	94°10'	ET	11	1973	1983
2357	Del Rio WB City	29°20'	100°53'	EP	12	1940	1951
2360	Del Rio WSO Airport	29°22'	100°55'	EP	67	1906	1994
2394	Denison Dam	33°49'	96°34'	NC	55	1940	1994
2404	Denton 2 SE	33°12'	97°06'	NC	49	1946	1994
2415	Deport	33°31'	95°19'	NC	50	1944	1994
2462	Dime Box	30°22'	96°50'	SC	14	1981	1994
2621	Dumont	33°48'	100°31'	LRP	24	1971	1994
2675	Eagle Lake and 2676[1]	29°36'	96°20'	SC	30	1965	1994
2679	Eagle Pass	28°42'	100°29'	ST	54	1941	1994
2715	Eastland	32°24'	98°51'	NC	33	1961	1994
2744	Eden 2	31°13'	99°51'	EP	47	1940	1986
2797	El Paso WSO Airport	31°48'	106°24'	TP	88	1906	1994
2811	Eldorado 1 N	30°53'	100°36'	EP	49	1940	1994
3005	Evant 4 SW	31°27'	98°13'	NC	52	1943	1994
3033	Fabens and 3034[1]	31°30'	106°09'	TP	26	1949	1977
3133	Ferris	32°32'	96°40'	NC	48	1946	1994
3171	Flat	31°19'	97°38'	NC	44	1951	1994
3189	Fletcher Ranch	30°10'	104°12'	TP	11	1942	1952
3270	Fort McKavett 7 N	30°56'	100°07'	EP	34	1961	1994
3278	Fort Stockton 35 SSW	30°23'	103°02'	TP	30	1958	1987
3283	Fort Worth International WSO Airport	32°50'	97°03'	NC	29	1940	1974
3284	Fort Worth Meach WSO Airport	32°49'	97°21'	NC	49	1940	1994
3285	Fort Worth Federal Building	32°45'	97°20'	NC	36	1948	1994
3329	Fredericksburg	30°16'	98°52'	EP	36	1940	1975
3370	Frisco	33°09'	96°50'	NC	29	1966	1994
3410	Gageby 2 NW	35°38'	100°22'	HP	51	1941	1994
3415	Gainesville	33°38'	97°08'	NC	54	1941	1994
3430	Galveston WSO City	29°18'	94°48'	UC	105	1890	1994
3442	Garcia Lake 12 ENE	34°55'	102°44'	HP	21	1943	1971
3446	Garden City 16 E	31°50'	101°12'	EP	24	1949	1972
3476	Garza Little Elm Dam	33°04'	97°01'	NC	16	1949	1964
3507	Georgetown Lake	30°41'	97°43'	NC	14	1981	1994
3546	Gilmer 2 W	32°44'	94°59'	ET	48	1941	1994
3642	Gordonville	33°48'	96°51'	NC	53	1942	1994
3646	Gorman	32°13'	98°40'	NC	44	1951	1994

Footnote at end of table.

Appendix 2. Hourly precipitation stations in Texas with at least 10 years of annual maxima data through 1994—Continued

Station no.	Station name	Latitude and longitude		Climatic region	Years of record	Beginning year of record	Ending year of record
3686	Granger Dam	30°42'	97°20'	NC	15	1980	1994
3691	Grapevine Dam	32°58'	97°03'	NC	46	1949	1994
3771	Groesbeck 2	31°32'	96°32'	NC	18	1977	1994
3831	Guyer	34°08'	98°56'	LRP	13	1940	1952
3871	Hall Ranch	30°08'	99°36'	EP	37	1940	1976
4040	Hazeldell	31°53'	98°18'	NC	12	1973	1984
4098	Hereford	34°49'	102°24'	HP	40	1955	1994
4100	Hereford 2 ESE	34°49'	102°23'	HP	13	1941	1953
4137	Hico	31°59'	98°02'	NC	18	1977	1994
4191	Hindes	28°43'	98°48'	ST	55	1940	1994
4257	Honey Grove	33°35'	95°54'	NC	49	1944	1994
4278	Hords Creek Dam	31°51'	99°34'	LRP	39	1956	1994
4299	Hot Springs	29°11'	103°00'	TP	10	1942	1952
4300	Houston WSCMO Airport	29°58'	95°21'	UC	25	1970	1994
4305	Houston WB City	29°46'	95°22'	UC	31	1940	1970
4309	Houston Addicks	29°46'	95°39'	UC	50	1943	1994
4311	Houston-Alief	29°43'	95°36'	UC	54	1940	1994
4329	Houston-Satsuma	29°56'	95°38'	UC	50	1940	1990
4375	Hunt 10 W	30°03'	99°31'	EP	19	1976	1994
4425	Imperial 2 W	31°16'	102°44'	TP	31	1963	1993
4440	Indian Gap Airport	31°40'	98°25'	NC	33	1951	1983
4476	Iredell	31°59'	97°53'	NC	32	1963	1994
4517	Jacksboro	33°14'	98°09'	NC	38	1940	1977
4520	Jacksboro 1 NNE	33°14'	98°09'	NC	18	1977	1994
4570	Jayton	33°15'	100°34'	LRP	54	1940	1994
4577	Jefferson 4 NE	32°50'	94°19'	ET	34	1944	1978
4591	Jewett	31°21'	96°09'	ET	51	1941	1991
4670	Junction	30°29'	99°47'	EP	55	1940	1994
4679	Justin	33°05'	97°18'	NC	41	1954	1994
4792	Killeen 3 S	31°04'	97°44'	NC	17	1978	1994
4866	Kopperl 5 NNE	32°08'	97°29'	NC	55	1940	1994
4878	Kountze 3 SE	30°20'	94°14'	ET	40	1940	1979
4880	Kress	34°22'	101°45'	HP	55	1940	1994
4920	La Pryor	28°57'	99°50'	ST	52	1940	1994
4972	Lake Bridgeport Dam	33°13'	97°50'	NC	49	1946	1994
4973	Lake Coffee Mill	33°44'	96°00'	NC	13	1946	1958

Footnote at end of table.

Appendix 2. Hourly precipitation stations in Texas with at least 10 years of annual maxima data through 1994—Continued

Station no.	Station name	Latitude and longitude		Climatic region	Years of record	Beginning year of record	Ending year of record
4974	Lake Colorado City	32°20'	100°55'	LRP	40	1954	1993
4975	Lake Crockett	33°44'	95°55'	NC	22	1973	1994
4982	Lake Kemp	33°45'	99°09'	LRP	21	1974	1994
5018	Lampasas	31°03'	98°11'	EP	10	1957	1994
5048	Langtry	29°48'	101°34'	EP	50	1942	1994
5057	Laredo WB Airport and 5060[1]	27°32'	99°28'	ST	29	1944	1972
5081	Latex	32°21'	94°06'	ET	22	1942	1963
5094	Lavon Dam	33°02'	96°29'	NC	46	1949	1994
5113	Leakey	29°44'	99°46'	EP	50	1940	1994
5192	Lewisville Dam	33°04'	97°01'	NC	31	1964	1994
5193	Lexington	30°25'	97°01'	SC	55	1940	1994
5247	Lipscomb	36°14'	100°16'	HP	55	1940	1994
5258	Little Elm	33°10'	96°56'	NC	21	1946	1966
5303	Loma Alta	29°55'	100°46'	EP	22	1942	1963
5312	London	30°40'	99°35'	EP	39	1956	1994
5348	Longview WSMO	32°21'	94°39'	ET	20	1975	1994
5358	Loraine	32°25'	100°43'	LRP	45	1940	1984
5398	Lovelady	31°08'	95°27'	ET	47	1940	1986
5410	Lubbock 9 N	33°42'	101°50'	HP	53	1942	1994
5411	Lubbock WSFO Airport	33°39'	101°49'	HP	42	1940	1994
5429	Luling	29°40'	97°39'	SC	23	1943	1965
5461	Mabank 4 SW and 5463[1]	32°20'	96°09'	ET	55	1940	1994
5528	Malone	31°55'	96°54'	NC	21	1973	1994
5591	Marfa-Charco M R	30°29'	104°07'	TP	20	1949	1968
5592	Marfa 9 W	30°18'	104°10'	TP	18	1952	1969
5596	Marfa 2	30°18'	104°01'	TP	27	1968	1994
5600	Marfa 16 SSE	30°08'	103°53'	TP	13	1969	1981
5656	Matador 2 and 5658[1]	34°01'	100°50'	LRP	54	1941	1994
5695	Maypearl	32°19'	97°01'	NC	52	1943	1994
5770	McLean	35°14'	100°36'	HP	55	1940	1994
5890	Midland/Odessa WSO Airport	31°57'	102°11'	HP	49	1941	1994
5897	Midlothian 2	32°29'	97°00'	NC	20	1974	1994
5957	Mineral Wells 1 SSW	32°47'	98°07'	NC	43	1952	1994
5996	Moline	31°23'	98°19'	NC	55	1940	1994
6104	Mount Locke	30°40'	104°00'	TP	47	1948	1994
6108	Mount Pleasant	33°10'	95°00'	ET	54	1940	1994

Footnote at end of table.

Appendix 2. Hourly precipitation stations in Texas with at least 10 years of annual maxima data through 1994—Continued

Station no.	Station name	Latitude and longitude		Climatic region	Years of record	Beginning year of record	Ending year of record
6136	Muleshoe 2	34°13'	102°44'	HP	53	1941	1994
6177	Nacogdoches	31°37'	94°38'	ET	42	1947	1994
6210	Navarro Mills Dam	31°57'	96°42'	NC	33	1962	1994
6211	Navasota	30°23'	96°07'	ET	12	1941	1952
6270	New Boston	33°27'	94°25'	ET	22	1973	1994
6335	New Summerfield 2 W	31°59'	95°08'	ET	33	1962	1994
6504	O'Donnell	32°58'	101°49'	HP	55	1940	1994
6615	Old "8" Camp (6666)	33°34'	100°11'	LRP	16	1973	1994
6736	Ozona 8 WSW and 6734[1]	30°41'	101°20'	EP	54	1940	1994
6757	Palestine 2 NE	31°47'	95°36'	ET	55	1940	1994
6775	Pampa and 6776[1]	35°32'	100°58'	HP	54	1941	1994
6792	Panther Junction	29°19'	103°13'	TP	40	1955	1994
6834	Pat Mayse Dam	33°52'	95°31'	NC	29	1966	1994
6893	Pecos 12 SSW	31°16'	103°36'	TP	35	1960	1994
6935	Pep	33°49'	102°34'	HP	39	1956	1994
6981	Pettit 4 NE	33°44'	102°28'	HP	13	1941	1955
7060	Pitchfork Ranch	33°36'	100°32'	LRP	22	1971	1994
7066	Pittsburg 5 S	32°56'	94°58'	ET	46	1949	1994
7074	Plains	33°11'	102°50'	HP	53	1942	1994
7116	Plemons	35°46'	101°20'	HP	19	1940	1958
7140	Point Comfort	28°40'	96°33'	UC	38	1957	1994
7173	Port Arthur	29°52'	93°56'	UC	37	1917	1953
7174	Port Arthur WSO Airport	29°57'	94°01'	UC	45	1947	1994
7213	Post Oak School	30°16'	96°43'	SC	19	1963	1981
7243	Prairie Mountain	30°35'	98°53'	EP	55	1940	1994
7274	Priddy 3 N	31°43'	98°31'	NC	11	1984	1994
7300	Proctor Reservoir	31°58'	98°30'	NC	22	1973	1994
7422	Randolph Field	29°32'	98°17'	EP	55	1940	1994
7431	Rankin	31°14'	101°57'	EP	45	1948	1994
7481	Red Bluff Dam	31°54'	103°55'	TP	47	1942	1994
7497	Red Rock and 7498[1]	29°58'	97°27'	SC	28	1967	1994
7499	Red Springs 2 ESE	33°36'	99°23'	LRP	52	1943	1994
7534	Reiley Ranch	30°38'	100°15'	EP	11	1940	1950
7556	Reno	32°57'	97°34'	NC	49	1946	1994
7594	Richmond and 7596[1]	29°35'	95°45'	UC	31	1964	1994
7608	Riesel	31°29'	96°53'	NC	29	1940	1968

Footnote at end of table.

Appendix 2. Hourly precipitation stations in Texas with at least 10 years of annual maxima data through 1994—Continued

Station no.	Station name	Latitude and longitude		Climatic region	Years of record	Beginning year of record	Ending year of record
7700	Rockland 2 NW	31°01'	94°24'	ET	35	1940	1974
7706	Rocksprings and 7718[1]	30°01'	100°13'	EP	52	1940	1994
7922	Salt Flat CAA Airport	31°45'	105°05'	TP	14	1942	1955
7936	Sam Rayburn Dam	31°04'	94°06'	ET	27	1968	1994
7943	San Angelo WSO Airport	31°22'	100°30'	EP	46	1949	1994
7945	San Antonio WSFO	29°32'	98°28'	EP	54	1941	1994
7948	San Antonio Nursery	29°18'	98°28'	EP	25	1944	1968
7951	San Augustine	31°32'	94°07'	ET	17	1962	1978
7981	San Manuel	26°34'	98°07'	ST	13	1941	1953
8023	Sanderson 5 NNW	30°13'	102°25'	TP	48	1947	1994
8047	Santa Anna	31°44'	99°19'	LRP	55	1940	1994
8081	Sarita 7 E	27°13'	97°41'	ST	54	1941	1994
8252	Sheffield	30°42'	101°50'	TP	53	1942	1994
8265	Shepherd 2 SW	30°29'	95°00'	ET	25	1940	1964
8305	Sierra Blanca	31°11'	105°21'	TP	51	1942	1994
8335	Simms 4 WNW	33°22'	94°34'	ET	30	1944	1973
8445	Somerville and 8446[1]	30°21'	96°31'	SC	55	1940	1994
8531	Spicewood 1 S	30°27'	98°10'	EP	27	1968	1994
8563	Springtown 4 S	32°54'	97°41'	NC	18	1977	1994
8566	Spur	33°29'	100°51'	LRP	17	1948	1964
8583	Stamford 1 and 8584[1]	32°56'	99°47'	LRP	54	1940	1994
8623	Stephenville WSMO	32°13'	98°11'	NC	28	1940	1994
8625	Stephenville 7 WSW	32°10'	98°19'	NC	29	1947	1975
8630	Sterling City	31°51'	100°59'	EP	18	1977	1994
8631	Sterling City 8 NE	31°55'	100°53'	EP	28	1949	1977
8646	Stillhouse Hollow Dam	31°02'	97°32'	NC	31	1964	1994
8647	Stinnett	35°50'	101°27'	HP	33	1959	1992
8743	Sulphur Springs	33°09'	95°38'	ET	53	1941	1994
8761	Sunray 4 SW	35°58'	101°52'	HP	29	1955	1984
8778	Swan 4 NW	32°27'	95°25'	ET	38	1957	1994
8845	Tarpley	29°40'	99°17'	EP	55	1940	1994
8859	Tatum	32°18'	94°31'	ET	36	1940	1975
8898	Telephone	33°47'	96°01'	NC	14	1959	1972
8911	Temple 3 SE	31°03'	97°21'	NC	20	1947	1968
8924	Terlingua	29°18'	103°33'	TP	21	1942	1962
8942	Texarkana	33°25'	94°05'	ET	27	1968	1994

Footnote at end of table.

Appendix 2. Hourly precipitation stations in Texas with at least 10 years of annual maxima data through 1994—Continued

Station no.	Station name	Latitude and longitude		Climatic region	Years of record	Beginning year of record	Ending year of record
8944	Texarkana Dam	33°18'	94°10'	ET	18	1955	1972
8996	Thompsons 3 WSW	29°29'	95°38'	UC	38	1957	1994
9037	Tinnin Ranch	31°18'	104°00'	TP	28	1942	1969
9163	Truscott 5 W	33°45'	99°55'	LRP	55	1940	1994
9270	Valentine	30°34'	104°29'	TP	36	1959	1994
9307	Vancourt 5 SW	31°21'	100°14'	EP	10	1940	1949
9363	Victoria WB Airport	28°47'	97°05'	UC	16	1946	1961
9364	Victoria WSO Airport	28°51'	96°55'	UC	40	1940	1994
9417	Waco Dam	31°36'	97°13'	NC	30	1965	1994
9419	Waco WSO Airport	31°37'	97°13'	NC	54	1941	1994
9491	Washington State Park	30°20'	96°09'	ET	43	1952	1994
9499	Water Valley	31°40'	100°43'	EP	42	1953	1994
9527	Wayside	34°48'	101°33'	HP	53	1941	1994
9532	Weatherford	32°46'	97°49'	NC	48	1947	1994
9565	Wellington and 9570[1]	34°50'	100°13'	LRP	45	1949	1994
9588	Weslaco 2 E	26°09'	97°58'	ST	45	1947	1994
9665	Wheelock	30°54'	96°23'	ET	55	1940	1994
9715	Whitney Dam	31°51'	97°22'	NC	43	1952	1994
9729	Wichita Falls WSO Airport	33°58'	98°29'	LRP	55	1940	1994
9772	William Harris Reservoir	29°15'	95°33'	UC	16	1949	1964
9817	Winchell and 9816[1]	31°28'	99°10'	EP	36	1949	1994
9829	Wink	31°46'	103°09'	TP	48	1942	1994
9858	Wolf Creek Dam	36°14'	100°40'	HP	34	1941	1974
9893	Woodson 5 NNE	33°06'	99°02'	NC	54	1941	1994
9916	Wright Patman Dam and Lake	33°18'	94°10'	ET	14	1981	1994
9976	Zapata	26°53'	99°18'	ST	55	1940	1994

[1] The record of this station was considered auxiliary and therefore combined with the identified station in the table.

Appendix 3. Daily precipitation stations in Texas with at least 10 years of annual maxima data through 1994

[Station name: WSO, Weather Service Office; LCRA, Lower Colorado River Authority; FAA, Federal Aviation Administration; WB, Weather Bureau; WSMO, Weather Service Meteorological Observatory; WSCMO, Weather Service Contract Meteorological Observatory; WSFO, Weather Service Forecast Observatory; CAA, Civilian Aeronautics Administration.

Climatic region: HP, High Plains; LRP, Low Rolling Plains; ST, South Texas; EP, Edwards Plateau; NC, North Central; TP, Trans-Pecos; ET, East Texas; UC, Upper Coast; SC, South Central.]

Station no.	Station name	Latitude and longitude		Climatic region	Years of record	Beginning year of record	Ending year of record
0012	Abernathy	33°50'	101°51'	HP	47	1948	1994
0016	Abilene WSO Airport	32°26'	99°41'	LRP	47	1948	1994
0025	Acker Ranch	28°08'	98°31'	ST	17	1978	1994
0034	Ackerly	32°32'	101°43'	HP	47	1948	1994
0050	Adamsville	31°17'	98°09'	EP	25	1963	1987
0068	Adrian	35°17'	102°40'	HP	11	1938	1948
0081	Agua Nueva	26°54'	98°36'	ST	17	1948	1964
0120	Albany	32°44'	99°17'	NC	94	1901	1994
0129	Aledo 4 SE	32°39'	97°34'	NC	35	1960	1994
0144	Alice	27°44'	98°04'	ST	78	1911	1994
0174	Alpine	30°22'	103°40'	TP	72	1900	1994
0190	Alto 5 SW	31°36'	95°08'	ET	47	1948	1994
0201	Alvarado	32°25'	97°13'	NC	17	1948	1964
0204	Alvin (Houston Area WSO)	29°25'	95°13'	UC	95	1898	1993
0211	Amarillo WSO Airport	35°14'	101°42'	HP	47	1948	1994
0225	Amistad Dam	29°28'	101°02'	EP	31	1964	1994
0235	Anahuac	29°47'	94°40'	UC	82	1909	1994
0244	Anderson	30°29'	95°59'	ET	59	1914	1972
0246	Andice 1 WNW	30°47'	97°52'	NC	27	1968	1994
0248	Andrews	32°19'	102°32'	HP	39	1914	1994
0257	Angleton 2 W	29°09'	95°27'	UC	82	1913	1994
0262	Anna	33°21'	96°31'	NC	51	1898	1994
0268	Anson	32°46'	99°54'	LRP	46	1898	1994
0271	Antelope	33°26'	98°22'	NC	58	1910	1994
0302	Aransas Pass 2	27°55'	97°08'	SC	31	1897	1971
0305	Aransas Wildlife Refuge	28°16'	96°48'	SC	24	1971	1994
0313	Archer City	33°35'	98°38'	NC	57	1910	1994
0337	Arlington	32°42'	97°07'	NC	47	1948	1994
0342	Armstrong	26°56'	97°48'	ST	34	1942	1978
0367	Arthur City	33°52'	95°30'	NC	72	1897	1970
0394	Aspermont 1 E	33°09'	100°13'	LRP	84	1911	1994
0404	Athens 3 SSE	32°10'	95°50'	ET	51	1903	1994

Footnote at end of table.

Appendix 3. Daily precipitation stations in Texas with at least 10 years of annual maxima data through 1994—Continued

Station no.	Station name	Latitude and longitude		Climatic region	Years of record	Beginning year of record	Ending year of record
0408	Atlanta	33°07'	94°10'	ET	51	1930	1994
0428	Austin WSO Airport	30°18'	97°42'	EP	65	1930	1994
0430	Austin Dam	30°18'	97°47'	EP	18	1948	1965
0432	Austin Montopolis Bridge	30°15'	97°41'	EP	16	1948	1963
0436	Austwell	28°23'	96°51'	SC	52	1897	1960
0437	Austwell Wildlife Refuge	28°16'	96°48'	SC	31	1940	1970
0440	Avalon	32°12'	96°47'	NC	31	1964	1994
0478	Baird	32°24'	99°24'	NC	32	1948	1980
0482	Bakersfield 2 NW	30°55'	102°19'	TP	47	1948	1994
0493	Ballinger 5 WSW	31°44'	100°03'	LRP	96	1897	1994
0498	Balmorhea	30°59'	103°45'	TP	72	1923	1994
0509	Bankersmith	30°08'	98°49'	EP	15	1948	1994
0518	Bardwell Dam	32°16'	96°38'	NC	30	1965	1994
0528	Barnhart	31°08'	101°10'	EP	17	1948	1964
0538	Barstow	31°28'	103°24'	TP	14	1906	1919
0558	Bateman Ranch 2	33°36'	100°13'	LRP	14	1974	1988
0560	Batesville	28°57'	99°37'	ST	30	1965	1994
0569	Bay City Waterworks	28°59'	95°59'	UC	62	1909	1994
0586	Baytown	29°50'	95°00'	UC	39	1946	1994
0611	Beaumont City	30°06'	94°06'	UC	94	1901	1994
0613	Beaumont Research Center	30°04'	94°17'	UC	34	1948	1994
0635	Bedias	30°47'	95°57'	ET	37	1949	1985
0639	Beeville 5 NE	28°27'	97°42'	SC	93	1901	1994
0655	Bellville	29°57'	96°16'	SC	16	1978	1993
0665	Belton Dam	31°06'	97°29'	NC	41	1951	1992
0689	Benavides and 0690[1]	27°36'	98°25'	ST	36	1948	1993
0691	Benbrook Dam	32°39'	97°27'	NC	46	1949	1994
0704	Benjamin 4 SSE	33°32'	99°46'	LRP	36	1940	1975
0708	Benjamin 15 W	33°35'	100°02'	LRP	15	1980	1994
0738	Bertram 3 ENE	30°45'	98°01'	EP	27	1968	1994
0776	Big Lake (LCRA 140)	31°12'	101°28'	EP	36	1948	1994
0786	Big Spring	32°15'	101°27'	HP	47	1948	1994
0787	Big Wells 1 W	28°35'	99°35'	ST	75	1916	1990
0805	Bishop	27°35'	97°48'	SC	26	1934	1959
0832	Blanco	30°06'	98°25'	EP	97	1897	1994
0839	Blanket	31°49'	98°47'	NC	18	1948	1965

Footnote at end of table.

Appendix 3. Daily precipitation stations in Texas with at least 10 years of annual maxima data through 1994—Continued

Station no.	Station name	Latitude and longitude		Climatic region	Years of record	Beginning year of record	Ending year of record
0852	Blewett 5 NW	29°14'	100°06'	EP	29	1957	1985
0861	Bloy's Campground	30°32'	104°08'	TP	10	1968	1977
0866	Blue	30°24'	97°09'	SC	22	1963	1984
0902	Boerne	29°48'	98°43'	EP	97	1897	1994
0917	Bon Wier	30°44'	93°39'	ET	41	1948	1988
0923	Bonham	33°36'	96°11'	NC	90	1903	1994
0944	Booker	36°27'	100°32'	HP	62	1922	1994
0950	Boquillas Ranger Station	29°11'	102°58'	TP	45	1910	1994
0955	Borger	35°39'	101°24'	HP	17	1944	1961
0958	Borger	35°39'	101°27'	HP	46	1949	1994
0984	Bowie	33°34'	97°51'	NC	70	1897	1994
0991	Boxelder	33°29'	94°53'	ET	46	1949	1994
0996	Boyd	33°04'	97°34'	NC	47	1948	1994
1000	Boys Ranch	35°32'	102°15'	HP	19	1964	1994
1007	Brackettville	29°19'	100°25'	EP	92	1900	1994
1013	Brackettville 26 N	29°41'	100°27'	EP	17	1978	1994
1017	Brady	31°07'	99°20'	EP	62	1897	1994
1033	Bravo	35°39'	103°00'	HP	47	1948	1994
1034	Brazoria	29°93'	95°34'	ET	32	1897	1929
1035	Brazos	32°40'	98°07'	NC	48	1915	1994
1042	Breckenridge and 1043[1]	32°45'	98°56'	NC	72	1898	1994
1045	Bremond	31°10'	96°41'	ET	32	1963	1994
1048	Brenham	30°09'	96°24'	SC	93	1902	1994
1063	Bridgeport	33°13'	97°46'	NC	79	1915	1994
1073	Brighton	27°39'	97°18'	SC	23	1897	1920
1089	Broaddus	31°19'	94°16'	ET	16	1977	1994
1094	Bronson	31°21'	94°01'	ET	52	1924	1979
1127	Brownfield and 1128[1]	33°11'	102°16'	HP	80	1914	1994
1136	Brownsville WSO Airport	25°54'	97°26'	ST	74	1898	1994
1138	Brownwood	31°43'	99°00'	NC	48	1947	1994
1165	Buchanan Dam	30°45'	98°25'	EP	22	1943	1964
1185	Buenavista 2 NNW	31°15'	102°40'	TP	23	1912	1951
1188	Buffalo	31°28'	96°03'	ET	41	1948	1988
1203	Buler 4 NNW	36°11'	100°50'	HP	30	1948	1977
1215	Bulverde	29°45'	98°27'	EP	55	1940	1994
1224	Bunker Hill	36°09'	102°56'	HP	43	1948	1990

Footnote at end of table.

Appendix 3. Daily precipitation stations in Texas with at least 10 years of annual maxima data through 1994—Continued

Station no.	Station name	Latitude and longitude		Climatic region	Years of record	Beginning year of record	Ending year of record
1239	Burkett	32°00'	99°14'	LRP	47	1948	1994
1245	Burleson 2 SSW and 1245[1]	32°31'	97°20'	NC	47	1948	1994
1248	Burlington 3 WSW	31°00'	97°02'	NC	28	1948	1975
1250	Burnet	30°44'	98°14'	EP	96	1896	1994
1285	Byrds 1 NNE	31°56'	99°02'	NC	18	1948	1965
1314	Caldwell	30°32'	96°42'	SC	32	1963	1994
1334	Callan	31°03'	99°43'	EP	18	1948	1965
1337	Calliham	28°27'	98°21'	ST	17	1978	1994
1348	Cameron	30°51'	96°59'	NC	87	1908	1994
1385	Camp San Saba	31°00'	99°16'	EP	18	1948	1965
1398	Camp Wood	29°41'	100°01'	EP	50	1944	1994
1412	Canadian 1 ENE	35°55'	100°22'	HP	89	1906	1994
1416	Candelaria	30°09'	104°41'	TP	47	1948	1994
1425	Canton 3 SSE	32°31'	95°51'	ET	43	1948	1994
1429	Canyon Dam	29°52'	98°12'	EP	34	1961	1994
1430	Canyon	34°59'	101°56'	HP	72	1923	1994
1439	Capps Ranch	30°50'	99°07'	EP	12	1948	1959
1481	Carr Ranch	30°10'	99°07'	EP	42	1920	1961
1486	Carrizo Springs	28°32'	99°53'	ST	70	1912	1994
1490	Carrollton	32°59'	96°54'	NC	47	1948	1994
1492	Carta Valley	29°48'	100°40'	EP	32	1963	1994
1500	Carthage	32°09'	94°22'	ET	45	1908	1994
1511	Case Ranch 3 S	31°38'	101°02'	EP	36	1948	1983
1521	Castell	30°42'	98°58'	EP	32	1948	1980
1524	Castolon	29°08'	103°30'	TP	21	1947	1994
1528	Catarina	28°21'	99°37'	ST	36	1959	1994
1541	Cedar Creek 4 SE	30°02'	97°28'	SC	17	1978	1994
1573	Celina	33°19'	96°48'	NC	35	1948	1982
1578	Center	31°48'	94°10'	ET	59	1922	1994
1580	Center City	31°28'	98°25'	NC	32	1963	1994
1596	Centerville	31°16'	95°59'	ET	58	1937	1994
1625	Chalk Mountain	32°09'	97°55'	NC	32	1963	1994
1646	Channing and 1649[1]	35°41'	102°20'	HP	29	1904	1994
1651	Chapman Ranch	27°35'	97°27'	SC	36	1959	1994
1655	Chappel	31°04'	98°34'	EP	12	1948	1959
1663	Charlotte 5 NNW	28°56'	98°45'	ST	33	1962	1994

Footnote at end of table.

Appendix 3. Daily precipitation stations in Texas with at least 10 years of annual maxima data through 1994—Continued

Station no.	Station name	Latitude and longitude		Climatic region	Years of record	Beginning year of record	Ending year of record
1696	Childress 3 W and 1968[1]	34°26'	100°15'	LRP	91	1897	1994
1701	Chillicothe	34°15'	99°31'	LRP	70	1906	1975
1715	Chisos Basin	29°16'	103°18'	TP	48	1947	1994
1720	Choke Canyon Dam	28°28'	98°16'	ST	12	1983	1994
1735	Christoval	31°12'	100°29'	EP	18	1948	1965
1741	Cibolo Creek	29°01'	97°56'	SC	35	1948	1982
1761	Clarendon	34°56'	100°53'	LRP	89	1904	1994
1772	Clarksville 2 NE	33°38'	95°02'	ET	90	1903	1994
1777	Classens Ranch	29°39'	98°22'	EP	26	1947	1972
1778	Claude	35°07'	101°22'	HP	91	1904	1994
1800	Cleburne	32°20'	97°24'	NC	87	1907	1994
1810	Cleveland	30°22'	95°05'	UC	41	1954	1994
1823	Clifton 10 E	31°48'	97°26'	NC	65	1911	1975
1832	Cline	29°15'	100°05'	EP	18	1940	1957
1838	Clodine	29°42'	95°41'	UC	49	1943	1994
1843	Cloudt Ranch	30°11'	100°22'	EP	16	1949	1964
1870	Coldspring 5 SSW	30°32'	95°09'	ET	41	1954	1994
1874	Coldwater	36°24'	102°34'	HP	42	1941	1983
1875	Coleman	31°50'	99°26'	LRP	98	1896	1994
1888	College Station 6 SW	30°32'	96°25'	SC	60	1901	1984
1889	College Station FAA Airport	30°35'	96°21'	ET	44	1951	1994
1903	Colorado City	32°23'	100°52'	LRP	71	1898	1994
1911	Columbus	29°43'	96°32'	SC	49	1915	1994
1914	Comanche	31°54'	98°35'	NC	81	1901	1994
1925	Comstock	29°41'	101°11'	EP	25	1903	1987
1946	Conlen	36°14'	102°14'	HP	47	1948	1994
1956	Conroe	30°20'	95°29'	ET	47	1948	1994
1970	Cooper	33°22'	95°41'	NC	47	1948	1994
1974	Cope Ranch	31°34'	101°15'	EP	47	1948	1994
1984	Copperas Cove and 1986[1]	31°07'	97°54'	NC	68	1915	1983
1990	Copperas Cove 5 NW	31°10'	97°58'	NC	12	1983	1994
2012	Cornudas Service Station	31°47'	105°28'	TP	47	1948	1994
2014	Corpus Christi	27°48'	97°24'	SC	35	1946	1980
2015	Corpus Christi WSO Airport	27°46'	97°30'	SC	47	1948	1994
2019	Corsicana	32°05'	96°28'	NC	95	1897	1994
2040	Cottonwood	30°10'	99°08'	EP	33	1962	1994

Footnote at end of table.

Appendix 3. Daily precipitation stations in Texas with at least 10 years of annual maxima data through 1994—Continued

Station no.	Station name	Latitude and longitude		Climatic region	Years of record	Beginning year of record	Ending year of record
2048	Cotulla	28°26'	99°15'	ST	86	1901	1994
2050	Cotulla FAA Airport	28°27'	99°13'	ST	33	1949	1981
2066	Cox Ranch	31°21'	99°53'	EP	18	1948	1965
2080	Crandall	32°38'	96°28'	NC	35	1960	1994
2082	Crane	31°23'	102°20'	TP	41	1928	1994
2096	Cresson	32°32'	97°37'	NC	47	1948	1994
2104	Crider Ranch	30°04'	99°44'	EP	28	1948	1975
2114	Crockett	31°18'	95°27'	ET	85	1904	1994
2121	Crosbyton	33°30'	101°15'	HP	97	1897	1994
2128	Cross Plains	32°07'	99°10'	NC	38	1939	1976
2142	Crowell	33°59'	99°43'	LRP	79	1916	1994
2160	Crystal City	28°41'	99°50'	ST	47	1948	1994
2173	Cuero	29°05'	97°19'	SC	93	1901	1994
2206	Cypress	29°58'	95°42'	UC	46	1948	1994
2210	Cypress Mill	30°23'	98°15'	EP	17	1948	1964
2218	Dacus	30°26'	95°47'	ET	41	1954	1994
2225	Daingerfield 9 S	32°55'	94°43'	ET	47	1948	1994
2239	Dalhart Experiment Station and 2240[1]	36°01'	102°35'	HP	91	1905	1994
2242	Dallas-Ft. Worth Regional WSO Airport	32°54'	97°02'	NC	21	1974	1994
2244	Dallas FAA Airport	32°51'	96°51'	NC	65	1897	1994
2266	Danevang 1 W	29°04'	96°13'	UC	97	1897	1994
2282	Darrouzett	36°26'	100°19'	HP	54	1941	1994
2295	Davilla	30°47'	97°16'	NC	47	1948	1994
2317	De Long Ranch	30°59'	100°48'	EP	11	1948	1958
2334	Decatur and 2338[1]	33°14'	97°36'	NC	55	1904	1994
2352	De Kalb	33°30'	94°36'	ET	47	1948	1994
2354	Dell City 5 SSW	31°54'	105°13'	TP	16	1979	1994
2357	Del Rio WB City	29°20'	100°53'	EP	13	1946	1963
2360	Del Rio WSO Airport	29°22'	100°55'	EP	39	1951	1994
2394	Denison Dam	33°49'	96°34'	NC	55	1940	1994
2397	Denison Hwy. 60 Bridge	33°49'	96°32'	NC	37	1909	1949
2403	Denton	33°14'	97°08'	NC	17	1949	1965
2404	Denton 2 SE	33°12'	97°06'	NC	82	1913	1994
2415	Deport	33°31'	95°19'	NC	15	1948	1994
2417	Derby 1 S	28°45'	99°08'	ST	17	1978	1994
2436	Deweyville 5 S	30°14'	93°44'	UC	33	1954	1986

Footnote at end of table.

Appendix 3. Daily precipitation stations in Texas with at least 10 years of annual maxima data through 1994—Continued

Station no.	Station name	Latitude and longitude		Climatic region	Years of record	Beginning year of record	Ending year of record
2444	Dialville 2 W	31°52'	95°16'	ET	97	1897	1994
2448	Dickens	33°37'	100°50'	LRP	21	1964	1984
2458	Dilley	28°40'	99°10'	ST	82	1910	1994
2462	Dime Box	30°22'	96°50'	SC	54	1941	1994
2463	Dimmitt 6 E	34°33'	102°13'	HP	63	1923	1985
2464	Dimmitt 2 N	34°35'	102°19'	HP	36	1959	1994
2527	Doole 6 NNE	31°29'	99°34'	EP	32	1948	1979
2541	Doss	30°27'	99°08'	EP	18	1948	1965
2585	Dripping Springs 6 E	30°13'	97°59'	EP	11	1984	1994
2590	Dryden	30°03'	102°07'	TP	29	1966	1994
2593	Dryden 10 NE	30°12'	101°50'	TP	13	1937	1993
2595	Dryer 1 NW	29°23'	97°16'	SC	36	1940	1975
2598	Dublin	32°06'	98°20'	NC	95	1898	1994
2617	Dumas	35°52'	101°58'	HP	58	1937	1994
2621	Dumont	33°48'	100°31'	LRP	24	1971	1994
2630	Duncan Wilson Ranch	30°48'	100°10'	EP	29	1966	1994
2633	Dundee 6 NNW	33°49'	98°56'	NC	73	1922	1994
2636	Dunk Ranch	30°22'	99°36'	EP	11	1948	1958
2669	Eads	32°34'	95°25'	ET	11	1948	1958
2677	Eagle Mountain Lake	32°53'	97°27'	NC	51	1940	1994
2679	Eagle Pass	28°42'	100°29'	5	94	1900	1994
2715	Eastland	32°24'	98°51'	NC	85	1904	1994
2741	Eden 1	31°13'	99°50'	EP	56	1923	1983
2768	Edna Hwy. 59 Bridge	28°58'	96°41'	UC	87	1909	1994
2772	Edom 3 NNW	32°25'	95°37'	ET	55	1940	1994
2786	El Campo	29°12'	96°17'	UC	34	1941	1974
2794	El Paso 15 ENE	31°50'	105°56'	TP	12	1983	1994
2797	El Paso WSO Airport	31°48'	106°24'	TP	47	1948	1994
2812	Eldorado 11 NW	30°58'	100°42'	EP	23	1959	1981
2814	Eldorado 19 SW	30°44'	100°53'	EP	33	1941	1975
2818	Electra	34°02'	98°55'	LRP	47	1948	1994
2820	Elgin	30°21'	97°22'	SC	33	1962	1994
2824	El Indio	28°31'	100°19'	ST	17	1978	1994
2902	Emory	32°52'	95°44'	ET	53	1897	1994
2906	Encinal	28°02'	99°22'	ST	88	1907	1994
2917	Engleman Gardens	26°20'	98°01'	ST	25	1946	1970

Footnote at end of table.

Appendix 3. Daily precipitation stations in Texas with at least 10 years of annual maxima data through 1994—Continued

Station no.	Station name	Latitude and longitude		Climatic region	Years of record	Beginning year of record	Ending year of record
2925	Ennis	32°20'	96°38'	NC	49	1940	1991
3000	Evadale	30°20'	94°05'	ET	42	1946	1994
3005	Evant 4 SW	31°27'	98°13'	NC	41	1941	1994
3033	Fabens	31°30'	106°09'	TP	30	1948	1977
3038	Fair Oaks Ranch	29°45'	98°38'	EP	28	1946	1973
3047	Fairfield 4 E	31°44'	96°06'	ET	53	1941	1994
3060	Falcon Dam	26°33'	99°08'	ST	33	1962	1994
3063	Falfurrias	27°14'	98°08'	ST	88	1907	1994
3065	Falls City 4 WSW	28°57'	98°04'	SC	49	1946	1994
3080	Farmersville	33°11'	96°22'	NC	48	1947	1994
3085	Farnsworth 3 NNW	36°22'	100°59'	HP	18	1941	1958
3112	Fedor	30°19'	97°03'	SC	32	1963	1994
3133	Ferris	32°32'	96°40'	NC	53	1940	1994
3142	Fife	31°23'	99°22'	EP	35	1941	1975
3156	Fischers Store	29°59'	98°16'	EP	54	1941	1994
3183	Flatonia	29°40'	97°07'	SC	87	1908	1994
3192	Flint	32°12'	95°21'	ET	40	1910	1949
3196	Flomot 4 NE	34°16'	100°56'	LRP	49	1946	1994
3199	Florence 3 SE	30°48'	97°46'	NC	32	1963	1994
3201	Floresville	29°08'	98°10'	SC	79	1916	1994
3214	Floydada	33°58'	101°20'	HP	56	1911	1994
3215	Floydada 9 SE	33°52'	101°15'	HP	48	1947	1994
3218	Flying V Ranch	31°05'	98°45'	EP	12	1948	1959
3225	Follett	36°26'	100°08'	HP	65	1930	1994
3247	Forestburg 5 S	33°28'	97°34'	NC	57	1897	1994
3253	Forsan	32°06'	101°22'	HP	46	1949	1994
3262	Fort Davis	30°36'	103°53'	TP	83	1902	1994
3266	Fort Hancock	31°17'	105°51'	TP	29	1966	1994
3267	Fort McIntosh	27°30'	99°31'	ST	32	1900	1931
3277	Fort Stockton 1	30°53'	102°53'	TP	51	1897	1948
3280	Fort Stockton	30°53'	102°52'	TP	54	1940	1994
3283	Fort Worth International WSO Airport	32°50'	97°03'	NC	27	1897	1973
3284	Fort Worth Meach WSO Airport	32°49'	97°21'	NC	11	1946	1994
3286	Fort Worth Vickery Blvd.	32°44'	97°20'	NC	19	1948	1994
3298	Four Notch Guard Station	30°39'	95°25'	ET	25	1940	1964
3299	Fowlerton 2 NW	28°29'	98°52'	ST	78	1913	1994

Footnote at end of table.

Appendix 3. Daily precipitation stations in Texas with at least 10 years of annual maxima data through 1994—Continued

Station no.	Station name	Latitude and longitude		Climatic region	Years of record	Beginning year of record	Ending year of record
3321	Franklin	31°02'	96°29'	ET	33	1962	1994
3329	Fredericksburg	30°16'	98°52'	EP	75	1896	1994
3340	Freeport 2 NW	28°59'	95°23'	UC	64	1931	1994
3341	Freer	27°53'	98°37'	ST	48	1947	1994
3344	Freer 18 WNW	27°57'	98°54'	ST	17	1978	1994
3366	Frio Town	29°02'	99°19'	ST	28	1947	1979
3368	Friona	34°38'	102°43'	HP	64	1927	1994
3370	Frisco	33°09'	96°50'	NC	29	1966	1994
3379	Frost	32°05'	96°48'	NC	40	1946	1985
3401	Funk Ranch (LCRA 127)	31°29'	100°48'	EP	47	1948	1994
3411	Gail	32°46'	101°27'	LRP	64	1897	1994
3415	Gainesville and 3420[1]	33°38'	97°08'	NC	96	1897	1994
3430	Galveston WSO City	29°18'	94°48'	UC	53	1900	1994
3431	Galveston WB Airport	29°16'	94°51'	UC	16	1948	1963
3445	Garden City	31°52'	101°29'	HP	83	1912	1994
3472	Gary	32°02'	94°22'	ET	19	1940	1958
3476	Garza Little Elm Dam	33°04'	97°01'	NC	15	1949	1963
3485	Gatesville	31°26'	97°46'	NC	88	1900	1994
3506	Georgetown	30°38'	97°41'	NC	54	1896	1983
3507	Georgetown Lake	30°41'	97°43'	NC	14	1981	1994
3508	George West 2 SSW	28°18'	98°07'	ST	79	1916	1994
3525	Giddings 3 ESE	30°10'	96°53'	SC	55	1940	1994
3546	Gilmer 2 W	32°44'	94°59'	ET	66	1929	1994
3557	Girvin	31°04'	102°24'	TP	33	1947	1979
3565	Gladewater 3 WSW	32°31'	94°58'	ET	31	1946	1976
3585	Glenfawn	31°55'	94°51'	ET	10	1949	1958
3591	Glen Rose 2 W	32°14'	97°48'	NC	32	1963	1994
3605	Gold	30°21'	98°43'	EP	47	1948	1994
3614	Goldthwaite 1 WSW	31°27'	98°35'	NC	64	1923	1994
3618	Goliad	28°40'	97°24'	SC	83	1912	1994
3619	Goliad 6 NE	28°43'	97°20'	SC	12	1948	1959
3620	Goliad 1 SE	28°40'	97°23'	SC	46	1949	1994
3622	Gonzales	29°30'	97°27'	SC	57	1915	1994
3640	Goose Creek	29°44'	94°58'	UC	36	1921	1956
3668	Graham	33°06'	98°35'	NC	92	1897	1994
3673	Granbury 2 ENE	32°27'	97°45'	NC	32	1943	1975

Footnote at end of table.

Appendix 3. Daily precipitation stations in Texas with at least 10 years of annual maxima data through 1994—Continued

Station no.	Station name	Latitude and longitude		Climatic region	Years of record	Beginning year of record	Ending year of record
3680	Grandfalls 3 SSE	31°18'	102°50'	TP	81	1909	1994
3685	Granger	30°43'	97°26'	NC	27	1968	1994
3686	Granger Dam	30°42'	97°20'	NC	15	1980	1994
3689	Grapeland	31°29'	95°29'	ET	40	1935	1975
3691	Grapevine Dam	32°58'	97°03'	NC	64	1901	1994
3734	Greenville 7 NW	33°12'	96°13'	NC	94	1900	1994
3770	Groesbeck	31°31'	96°32'	NC	13	1963	1975
3778	Groveton	31°04'	95°08'	ET	57	1923	1994
3787	Gruver	36°15'	101°24'	HP	54	1941	1994
3822	Gunter 5 S	33°22'	96°46'	NC	47	1948	1994
3828	Guthrie	33°37'	100°19'	LRP	46	1947	1994
3841	Hackberry	33°56'	100°08'	LRP	17	1971	1987
3846	Hagansport	33°21'	95°15'	ET	82	1909	1994
3862	Hale Center	34°05'	101°51'	HP	18	1901	1957
3864	Hale Center 14 WNW	34°08'	102°03'	HP	13	1946	1958
3873	Hallettsville 2 N	29°28'	96°57'	SC	97	1897	1994
3884	Hamilton 1 NW	31°43'	98°09'	NC	47	1915	1990
3890	Hamlin	32°53'	100°08'	LRP	68	1910	1994
3941	Harleton	32°40'	94°34'	ET	46	1949	1994
3943	Harlingen	26°12'	97°40'	ST	82	1911	1994
3954	Harper	30°18'	99°15'	EP	54	1909	1994
3972	Hart	34°22'	102°05'	HP	42	1947	1994
3981	Hartley	35°53'	102°24'	HP	48	1947	1994
3992	Haskell	33°10'	99°44'	LRP	97	1897	1994
3994	Haskell 6 NW	33°14'	99°48'	LRP	23	1941	1963
4020	Hawkins 1 E	32°35'	95°11'	ET	47	1924	1994
4026	Hawley	32°38'	99°49'	LRP	22	1973	1994
4033	Haynes Ranch	30°28'	98°25'	EP	11	1948	1958
4058	Hebbronville	27°19'	98°41'	ST	89	1905	1994
4076	Hemphill	31°21'	93°50'	ET	26	1967	1992
4080	Hempstead	30°06'	96°05'	ET	33	1946	1978
4081	Henderson	32°10'	94°48'	ET	87	1908	1994
4088	Henly	30°12'	98°13'	EP	18	1948	1965
4093	Henrietta	33°49'	98°12'	NC	94	1897	1994
4098	Hereford	34°49'	102°24'	HP	67	1905	1994
4122	Hewitt 1 SE	31°27'	97°11'	NC	109	1879	1994

Footnote at end of table.

Appendix 3. Daily precipitation stations in Texas with at least 10 years of annual maxima data through 1994—Continued

Station no.	Station name	Latitude and longitude		Climatic region	Years of record	Beginning year of record	Ending year of record
4137	Hico	31°59'	98°02'	NC	85	1910	1994
4140	Higgins	36°07'	100°02'	HP	50	1907	1994
4182	Hillsboro	32°01'	97°07'	NC	92	1903	1994
4196	Hitchland 6 SSW	36°25'	101°21'	HP	27	1947	1973
4254	Hondo	29°21'	99°08'	EP	76	1900	1975
4256	Hondo WSMO Airport	29°21'	99°10'	EP	20	1975	1994
4257	Honey Grove	33°35'	95°54'	NC	80	1898	1994
4278	Hords Creek Dam	31°51'	99°34'	LRP	42	1953	1994
4280	Horger	31°00'	94°10'	ET	37	1946	1982
4300	Houston WSCMO Airport	29°58'	95°21'	UC	26	1969	1994
4305	Houston WB City	29°46'	95°22'	UC	29	1941	1969
4307	Houston FAA Airport	29°39'	95°17'	UC	54	1941	1994
4311	Houston-Alief	29°43'	95°36'	UC	17	1948	1964
4313	Houston-Barker	29°49'	95°44'	UC	47	1948	1994
4315	Houston Deer Park	29°43'	95°08'	UC	50	1945	1994
4321	Houston-Heights	29°47'	95°26'	UC	43	1948	1994
4323	Houston Independence Heights	29°52'	95°25'	UC	47	1948	1994
4325	Houston-Westbury	29°40'	95°28'	UC	47	1948	1994
4327	Houston North Houston	29°53'	95°32'	UC	47	1948	1994
4328	Houston San Jacinto Dam	29°55'	95°09'	UC	41	1954	1994
4329	Houston-Satsuma	29°56'	95°38'	UC	26	1923	1964
4331	Houston Spring Branch	29°48'	95°30'	UC	39	1954	1994
4343	Huckabay 2 NW	32°21'	98°19'	NC	30	1963	1994
4362	Humble	30°00'	95°15'	UC	32	1954	1985
4363	Humble Pump Station 5 WNW	30°22'	100°18'	EP	46	1948	1994
4374	Hunt	30°04'	99°21'	EP	48	1947	1994
4382	Huntsville	30°43'	95°33'	ET	49	1946	1994
4390	Hurst Springs	31°39'	97°43'	NC	32	1963	1994
4402	Hye	30°15'	98°34'	EP	47	1948	1994
4425	Imperial 2 W	31°16'	102°44'	TP	47	1947	1993
4440	Indian Gap	31°40'	98°25'	NC	37	1947	1983
4471	Iowa Park Experiment Station	33°55'	98°39'	LRP	25	1940	1964
4483	Iron Bridge Dam	32°49'	95°55'	ET	19	1975	1993
4517	Jacksboro	33°14'	98°09'	NC	54	1941	1994
4523	Jackson Hill Guard Station	31°19'	94°17'	ET	30	1947	1976
4524	Jacksonville Experiment Station	31°59'	95°17'	ET	17	1947	1963

Footnote at end of table.

Appendix 3. Daily precipitation stations in Texas with at least 10 years of annual maxima data through 1994—Continued

Station no.	Station name	Latitude and longitude		Climatic region	Years of record	Beginning year of record	Ending year of record
4525	Jacksonville	31°58'	95°16'	ET	41	1953	1994
4538	James River Ranch	30°32'	99°23'	EP	28	1948	1975
4556	Jarrell	30°49'	97°36'	NC	68	1926	1994
4563	Jasper	30°56'	94°00'	ET	54	1898	1994
4570	Jayton	33°15'	100°34'	LRP	47	1910	1994
4575	Jeddo 1 SW	29°48'	97°20'	SC	48	1947	1994
4577	Jefferson 4 NE	32°50'	94°19'	ET	85	1903	1994
4591	Jewett	31°21'	96°09'	ET	46	1904	1991
4597	Joe Pool Lake	32°38'	97°01'	NC	11	1984	1994
4605	Johnson City	30°17'	98°25'	EP	29	1964	1994
4608	Johnson Ranch	31°14'	99°29'	EP	18	1948	1965
4627	Jones CB Ranch	30°49'	100°08'	EP	16	1948	1964
4630	Jones MW Ranch	30°57'	100°16'	EP	11	1948	1958
4647	Jourdanton	28°54'	98°33'	ST	55	1916	1994
4670	Junction	30°29'	99°47'	EP	86	1897	1994
4671	Junction FAA Airport	30°30'	99°46'	EP	22	1948	1969
4672	Juno	30°09'	101°07'	EP	12	1964	1975
4693	Karnack	32°41'	94°09'	ET	53	1942	1994
4696	Karnes City	28°53'	97°55'	SC	75	1919	1994
4704	Katy-Wolf Hill	29°51'	95°50'	UC	40	1952	1993
4705	Kaufman 3 SE	32°33'	96°16'	NC	93	1902	1994
4745	Kempner	31°05'	98°00'	EP	22	1963	1987
4752	Kenedy	28°49'	97°51'	SC	30	1948	1977
4761	Kennedale 6 SSW	32°33'	97°14'	NC	33	1949	1981
4767	Kent 5 E	31°04'	104°09'	TP	40	1898	1976
4780	Kerrville and 4782[1]	30°03'	99°09'	EP	95	1897	1994
4791	Killeen	31°07'	97°42'	NC	33	1912	1978
4792	Killeen 3 S	31°04'	97°44'	NC	17	1978	1994
4810	Kingsville	27°33'	97°53'	SC	77	1902	1993
4819	Kirbyville 5 ESE	30°37'	93°49'	ET	53	1929	1994
4841	Knapp 2 SW	32°38'	101°08'	LRP	63	1931	1994
4852	Knox City	33°25'	99°49'	LRP	31	1935	1965
4866	Kopperl 5 NNE	32°08'	97°29'	NC	11	1900	1994
4878	Kountze 3 SE	30°20'	94°14'	ET	11	1948	1994
4903	La Grange	29°55'	96°52'	SC	85	1910	1994
4914	Lake Ray Hubbard	32°48'	96°29'	NC	16	1978	1993

Footnote at end of table.

Appendix 3. Daily precipitation stations in Texas with at least 10 years of annual maxima data through 1994—Continued

Station no.	Station name	Latitude and longitude		Climatic region	Years of record	Beginning year of record	Ending year of record
4920	La Pryor	28°57'	99°50'	ST	76	1915	1994
4931	La Tuna 1 S	31°58'	106°36'	TP	52	1943	1994
4950	Lajitas	29°15'	103°47'	TP	17	1978	1994
4960	Lake Abilene	32°14'	99°54'	LRP	33	1962	1994
4974	Lake Colorado City	32°20'	100°55'	LRP	34	1954	1993
4977	Lake Dallas	33°07'	97°02'	NC	10	1947	1956
4978	Lake Kickapoo	33°40'	98°47'	NC	18	1947	1964
4981	Lake Victor 3 W	30°54'	98°14'	EP	18	1948	1965
4982	Lake Kemp	33°45'	99°09'	LRP	27	1962	1994
5013	Lamesa 1 SSE	32°42'	101°56'	HP	85	1910	1994
5018	Lampasas	31°03'	98°11'	EP	97	1897	1994
5048	Langtry	29°48'	101°34'	EP	53	1897	1994
5057	Laredo WB Airport	27°32'	99°28'	ST	24	1915	1965
5060	Laredo 2	27°34'	99°30'	ST	33	1946	1994
5081	Latex	32°21'	94°06'	ET	17	1947	1963
5086	Latimer Ranch	33°53'	100°23'	LRP	24	1971	1994
5094	Lavon Dam	33°02'	96°29'	NC	46	1949	1994
5097	Lawn	32°09'	99°45'	LRP	47	1948	1994
5109	Leaday	31°34'	99°40'	LRP	18	1948	1965
5158	Lenorah	32°18'	101°53'	HP	53	1941	1994
5183	Levelland	33°34'	102°23'	HP	59	1926	1994
5191	Lewisville and 5190[1], 5192[1]	33°03'	97°00'	NC	47	1909	1994
5193	Lexington	30°25'	97°01'	SC	37	1948	1994
5196	Liberty	30°03'	94°48'	UC	91	1904	1994
5202	Liberty Hill	30°40'	97°55'	NC	18	1948	1965
5216	Lillian	32°30'	97°11'	NC	13	1947	1959
5218	Lillian 3 W	32°30'	97°14'	NC	14	1981	1994
5228	Lindale 5 SE	32°27'	95°22'	ET	35	1931	1965
5229	Linden	33°01'	94°21'	ET	46	1948	1994
5243	Lipan	32°31'	98°03'	NC	46	1949	1994
5247	Lipscomb	36°14'	100°16'	HP	47	1948	1994
5258	Little Elm	33°10'	96°56'	NC	21	1946	1966
5263	Littlefield and 5265[1]	33°55'	102°20'	HP	70	1916	1994
5271	Livingston 2 NNE	30°44'	94°56'	ET	58	1937	1994
5272	Llano	30°45'	98°41'	EP	98	1896	1994
5284	Lockhart	29°53'	97°42'	SC	48	1947	1994

Footnote at end of table.

Appendix 3. Daily precipitation stations in Texas with at least 10 years of annual maxima data through 1994—Continued

Station no.	Station name	Latitude and longitude		Climatic region	Years of record	Beginning year of record	Ending year of record
5308	Lometa	31°13'	98°24'	EP	18	1948	1965
5327	Long Lake 5 SW	31°37'	95°51'	ET	37	1915	1980
5341	Longview	32°28'	94°44'	ET	93	1902	1994
5348	Longview WSMO	32°21'	94°39'	ET	20	1975	1994
5351	Loop	32°54'	102°25'	HP	46	1948	1994
5363	Lorenzo	33°40'	101°32'	HP	46	1947	1993
5398	Lovelady	31°08'	95°27'	ET	29	1948	1986
5410	Lubbock 9 N	33°42'	101°50'	HP	19	1946	1964
5411	Lubbock WSFO Airport	33°39'	101°49'	HP	84	1911	1994
5415	Lufkin 7 NW	31°25'	94°48'	ET	12	1983	1994
5424	Lufkin FAA Airport	31°14'	94°45'	ET	88	1906	1994
5429	Luling	29°40'	97°39'	SC	94	1901	1994
5449	Lynxhaven Ranch	29°58'	99°27'	EP	30	1947	1976
5454	Lytle 3 W	29°14'	98°50'	EP	19	1976	1994
5477	Madisonville	30°57'	95°55'	ET	68	1918	1994
5496	Magnolia 1 W	30°13'	95°47'	ET	31	1954	1986
5538	Manchaca	30°08'	97°50'	EP	18	1948	1965
5560	Mansfield	32°34'	97°09'	NC	18	1947	1964
5561	Mansfield Dam	30°24'	97°55'	EP	21	1944	1964
5579	Marathon	30°13'	103°14'	TP	61	1897	1994
5583	Marco	31°06'	99°34'	EP	27	1948	1974
5589	Marfa CAA Airport	30°15'	103°53'	TP	16	1907	1954
5593	Marfa 19 S	30°02'	104°01'	TP	11	1950	1961
5596	Marfa 2	30°18'	104°01'	TP	37	1958	1994
5611	Marlin 3 NE	31°20'	96°51'	NC	68	1902	1994
5618	Marshall	32°32'	94°21'	ET	87	1908	1994
5626	Martin Ranch	30°38'	99°10'	EP	18	1948	1965
5646	Marys Creek	32°44'	97°30'	NC	27	1947	1973
5650	Mason	30°45'	99°14'	EP	54	1941	1994
5658	Matador	34°01'	100°50'	LRP	48	1947	1994
5659	Matagorda 2	28°42'	95°58'	UC	85	1910	1994
5661	Mathis 4 SSW	28°02'	97°52'	ST	31	1964	1994
5667	Maud 1 S	33°19'	94°20'	ET	49	1946	1994
5670	Maurbro	28°55'	96°28'	UC	23	1944	1966
5701	McAllen	26°12'	98°13'	ST	53	1941	1993
5702	McAllen FAA Airport	26°11'	98°14'	ST	34	1961	1994

Footnote at end of table.

Appendix 3. Daily precipitation stations in Texas with at least 10 years of annual maxima data through 1994—Continued

Station no.	Station name	Latitude and longitude		Climatic region	Years of record	Beginning year of record	Ending year of record
5707	McCamey	31°08'	102°12'	EP	63	1932	1994
5721	McCook	26°29'	98°23'	ST	54	1941	1994
5742	Medina	29°48'	99°15'	EP	29	1966	1994
5757	McGregor	31°26'	97°25'	NC	85	1910	1994
5761	McIntosh Ranch	30°44'	100°30'	EP	18	1948	1965
5766	McKinney 3 S	33°10'	96°37'	NC	86	1903	1994
5770	McLean	35°14'	100°36'	HP	37	1948	1994
5821	Memphis	34°44'	100°32'	LRP	89	1905	1994
5822	Menard	30°55'	99°47'	EP	90	1897	1994
5828	Mentone 2 S	31°41'	103°36'	TP	26	1949	1974
5832	Menzies Al Ranch	31°04'	99°56'	EP	12	1948	1959
5836	Mercedes 6 SSE	26°04'	97°54'	ST	80	1914	1994
5845	Meridian	31°56'	97°40'	NC	13	1982	1994
5847	Meridian State Park	31°53'	97°42'	NC	20	1963	1982
5854	Merrill Ranch	30°32'	104°03'	TP	29	1939	1967
5859	Mertzon	31°16'	100°49'	EP	47	1941	1987
5869	Mexia	31°41'	96°29'	NC	89	1904	1994
5875	Miami	35°42'	100°38'	HP	90	1905	1994
5878	Mid City	33°50'	95°31'	NC	25	1970	1994
5888	Midkiff	31°38'	101°50'	EP	14	1981	1994
5890	Midland/Odessa WSO Airport	31°57'	102°11'	HP	47	1948	1994
5891	Midland 4 ENE	32°01'	102°01'	HP	48	1947	1994
5896	Midlothian	32°29'	97°03'	NC	18	1947	1964
5904	Midway 4 NE	31°04'	95°43'	ET	17	1978	1994
5930	Miller Ranch	30°58'	98°56'	EP	18	1948	1966
5954	Mineola 7 SSW	32°35'	95°33'	ET	49	1946	1994
5956	Mineola 8 ENE	32°43'	95°22'	ET	28	1966	1994
5958	Mineral Wells FAA Airport	32°47'	98°04'	NC	42	1948	1994
5971	Mirando City	27°27'	99°00'	ST	16	1948	1963
5972	Mission 4 W	26°13'	98°24'	ST	84	1910	1994
5987	Mobeetie	35°32'	100°26'	LRP	27	1947	1974
5999	Monahans and 6000[1]	31°35'	102°53'	TP	42	1900	1994
6014	Montague	33°40'	97°45'	NC	22	1943	1964
6019	Montell	29°32'	100°01'	EP	33	1912	1944
6024	Montgomery	30°23'	95°42'	ET	41	1954	1994
6058	Morgan 3 WNW	32°01'	97°39'	NC	30	1965	1994

Footnote at end of table.

Appendix 3. Daily precipitation stations in Texas with at least 10 years of annual maxima data through 1994—Continued

Station no.	Station name	Latitude and longitude		Climatic region	Years of record	Beginning year of record	Ending year of record
6060	Morgan Mill	32°22'	98°10'	NC	46	1949	1994
6070	Morse	36°04'	101°29'	HP	53	1941	1994
6074	Morton 1 WNW	33°44'	102°47'	HP	52	1935	1994
6078	Moscow	30°55'	94°50'	ET	23	1947	1969
6085	Moss Ranch	30°33'	98°41'	EP	18	1948	1965
6104	Mount Locke	30°40'	104°00'	TP	60	1935	1994
6108	Mount Pleasant	33°10'	95°00'	ET	79	1905	1994
6116	Mountain Creek	32°43'	96°56'	NC	18	1947	1964
6119	Mount Vernon	33°11'	95°14'	ET	29	1966	1994
6130	Muenster	33°39'	97°22'	NC	48	1947	1994
6135	Muleshoe 1	34°14'	102°45'	HP	74	1921	1994
6137	Muleshoe Wildlife Refuge	33°57'	102°47'	HP	15	1980	1994
6140	Mullin	31°34'	98°40'	NC	47	1948	1994
6146	Munday	33°27'	99°38'	LRP	83	1912	1994
6158	Murr Ranch	30°41'	100°05'	EP	17	1948	1965
6176	Nacogdoches and 6177[1]	31°36'	94°39'	ET	95	1900	1994
6190	Naples 1 SW	33°11'	94°41'	ET	73	1909	1981
6195	Naples 5 NE	33°15'	94°37'	ET	13	1982	1994
6205	Natalia	29°12'	98°51'	EP	41	1909	1976
6210	Navarro Mills Dam	31°57'	96°42'	NC	32	1963	1994
6219	Neal Ranch	31°11'	99°09'	EP	12	1948	1959
6247	Negley 1 SE	33°44'	95°03'	ET	47	1948	1994
6257	Nelson Ranch	29°57'	99°31'	EP	22	1962	1983
6265	Neuville	31°40'	94°09'	ET	29	1947	1975
6270	New Boston	33°27'	94°25'	ET	15	1980	1994
6276	New Braunfels	29°44'	98°07'	EP	97	1897	1994
6280	New Caney 2 E	30°08'	95°11'	ET	43	1952	1994
6286	New Gulf	29°16'	95°54'	UC	49	1946	1994
6331	Newport	33°29'	98°02'	NC	46	1947	1994
6339	Newton	30°51'	93°46'	ET	12	1966	1977
6341	Newton 6 SE	30°47'	93°43'	ET	12	1980	1991
6367	Nix Store 1 W	31°07'	98°22'	EP	47	1948	1994
6368	Nixon	29°16'	97°46'	SC	74	1921	1994
6382	Nogalus Guard Station	31°16'	95°08'	ET	21	1947	1969
6433	Northfield	34°17'	100°36'	LRP	47	1948	1994
6477	Notla 3 SE	36°06'	100°36'	HP	47	1947	1994

Footnote at end of table.

Appendix 3. Daily precipitation stations in Texas with at least 10 years of annual maxima data through 1994—Continued

Station no.	Station name	Latitude and longitude		Climatic region	Years of record	Beginning year of record	Ending year of record
6484	Novice 1 E	31°59'	99°37'	LRP	26	1948	1973
6494	Nugent 1 ESE	32°41'	99°40'	LRP	30	1943	1972
6495	Oak Creek Lake	32°03'	100°18'	EP	33	1962	1994
6496	Oakwood 2 NNE	31°37'	95°51'	ET	15	1980	1994
6499	O.C. Fisher Dam	31°28'	100°29'	EP	20	1975	1994
6502	Odessa	31°53'	102°24'	TP	45	1950	1994
6636	Olney	33°22'	98°46'	NC	39	1956	1994
6641	Olney 5 NNW	33°26'	98°47'	NC	54	1941	1994
6644	Olton	34°11'	102°08'	HP	53	1928	1994
6664	Orange 4 NW	30°07'	93°47'	UC	60	1905	1994
6722	Overton	32°16'	94°59'	ET	45	1943	1987
6734	Ozona 2 SSW	30°41'	101°20'	EP	47	1948	1994
6740	Paducah and 6743[1]	34°01'	100°18'	LRP	81	1913	1994
6742	Paducah 15 S	33°48'	100°17'	LRP	24	1971	1994
6747	Paint Rock	31°30'	99°55'	EP	77	1918	1994
6750	Palacios FAA Airport	28°43'	96°15'	UC	52	1943	1994
6757	Palestine 2 NE	31°47'	95°36'	ET	63	1930	1994
6766	Palo Pinto	32°46'	98°19'	NC	46	1949	1994
6775	Pampa and 6776[1]	35°32'	100°58'	HP	71	1908	1994
6780	Pandale 2 NE	30°12'	101°33'	EP	49	1909	1994
6781	Pandale 11 NE	30°16'	101°27'	EP	13	1982	1994
6785	Panhandle	35°21'	101°23'	HP	70	1911	1993
6790	Panter	32°20'	97°52'	NC	17	1901	1917
6792	Panther Junction	29°19'	103°13'	TP	40	1955	1994
6794	Paris	33°40'	95°34'	NC	94	1896	1994
6879	Pearsall	28°53'	99°05'	ST	90	1902	1994
6892	Pecos	31°25'	103°30'	TP	66	1904	1994
6932	Penwell	31°44'	102°35'	TP	40	1955	1994
6950	Perryton 5 NNE	36°28'	100°47'	HP	84	1907	1994
6952	Perryton 21 S	36°06'	100°49'	HP	17	1978	1994
6953	Perryton 11 WNW	36°27'	101°00'	HP	48	1947	1994
6959	Persimmon Gap	29°40'	103°10'	TP	16	1952	1994
6992	Pflugerville	30°26'	97°37'	EP	18	1948	1965
7020	Pierce 1 E	29°14'	96°11'	UC	91	1904	1994
7028	Pilot Point	33°23'	96°58'	NC	47	1947	1994
7040	Pineland	31°15'	93°58'	ET	18	1965	1994

Footnote at end of table.

Appendix 3. Daily precipitation stations in Texas with at least 10 years of annual maxima data through 1994—Continued

Station no.	Station name	Latitude and longitude		Climatic region	Years of record	Beginning year of record	Ending year of record
7044	Pine Springs 1 NE	31°54'	104°48'	TP	15	1939	1994
7060	Pitchfork Ranch	33°36'	100°32'	LRP	24	1971	1994
7066	Pittsburg 5 S	32°56'	94°58'	ET	46	1949	1994
7072	Placid	31°19'	99°11'	EP	18	1948	1965
7074	Plains	33°11'	102°50'	HP	60	1925	1994
7079	Plainview	34°11'	101°42'	HP	87	1908	1994
7091	Plata	29°51'	104°01'	TP	14	1964	1977
7116	Plemons	35°46'	101°20'	HP	25	1906	1951
7140	Point Comfort	28°40'	96°33'	UC	38	1957	1994
7146	Polar	33°01'	101°04'	LRP	29	1947	1975
7164	Pontotoc	30°55'	98°59'	EP	16	1948	1965
7165	Poolville	32°58'	97°52'	NC	11	1947	1957
7172	Port Arthur City	29°54'	93°56'	UC	20	1975	1994
7173	Port Arthur	29°52'	93°56'	UC	28	1911	1967
7174	Port Arthur WSO Airport	29°57'	94°01'	UC	48	1947	1994
7179	Port Isabel	26°04'	97°13'	ST	65	1897	1994
7182	Port Lavaca 2	28°37'	96°38'	UC	69	1901	1988
7184	Port Mansfield	26°33'	97°26'	ST	37	1958	1994
7186	Port O'Connor	28°26'	96°25'	UC	45	1948	1994
7205	Possum Kingdom Dam	32°52'	98°26'	NC	37	1939	1975
7206	Post 3 ENE	33°12'	101°20'	LRP	85	1910	1994
7213	Post Oak School	30°16'	96°43'	SC	19	1963	1981
7215	Poteet	29°02'	98°35'	ST	54	1941	1994
7230	Poynor 1 NE	32°05'	95°35'	ET	29	1947	1975
7232	Prade Ranch	29°55'	99°46'	EP	35	1955	1994
7262	Presidio	29°34'	104°23'	TP	68	1927	1994
7271	Price 2 SW	32°07'	94°58'	ET	35	1941	1975
7274	Priddy 3 N	31°43'	98°31'	NC	11	1984	1994
7299	Provident City	29°17'	96°38'	SC	20	1947	1966
7300	Proctor Reservoir	31°58'	98°30'	NC	32	1963	1994
7327	Putnam	32°22'	99°11'	NC	84	1911	1994
7336	Quanah 5 SE	34°15'	99°41'	LRP	91	1904	1994
7358	Quinlan	32°55'	96°08'	NC	13	1962	1974
7361	Quitaque	34°22'	101°03'	HP	42	1934	1976
7363	Quitman	32°47'	95°26'	ET	40	1948	1987
7388	Rainbow	32°16'	97°42'	NC	49	1946	1994

Footnote at end of table.

Appendix 3. Daily precipitation stations in Texas with at least 10 years of annual maxima data through 1994—Continued

Station no.	Station name	Latitude and longitude		Climatic region	Years of record	Beginning year of record	Ending year of record
7426	Ranger 1 W	32°28'	98°42'	NC	29	1947	1975
7431	Rankin	31°14'	101°57'	EP	27	1948	1984
7458	Raymondville	26°29'	97°48'	ST	85	1910	1994
7480	Red Bluff Crossing	31°13'	98°35'	EP	47	1948	1994
7481	Red Bluff Dam	31°54'	103°55'	TP	53	1939	1994
7495	Red Oak	32°31'	96°48'	NC	31	1964	1994
7497	Red Rock	29°58'	97°27'	SC	30	1965	1994
7529	Refugio and 7530[1]	28°18'	97°17'	SC	41	1948	1994
7533	Refugio 7 N	28°24'	97°17'	SC	10	1985	1994
7547	Reklaw 3 NNE	31°54'	94°59'	ET	31	1958	1988
7552	Rendham	33°35'	99°09'	LRP	12	1947	1958
7572	Rhineland	33°32'	99°39'	LRP	10	1897	1907
7580	Ricardo	27°25'	97°49'	SC	67	1909	1975
7586	Richards	30°33'	95°51'	ET	41	1954	1994
7588	Richardson	32°59'	96°45'	NC	46	1948	1994
7593	Richland Springs	31°16'	98°57'	EP	47	1948	1994
7594	Richmond	29°35'	95°45'	UC	50	1919	1994
7612	Riley Ben Ranch	30°26'	98°49'	EP	18	1948	1965
7614	Ringgold	33°49'	97°56'	NC	48	1947	1994
7622	Rio Grande City 3 W	26°23'	98°52'	ST	76	1900	1994
7628	Riomedina 2 N	29°28'	98°53'	EP	73	1922	1994
7633	Rising Star	32°06'	98°58'	NC	53	1942	1994
7651	Riverside	30°51'	95°24'	ET	27	1915	1970
7659	Roanoke	33°00'	97°14'	NC	48	1947	1994
7669	Robert Lee (LCRA 55)	31°54'	100°29'	EP	51	1908	1994
7677	Robstown	27°47'	97°40'	SC	55	1922	1994
7678	Roby	32°44'	100°23'	LRP	65	1897	1975
7680	Rochelle	30°13'	99°13'	EP	21	1915	1935
7685	Rockdale	30°39'	97°01'	NC	32	1963	1994
7700	Rockland 2 NW	31°01'	94°24'	ET	38	1904	1979
7704	Rockport and 7705[1]	28°01'	97°03'	SC	63	1901	1994
7706	Rocksprings	30°01'	100°13'	EP	56	1932	1994
7707	Rockwall	32°56'	96°28'	NC	49	1946	1994
7712	Rocksprings 18 SW	29°47'	100°25'	EP	31	1963	1993
7714	Rocksprings 15 NE	30°11'	100°02'	EP	11	1978	1989
7730	Romero	35°43'	102°55'	HP	26	1910	1936

Footnote at end of table.

Appendix 3. Daily precipitation stations in Texas with at least 10 years of annual maxima data through 1994—Continued

Station no.	Station name	Latitude and longitude		Climatic region	Years of record	Beginning year of record	Ending year of record
7735	Roosevelt 2 E	30°29'	100°02'	EP	18	1948	1965
7743	Roscoe	32°27'	100°32'	LRP	60	1935	1994
7744	Rosebud	31°05'	96°58'	NC	22	1965	1994
7756	Rosenberg	29°33'	95°47'	UC	22	1915	1960
7768	Ross	31°43'	97°07'	NC	36	1940	1975
7773	Rosser	32°28'	96°27'	NC	48	1947	1994
7779	Rossville	29°06'	98°41'	ST	20	1907	1926
7782	Rotan	32°51'	100°28'	LRP	71	1924	1994
7787	Round Mountain 4 WNW	30°28'	98°25'	EP	37	1958	1994
7791	Round Rock 3 NE	30°32'	97°38'	NC	27	1968	1994
7836	Runge	28°53'	97°43'	SC	97	1897	1994
7841	Rusk	31°48'	95°09'	ET	53	1942	1994
7852	Rust Circle Bar Ranch	31°12'	100°10'	EP	10	1948	1958
7873	Sabinal	29°20'	99°29'	EP	91	1903	1994
7903	Salado	30°57'	97°32'	NC	10	1910	1919
7920	Salt Flat	31°45'	105°05'	TP	17	1978	1994
7921	Salt Flat 10 ENE	31°47'	104°54'	TP	19	1959	1977
7936	Sam Rayburn Dam	31°04'	94°06'	ET	27	1968	1994
7940	San Angelo Dam	31°28'	100°29'	EP	23	1953	1975
7943	San Angelo WSO Airport	31°22'	100°30'	EP	49	1946	1994
7945	San Antonio WSFO	29°32'	98°28'	EP	49	1946	1994
7948	San Antonio Nursery	29°18'	98°28'	EP	38	1897	1951
7951	San Augustine	31°32'	94°07'	ET	29	1909	1994
7952	San Benito	26°08'	97°38'	ST	53	1920	1975
7983	San Marcos	29°51'	97°57'	EP	95	1896	1994
7992	San Saba	31°11'	98°43'	EP	64	1901	1994
8022	Sanderson	30°09'	102°24'	TP	62	1897	1994
8036	Sandy 2 S	30°20'	98°28'	EP	17	1949	1965
8043	Sanger	33°22'	97°10'	NC	30	1947	1994
8045	San Jacinto	30°37'	95°43'	ET	10	1977	1986
8059	Santa Rosa 3 WNW and 8060[1]	26°16'	97°52'	ST	11	1948	1994
8081	Sarita 7 E	27°13'	97°41'	ST	95	1900	1994
8126	Schulenburg	29°42'	96°54'	SC	48	1947	1994
8160	Sealy	29°47'	96°08'	SC	80	1910	1994
8186	Seguin	29°35'	97°57'	SC	51	1922	1972
8201	Seminole	32°43'	102°40'	HP	72	1922	1994

Footnote at end of table.

Appendix 3. Daily precipitation stations in Texas with at least 10 years of annual maxima data through 1994—Continued

Station no.	Station name	Latitude and longitude		Climatic region	Years of record	Beginning year of record	Ending year of record
8221	Seymour	33°36'	99°15'	LRP	82	1905	1994
8235	Shamrock	35°12'	100°15'	LRP	59	1929	1987
8236	Shamrock No. 2	35°13'	100°15'	LRP	33	1962	1994
8252	Sheffield	30°42'	101°50'	TP	39	1938	1994
8274	Sherman	33°38'	96°37'	NC	95	1897	1994
8279	Sherwood	31°17'	100°48'	EP	18	1948	1965
8305	Sierra Blanca	31°11'	105°21'	TP	35	1948	1994
8323	Silverton	34°29'	101°19'	HP	49	1946	1994
8326	Silver Valley	31°58'	99°34'	LRP	22	1973	1994
8335	Simms 4 WNW	33°22'	94°34'	ET	15	1948	1973
8354	Sinton	28°03'	97°30'	SC	70	1921	1994
8373	Slaton 5 SE	33°22'	101°36'	HP	46	1949	1994
8378	Slidell	33°21'	97°23'	NC	48	1947	1994
8382	Sloan	31°09'	98°55'	EP	41	1935	1975
8414	Smithsons Valley	29°49'	98°20'	EP	10	1946	1955
8415	Smithville	30°01'	97°09'	SC	77	1917	1994
8433	Snyder	32°43'	100°55'	LRP	84	1911	1994
8435	Socorro	31°39'	106°17'	TP	32	1918	1950
8445	Somerville	30°21'	96°31'	SC	25	1908	1951
8446	Somerville Dam	30°20'	96°32'	SC	31	1963	1994
8449	Sonora	30°34'	100°39'	EP	61	1902	1994
8468	South Camp (6666)	33°30'	100°27'	LRP	10	1971	1980
8519	Speaks 2	29°16'	96°42'	SC	27	1967	1994
8523	Spearman	36°11'	101°11'	HP	75	1920	1994
8531	Spicewood 1 S	30°27'	98°10'	EP	27	1968	1994
8536	Spinks Ranch	30°46'	99°50'	EP	17	1948	1964
8544	Spring Branch	29°52'	98°24'	EP	39	1956	1994
8561	Springtown	32°58'	97°40'	NC	22	1957	1978
8566	Spur	33°29'	100°51'	LRP	62	1911	1994
8568	Spurger Dam B	30°48'	94°11'	ET	18	1953	1970
8583	Stamford 1	32°56'	99°47'	LRP	79	1911	1994
8623	Stephenville WSMO	32°13'	98°11'	NC	60	1918	1994
8628	Sterley	34°12'	101°24'	HP	14	1947	1960
8630	Sterling City	31°51'	100°59'	EP	69	1926	1994
8631	Sterling City 8 NE	31°55'	100°53'	EP	21	1949	1994
8632	Sterling City 9 NW	31°54'	101°08'	EP	12	1949	1960

Footnote at end of table.

Appendix 3. Daily precipitation stations in Texas with at least 10 years of annual maxima data through 1994—Continued

Station no.	Station name	Latitude and longitude		Climatic region	Years of record	Beginning year of record	Ending year of record
8646	Stillhouse Hollow Dam	31°02'	97°32'	NC	32	1963	1994
8658	Stockdale 4 N	29°18'	97°58'	SC	23	1940	1994
8692	Stratford	36°21'	102°05'	HP	73	1911	1994
8696	Strawn 8 NNE	32°40'	98°28'	NC	46	1949	1994
8721	Substation 14	30°16'	100°35'	EP	31	1922	1952
8728	Sugar Land	29°37'	95°38'	UC	49	1946	1994
8743	Sulphur Springs	33°09'	95°38'	ET	86	1897	1994
8761	Sunray 4 SW	35°58'	101°52'	HP	28	1932	1984
8818	Tahoka	33°10'	101°89'	HP	70	1913	1994
8824	Talpa	31°46'	99°42'	LRP	18	1948	1965
8833	Tampico	34°28'	100°49'	LRP	38	1947	1984
8845	Tarpley	29°40'	99°17'	EP	29	1937	1965
8852	Tascosa	3°53'	410°21'	HP	38	1947	1984
8861	Taylor	30°34'	97°25'	NC	66	1929	1994
8863	Taylor Ranch	30°58'	98°56'	EP	29	1966	1994
8877	Teague Ranch	30°26'	98°49'	EP	29	1966	1994
8897	Telegraph	30°21'	99°54'	EP	46	1948	1994
8898	Telephone	33°47'	96°01'	NC	12	1947	1958
8910	Temple	31°05'	97°22'	NC	97	1897	1994
8920	Tennyson	31°44'	100°18'	EP	18	1948	1965
8929	Terrell	32°45'	96°17'	NC	48	1947	1994
8939	Tesco	32°30'	100°15'	LRP	28	1944	1971
8942	Texarkana	33°25'	94°05'	ET	27	1968	1994
8944	Texarkana Dam	33°18'	94°10'	ET	19	1956	1974
8996	Thompsons 3 WSW	29°29'	95°38'	UC	42	1942	1994
9001	Thorndale	30°37'	97°13'	NC	27	1968	1994
9004	Thornton	31°25'	96°35'	NC	48	1947	1994
9009	Three Rivers and 9007[1]	28°28'	98°11'	ST	73	1922	1994
9014	Throckmorton 2 W	33°11'	99°12'	NC	71	1924	1994
9015	Thurber 5 NE	32°32'	98°20'	NC	54	1910	1991
9031	Tilden	28°25'	98°32'	ST	46	1904	1994
9068	Toledo Bend Dam	31°11'	93°34'	ET	20	1975	1994
9076	Tomball	30°06'	95°37'	UC	49	1946	1994
9088	Tornillo 2 SSE	31°25'	106°05'	TP	17	1946	1994
9099	Tow	30°53'	98°28'	EP	17	1978	1994
9101	Town Bluff Dam	30°48'	94°11'	ET	25	1970	1994

Footnote at end of table.

Appendix 3. Daily precipitation stations in Texas with at least 10 years of annual maxima data through 1994—Continued

Station no.	Station name	Latitude and longitude		Climatic region	Years of record	Beginning year of record	Ending year of record
9106	Toyah	31°18'	103°48'	TP	30	1947	1977
9122	Trent 2 SSW	32°28'	100°08'	LRP	47	1948	1994
9125	Trenton	33°26'	96°20'	NC	48	1947	1994
9132	Trickham	31°35'	99°13'	LRP	18	1948	1965
9136	Trinidad 1 SW and 9137[1]	32°08'	96°06'	ET	47	1915	1990
9147	Troup	32°09'	95°07'	ET	19	1913	1931
9153	Troy	31°12'	97°18'	NC	48	1947	1994
9154	Truby 3 ESE	32°38'	99°53'	LRP	26	1947	1972
9163	Truscott 5 W	33°45'	99°55'	LRP	36	1948	1994
9175	Tulia	34°32'	101°46'	HP	48	1947	1994
9176	Tulia 6 NE	34°36'	101°42'	HP	50	1897	1952
9191	Turkey 2 WSW	34°23'	100°56'	LRP	40	1947	1994
9207	Tyler	32°20'	95°16'	ET	11	1984	1994
9213	Tyler CAA Airport	32°21'	95°24'	ET	20	1898	1954
9214	Tyler 5 NE	32°24'	95°16'	ET	30	1955	1984
9224	Umbarger	34°57'	102°06'	HP	48	1947	1994
9265	Uvalde and 9268[1]	29°13'	99°46'	EP	90	1905	1994
9270	Valentine	30°34'	104°29'	TP	17	1978	1994
9275	Valentine 10 WSW	30°30'	104°38'	TP	65	1897	1994
9280	Valley Junction	30°50'	96°38'	ET	39	1902	1977
9286	Valley View	33°29'	97°10'	NC	48	1947	1994
9295	Van Horn	31°04'	104°47'	TP	56	1939	1994
9304	Vancourt	31°21'	100°11'	EP	18	1948	1965
9311	Vanderpool	29°45'	99°34'	EP	16	1978	1993
9330	Vega	35°15'	102°25'	HP	61	1923	1983
9337	Venus	32°26'	97°06'	NC	18	1947	1964
9346	Vernon 4 S	34°05'	99°18'	LRP	65	1904	1994
9363	Victoria WB Airport	28°47'	97°05'	UC	16	1946	1961
9364	Victoria WSO Airport	28°51'	96°55'	UC	34	1961	1994
9365	Victoria Cp & L	28°48'	97°01'	UC	34	1922	1994
9410	Voss 1 WSW	31°37'	99°35'	LRP	33	1949	1981
9417	Waco Dam	31°36'	97°13'	NC	30	1965	1994
9419	Waco WSO Airport	31°37'	97°13'	NC	63	1930	1994
9421	Waco	31°32'	97°04'	NC	12	1946	1957
9424	Waelder 7 S	29°36'	97°19'	SC	46	1947	1993
9448	Waller 3 SSW	30°01'	95°56'	ET	48	1947	1994

Footnote at end of table.

Appendix 3. Daily precipitation stations in Texas with at least 10 years of annual maxima data through 1994—Continued

Station no.	Station name	Latitude and longitude		Climatic region	Years of record	Beginning year of record	Ending year of record
9480	Warren	30°37'	94°25'	ET	51	1935	1992
9491	Washington State Park	30°20'	96°09'	ET	49	1915	1994
9499	Water Valley	31°40'	100°43'	EP	48	1898	1994
9500	Water Valley 11 ENE	31°42'	100°32'	EP	10	1949	1958
9501	Water Valley 10 NNE	31°48'	100°39'	EP	36	1959	1994
9504	Watson	30°56'	98°01'	EP	27	1968	1994
9522	Waxahachie	32°25'	96°51'	NC	97	1897	1994
9532	Weatherford	32°46'	97°49'	NC	93	1902	1994
9538	Webb	32°42'	97°04'	NC	13	1947	1959
9559	Welder Wildlife Foundation	28°06'	97°25'	SC	31	1964	1994
9565	Wellington	34°50'	100°13'	LRP	55	1912	1994
9588	Weslaco 2 E	26°09'	97°58'	ST	48	1947	1994
9655	Wharton	29°19'	96°06'	UC	59	1902	1994
9662	Wheeler	35°26'	100°17'	LRP	16	1979	1994
9715	Whitney Dam	31°51'	97°22'	NC	46	1949	1994
9716	Whitsett 3 SW	28°38'	98°16'	ST	49	1914	1964
9717	Whitsett	28°38'	98°16'	ST	31	1964	1994
9729	Wichita Falls WSO Airport	33°58'	98°29'	LRP	94	1897	1994
9730	Wichita Valley Farm 29	33°56'	98°35'	LRP	29	1939	1972
9732	Wichita Valley 55	33°56'	98°37'	LRP	16	1939	1954
9734	Wiergate	31°01'	93°43'	ET	19	1925	1943
9772	William Harris Reservoir	29°15'	95°33'	UC	16	1949	1964
9780	Willis	30°26'	95°29'	ET	11	1907	1928
9800	Wills Point	32°42'	96°01'	ET	75	1905	1994
9813	Wilson Ranch	29°54'	99°36'	EP	16	1947	1962
9815	Wimberley 2	29°59'	98°03'	EP	11	1984	1994
9816	Winchell 1 WNW	31°29'	99°11'	EP	18	1948	1965
9826	Winfield	33°09'	95°08'	ET	27	1910	1936
9830	Wink FAA Airport	31°47'	103°12'	TP	53	1938	1994
9836	Winnsboro 6 SW	32°53'	95°20'	ET	47	1947	1994
9842	Winter Haven Experiment Station	28°38'	99°52'	ST	18	1947	1964
9845	Winters 9 NNE	32°06'	99°54'	LRP	44	1911	1968
9847	Winters 1 NNE	31°58'	99°57'	LRP	27	1968	1994
9859	Wolfe City	33°22'	96°04'	NC	48	1947	1994
9892	Woodsboro	28°14'	97°20'	SC	49	1916	1964
9898	Woodville and 9896[1]	30°46'	94°25'	ET	10	1917	1994

Footnote at end of table.

Appendix 3. Daily precipitation stations in Texas with at least 10 years of annual maxima data through 1994—Continued

Station no.	Station name	Latitude and longitude		Climatic region	Years of record	Beginning year of record	Ending year of record
9916	Wright Patman Dam and Lake	33°18'	94°10'	ET	21	1974	1994
9952	Yoakum	29°17'	97°08'	SC	73	1917	1994
9953	Yorktown	28°59'	97°30'	SC	48	1947	1994
9966	Ysleta	31°42'	106°19'	TP	56	1939	1994
9976	Zapata	26°53'	99°18'	ST	39	1909	1994

[1] The record of this station was considered auxiliary and therefore combined with the identified station in the table.

District Chief
U.S. Geological Survey
8011 Cameron, Rd.
Austin, TX 78754–3898